Journal Information

Maejo International Journal of Science and Technology (ISSN 1905-7873 © 2013), the international journal for preliminary communications in Science and Technology is the first peer-refereed scientific journal of Maejo University (www.mju.ac.th). Intended as a medium for communication, discussion, and rapid dissemination of important issues in Science and Technology, articles are published online in an open access format, which thereby gives authors the chance to communicate with a wide range of readers in an international community.

Publication Information

MIJST is published triannually. Articles are available online and can be accessed free of charge at http://www.mijst.mju.ac.th. Printed and bound copies of each volume are produced and distributed to selected groups or individuals.

Abstracting/Indexing Information

MIJST is covered and cited by Science Citation Index Expanded, SCOPUS, Journal Citation Reports/Science Edition, Zoological Record, Directory of Open Access Journals (DOAJ), CAB Abstracts, ProQuest, Google Scholar and EBSCO.

Contact Information

Editorial office: Maejo International Journal of Science and Technology (MIJST), 1st floor, Orchid Building, Maejo University, San Sai, Chiang Mai 50290, Thailand

Tel: +66-53-87-3880
E-mail: duang@mju.ac.th

MAEJO INTERNATIONAL JOURNAL OF SCIENCE AND TECHNOLOGY

MAEJO INTERNATIONAL JOURNAL OF SCIENCE AND TECHNOLOGY

The International Journal for the Publication of Preliminary Communications in Science and Technology

http://www.mijst.mju.ac.th
ISSN 1905-7873

MAEJO INTERNATIONAL JOURNAL
OF SCIENCE AND TECHNOLOGY

Volume 7, Issue 3 (September-December 2013)

CONTENTS

http://www.mijst.mju.ac.th
ISSN 1905-7873

http://www.mijst.mju.ac.th
ISSN 1905-7873

MAEJO INTERNATIONAL JOURNAL
OF SCIENCE AND TECHNOLOGY

Volume 7, Issue 3 (September-December 2013)

Author Index

Instructions for Authors

A proper introductory e-mail page containing the title of the submitted article and certifying its originality should be sent to the editor (Duang Buddhasukh, e-mail: duang@mju.ac.th). The manuscript proper together with a list of suggested referees should be attached in separate files. The list should contain at least 5 referees with appropriate expertise. Three referees should be non-native from 3 different countries. Each referee's academic/professional position, scientific expertise, affiliation and e-mail address must be given. The referees should not be affiliated to the same university/institution as any of the authors, nor should any two referees come from the same university/institution. The editorial team, however, retain the sole right to decide whether or not the suggested referees are approached.

Failure to conform to the above instructions will result in non-consideration of the submission.

Please also ensure that English and style is properly edited before submission. UK style of spelling should be used. Authors who would like to consult a professional service can visit www.proof-reading-service.com, www.editage.com, www.bioedit.co.uk (bioscience and medical papers), www.bioscienceeditingsolutions.com, www.scribendi.com, www.letpub.com, www.papersconsulting.com, www.stickle rediting.com, Cambridge Proofreading (http://proofreading.org/), www.ProofreadingServices.com, www.horizonproofreaders.org, www.manuscript-proofreding.com or Quality Proofreading.

Important : Manuscript with substandard English and style will not be considered.

Warning : Plagiarism (including self-plagiarism) may be checked for at *the last* stage of processing and, if detected, will result in a rejection and blacklisting.

Manuscript Preparation

Manuscripts must be prepared in English using a word processor. MS Word for Macintosh or Windows, and .doc or .rtf files are preferred. Manuscripts may be prepared with other software provided that the full document (with figures, schemes and tables inserted into the text) is exported to a MS Word format for submission. Times or Times New Roman font is preferred. The font size should be 12 pt and the line spacing 'at least 17 pt'. A4 paper size is used and margins must be 1.5 cm on top, 2.0 cm at the bottom and 2.0 cm on both left and right sides of the paper. Although our final output is in .pdf format, authors are asked NOT to send manuscripts in this format as editing them is much more complicated. Under the above settings, a manuscript submitted should not be longer than **15 pages** for a full paper or **20 pages** for a review paper.

A template file may be downloaded from the *Maejo Int. J. Sci. Technol.* homepage. (DOWNLOAD HERE)

Authors' full mailing addresses, homepage addresses, phone and fax numbers, and e-mail addresses homepages can be included in the title page and these will be published in the manuscripts and the Table of Contents. The corresponding author should be clearly identified. It is the corresponding author's responsibility to ensure that all co-authors are aware of and approve of the contents of a submitted manuscript.

A brief (200 word maximum) Abstract should be provided. The use in the Abstract of numbers to identify compounds should be avoided unless these compounds are also identified by names.

A list of three to five keywords must be given and placed after the Abstract. Keywords may be single words or very short phrases.

Although variations in accord with contents of a manuscript are permissible, in general all papers should have the following sections: Introduction, Materials and Methods, Results and Discussion, Conclusions, Acknowledgments (if applicable) and References.

Authors are encouraged to prepare Figures and Schemes in colour. Full colour graphics will be published free of charge.

Tables and Figures should be inserted into the main text, and numbers and titles supplied for all Tables and Figures. All table columns should have an explanatory heading. To facilitate layout of large tables, smaller fonts may be used, but in no case should these be less than 10 pt in size. Authors should use the Table option of MS Word to create tables, rather than tabs, as tab-delimited columns are often difficult to format in .pdf for final output.

Figures, tables and schemes should also be placed in numerical order in the appropriate place within the main text. Numbers, titles and legends should be provided for all tables, schemes and figures. Chemical structures and reaction schemes should be drawn using an appropriate software package designed for this purpose. As a guideline, these should be drawn to a scale such that all the details and text are clearly legible when placed in the manuscript (i.e. text should be no smaller than 8-9 pt).

For bibliographic citations, the reference numbers should be placed in square brackets, i.e. [ ], and placed before the punctuation, for example [4] or [1-3], and all the references should be listed separately and as the last section at the end of the manuscript.

Format for References

Journal :

1. D. Buddhasukh, J. R. Cannon, B. W. Metcalf and A. J. Power, "Synthesis of 5-n-alkylresorcinol dimethyl ethers and related compounds *via* substituted thiophens", *Aust. J. Chem.*, **1971**, *24*, 2655-2664.

Text :

2. A. I. Vogel, "A Textbook of Practical Organic Chemistry", 3rd Edn., Longmans, London, **1956,** pp. 130-132.

Chapter in an edited text :

3. W. Leistritz, "Methods of bacterial reduction in spices", in "Spices: Flavor Chemistry and Antioxidant Porperties" (Ed. S. J. Risch and C-T. Ito), American Chemical Society, Washington, DC, **1997**, Ch. 2.

Thesis / Dissertation :

4. W. phutdhawong, "Isolation of glycosides by electrolytic decolourisation and synthesis of pentinomycin", *PhD Thesis*, **2002**, Chiang Mai University, Thailand.

Patent :

5. K. Miwa, S. Maeda and Y. Murata, "Purification of stevioside by electrolysis", *Jpn. Kokai Tokkyo Koho 79 89,066* (**1979**).

Proceedings :

6. P. M. Sears, J. Peele, M. Lassauzet and P. Blackburn, "Use of antimicrobial proteins in the treatment of bovine mastitis", Proceedings of the 3rd International Mastitis Seminars, **1995**, Tel-Aviv, Israel, pp. 17-18.

Websites :

7. S. Simon, "What is an odds ratio?", **2008**, http://www.childrensmercy.org/stats/definitions/or.htm (Accessed: October 2011).

Manuscript Revision Time

Authors who are instructed to revise their manuscript should do so within **45** days. Otherwise the revised manuscript will be regarded as a new submission.

Manuscript Processing Time

As a result of a large number of submissions, there may be a long delay in the evaluation or publication of a paper. A duration of at least 6-8 months between submission and acceptance (or rejection) can normally be expected.

Maejo International Journal of Science and Technology

ISSN 1905-7873
Available online at www.mijst.mju.ac.th

Full Paper

Antioxidant activity changes during hot-air drying of *Moringa oleifera* leaves

Wiwat Wangcharoen* and Sompoch Gomolmanee

Faculty of Engineering and Agro-Industry, Maejo University, Chiang Mai 50290, Thailand

*Corresponding author, e-mail: wiwat@mju.ac.th

Received: 19 April 2012 / Accepted: 1 September 2013 / Published: 3 September 2013

Abstract: Dried *Moringa oleifera* leaf powder in capsule is now a popular food supplement in Thailand. To investigate its health benefits, antioxidant activities of *M. oleifera* leaves (3 varieties: Num Phrae, Ang Thong and PKM1) during drying in hot-air oven at 50°C and 100°C were studied by 3 different methods, viz. ferric reducing antioxidant power (FRAP), DPPH free radical scavenging activity and ABTS radical cation decolourisation, together with the determination of total phenolic content and browning pigment formation. It was found that the antioxidant activities and total phenolic content tend to decrease in the early stage of drying and then increase in the later stage, and that the dried leaves still have at least 60% of antioxidant activities compared to fresh leaves.

Key words: *Moringa oleifera*, antioxidant activity, total phenolic content, browning pigment formation, hot-air drying

INTRODUCTION

Moringa oleifera, Lam. Syn. *Moringa pterygosperma* Gaertn. (family Moringaceae) is commonly known as drumstick tree or horseradish tree and widely cultivated in the tropics and subtopics of Asia and Africa [1]. Almost all the parts of this plant are used for various ailments in the indigenous medicine of South Asia [2]. Its young leaves and green pods are common vegetables in some countries such as India [3] and Thailand, and the dried leaf powder has now become popular among many Thais.

M. oleifera leaves are highly nutritious. In 100 g dry matter, they contain 29±6 g of protein, 28±6 mg of iron, 1,924±288 mg of calcium, 15,620±6,475 IU of vitamin A and 773±91 mg of vitamin C. This is at least twice the protein in milk and half the protein in egg, and has more iron than in beef, more calcium than in milk, equal vitamin A to carrot and more vitamin C than in orange [5]. In addition, the leaves of this plant are reported to have various biological

activities such as diuretic [6], immune boosting and hypotensive [7], antiinflammatory [8-10], antiulcer [11], antihepatotoxic [10], antitumour [12], thyroid hormone status regulating [13], hypocholesterolaemic [14-15], radioprotective [16], hypolipidaemic [17], antiatherosclerotic [17], antidiabetic [18] and antioxidant [4, 17, 19-23].

The free radical accumulation or oxidative stress in the human body plays multiple important roles in tissue damage and loss of function in a number of tissues and organs [24], which consequently may adversely affect the immune functions and contribute to pathological conditions and chronic human diseases such as aging, carcinogenesis, diabetes, gastric ulcer and rheumatic joint inflammation [25-26]. Phenolic compounds in plants have been shown to be effective antioxidant constituents and many polyphenolics have a more powerful antioxidant effect than that of vitamin E [27].

M. oleifera leaves with a high content of phenolics and flavonoids [4, 21, 28] show greater antioxidant activity, anti-radical power, reducing power, inhibition of lipid peroxidation, protein oxidation and OH·-induced deoxyribose degradation, and scavenging power of superoxide anions and nitric oxide radicals than do its fruits and seeds [4, 21]. The antioxidant activity of *M. oleifera* leaf extract was found to be higher than that of standard vitamin E [20, 21] and remain unaffected at pH 4 and pH 9 in the dark at 5°C and 25°C respectively for 15 days, although the activity significantly decreases when heated at 100°C for 15 min [20]. In addition, the activity can vary with such factors as variety [4], season and production location [19] and stage of maturity [22].

Dried *M. oleifera* leaf powder in capsules has become a popular food supplement for many people in Thailand [4]. However, heat treatment may affect the stability of *M. oleifera* extracts [20]. This study aims to follow changes in the antioxidant activity of *M. oleifera* leaves during hot-air drying, a conventional process for their drying. Three varieties of *M. oleifera* (Num Phrae, Ang Thong and PKM1) were studied, and the total phenolic content (TPC) and browning pigment formation, which may affect the antioxidant activities, were also determined.

MATERIALS AND METHODS

Chemicals and Apparatus

2,2-Diphenyl-1-picrylhydrazyl (DPPH), 2,4,6-tripyridyl-s-triazine (TPTZ), 2,2'-azinobis (3-ethylbenzothiazoline-6-sulphonic acid) (ABTS), ferric chloride, Folin-Ciocalteu phenol reagent, gallic acid, glacial acetic acid, hydrochloric acid, potassium persulphate, sodium acetate, sodium carbonate and vitamin C were obtained from Sigma-Aldrich and all of them were of analytical grade.

A spectronic 20D+ spectrophotometer (Milton Roy) was used for all assays.

Preparation of Leaf Extract

Fresh leaves of *M. oleifera* (variety: Num Phrae, Ang Thong and PKM1) grown in Chiang Mai province were harvested in April–June 2010. Num Phrae and Ang Thong are local varieties from Amphoe Mueang, Phrae province and Amphoe Pamok, Ang Thong province respectively, while PKM1 is an Indian variety available from Chaipattana Foundation in Bangkok.

Fresh leaves (71-78% moisture content) were macerated using a blender. Two grams of the blended leaves were transferred into each 25x150 cm sample tube and dried in a hot-air oven at 50°C for 12.5 hr or at 100°C for 2.5 hr. Sampling of the leaves was done before drying and then every 2.5 hr for leaves heated at 50°C and every 0.5 hr for leaves heated at 100°C. To

prepare a crude extract, 10 mL of deionised water was added to the collected sample tube and the mixture was shaken by a vortex mixer for 60 seconds [29] and filtered. The filtrate was adjusted to 10 mL and the resulting extract solution was used for the determination of antioxidant activities, total phenolic content and browning pigment formation.

Ferric Reducing Antioxidant Power (FRAP) Assay

The total reducing power of electron donating substances was determined according to Benzie and Strain [30]. Briefly, 6 mL of FRAP reagent (0.1M acetate buffer : 0.02M $FeCl_3$: 0.01M TPTZ = 10:1:1) prepared daily were mixed with 20 µL of the extract solution. The absorbance at 593 nm was recorded after a 30-min. incubation at 37°C. FRAP values were obtained by comparison with a standard curve created using vitamin C (0-15 µg) and reported as mg vitamin C equivalent per gram (dried leaves).

DPPH Free Radical Scavenging Activity

The method of Brand-Williams et al. [31] based on the reduction of DPPH radical solution in the presence of hydrogen donating antioxidants was used with some modifications. Twenty µL of the extract solution were diluted with deionised water : 95% ethanol (1:1) to 5.4 mL and then 0.6 mL of DPPH radical solution (0.8 mM in 95% ethanol) was added and the mixture was shaken vigorously. The decrease of absorbance at 517 nm was recorded at 1 min. after mixing. Vitamin C (0-40 µg) was used as standard and the results were reported as mg vitamin C equivalent per gram (dried leaves).

ABTS Radical Cation Decolourisation Assay

The method of Re et al. [32] based on the ability of antioxidant molecules to quench the long-lived ABTS radical cation ($ABTS^{\bullet+}$) was modified. $ABTS^{\bullet+}$ was produced by reacting 7 mM ABTS stock solution with 2.45 mM postassium persulphate (final concentration) and allowing the mixture to stand in the dark at room temperature for 12-16 hr before use. The $ABTS^{\bullet+}$ solution was diluted with deionised water : 95% ethanol (1:1) to an absorbance of 0.70 ($\pm$0.02) at 734 nm. Twenty µL of the extract solution were mixed with 6 mL of the diluted $ABTS^{\bullet+}$ solution. The decrease of absorbance was recorded at 1 min. after mixing. Vitamin C (0-20 µg) was used as standard and the results were reported as mg vitamin C equivalent per gram (dried leaves).

Total Phenolic Content (TPC)

The Folin-Ciocalteau micro method of Waterhouse [33] was used. Twenty µL of the extract solution were diluted with deionised water to 4.8 mL and 300 µL Folin-Ciocalteau reagent were added and shaken. After 8 min., 900 µL of 20% sodium carbonate were added with mixing. The mixture was allowed to stand at 40°C for 30 min. before the absorbance at 765 nm was read. Gallic acid (0-50 µg) was used as standard and the results for TPC were reported as mg gallic acid equivalent per gram (dried leaves).

Formation of Browning Pigments

Browning pigment formation was determined by the official method of the Association for Dehydrated Onion and Garlic Products (ADOGA) [34]. Three mL of the extract solution were mixed with 3 mL of deionised water and its absorbance was measured at 420 nm.

Experimental Values for Antioxidant Assays and TPC

The experimental values for TPC and antioxidant assays by FRAP, ABTS and DPPH methods (mg standard equivalent per gram of dried leaves) were calculated as:

$$= \frac{\left[\frac{[SA - BA]}{Slope} \times [10/U]\right]}{\left[2 * \left[1 - \frac{\%mc}{100}\right]\right][1{,}000]}$$

where: SA = Sample absorbance for FRAP method or TPC, or absorbance decrease of sample for ABTS or DPPH method
BA = Blank absorbance for FRAP method or TPC, or absorbance decrease of blank for ABTS or DPPH method
Slope = Slope of standard curve
10/U = Total volume of extract solution (10 mL) / Used volume of extract (mL)
2 = Weight of blended fresh leaves (g)
% mc = % moisture content
1,000 = Factor for converting µg to mg

Statistical Analysis

The relation between the three antioxidant activities and total phenolic content or browning pigment formation was analysed by Bivariate correlation. All statistical analysis was done by SPSS 16.0 Family.

RESULTS AND DISCUSSION

Changes at 50°C

As shown in Figure 1, the values from the results of FRAP assay and TPC gradually declined while some values slightly increased in the later stage of the drying process. On the other hand, the values from the results of DPPH and ABTS assays rapidly decreased in the first 2.5 hours and then were quite constant, although some values slightly increased at the end of the drying process.

The drop in TPC could be explained by thermal oxidation and decomposition of phenolic compounds [35], which might be the main reason for the antioxidant activity decrease of *M. oleifera* leaves, as shown by a significant correlation between TPC and all antioxidant activities in Table 1. The FRAP, rather than the DPPH and ABTS assay values, was highly dependent on the TPC. The decrease in the capacity to allay DPPH and ABTS radicals at the first 2.5 hours was faster than the decrease in TPC, possibly due to thermal oxidation and decomposition of non-phenolic antioxidant substances in *M. oleifera* leaves, especially vitamin C [5].

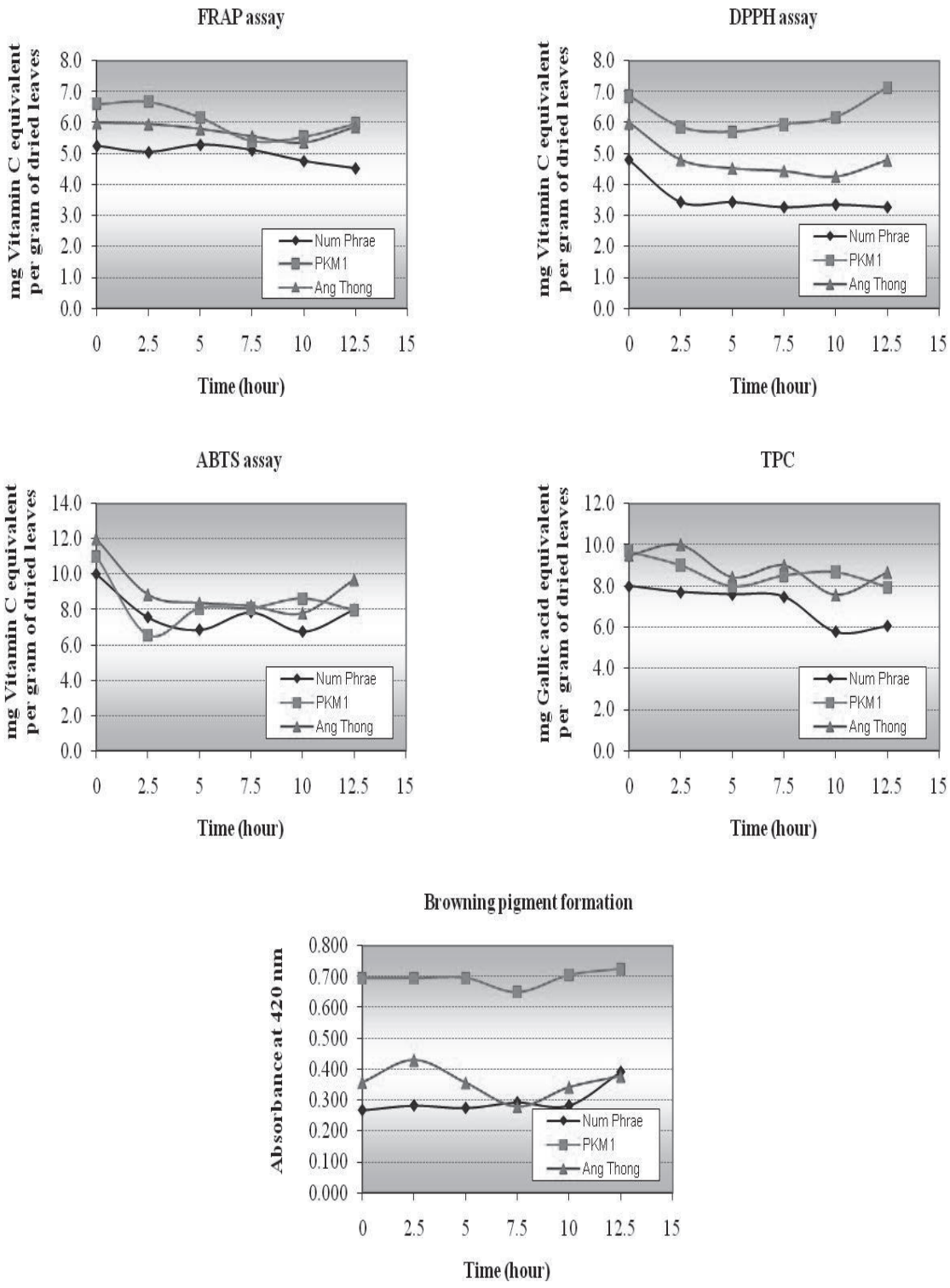

Figure 1. Antioxidant activities (FRAP, DPPH and ABTS assays), TPC and browning pigment formation of *M. oleifera* leaves during drying in hot-air oven at 50°C (Coefficient of variation = 4.76 -13.82%)

Table 1. Correlation coefficients between TPC/browning pigment formation and antioxidant activities of *M. oleifera* leaves during drying in hot-air oven at 50°C and 100°C

	Correlation coefficient	
	TPC	Browning pigment formation (absorbance at 420 nm)
At 50°C		
FRAP	0.790**	0.627**
DPPH	0.626**	0.834**
ABTS	0.561*	0.035
At 100°C		
FRAP	0.366	0.055
DPPH	0.586*	-0.005
ABTS	0.587*	-0.395
Pooled data		
FRAP	0.621**	0.354*
DPPH	0.587**	0.563**
ABTS	0.558**	-0.037

* Correlation is significant ($p<0.05$). ** Correlation is highly significant ($p<0.01$).

At the later stage of the drying process, some observed increase in antioxidant activity could be attributable to the occurance of antioxidant substances or phenolic compounds by thermal reactions such as non-enzymatic browning reactions [35-39]. This is supported by a significant correlation between the browning pigment formation and results of DPPH or FRAP assay in Table 1. The capacity to trap DPPH radicals was more dependent on the browning pigment formation than the electron donating power (FRAP) results. This high correlation between browning pigment formation and results of DPPH or FRAP assay was also found in our previous work [40]. However, the increase in browning pigment formation (0.020-0.124) during drying at 50°C was not much. Thus, the antioxidant activities in this case could be considered to stem more from natural heat-stable antioxidant substances in *M. oleifera* leaves than from non-enzymatic browning products. As for the capacity to trap ABTS radicals, it was not related to the browning pigment formation but correlated with the TPC only. The increase in the ABTS values could therefore be the results of phenolic compounds from other thermal reactions such as the thermal degradation of insoluble and bound phenolic compounds [41].

From Figure 1, it is evident that the antioxidant activities and TPC of *M. oleifera* leaves significantly decreased during drying at 50°C. Although some of the values were regained in the later stage of the drying process, almost all of them were significantly lower than those for the fresh leaves. However, the antioxidant activity of all dried leaves was at least 60% of that of the fresh leaves. Moreover, the values for antioxidant activities and phenolic content of the three leaf varieties during drying at 50°C were similarly changed: compared to those from fresh leaves (treated as 100%) the values varied between 68-101% (for Num Phrae), 60-104% (for PKM1) and 65-105% (for Ang Thong).

Changes at 100°C

As shown in Figure 2, the electron donating power (FRAP) value appeared to decrease except that for Num Phrae variety, whose FRAP showed little change. The values for DPPH and

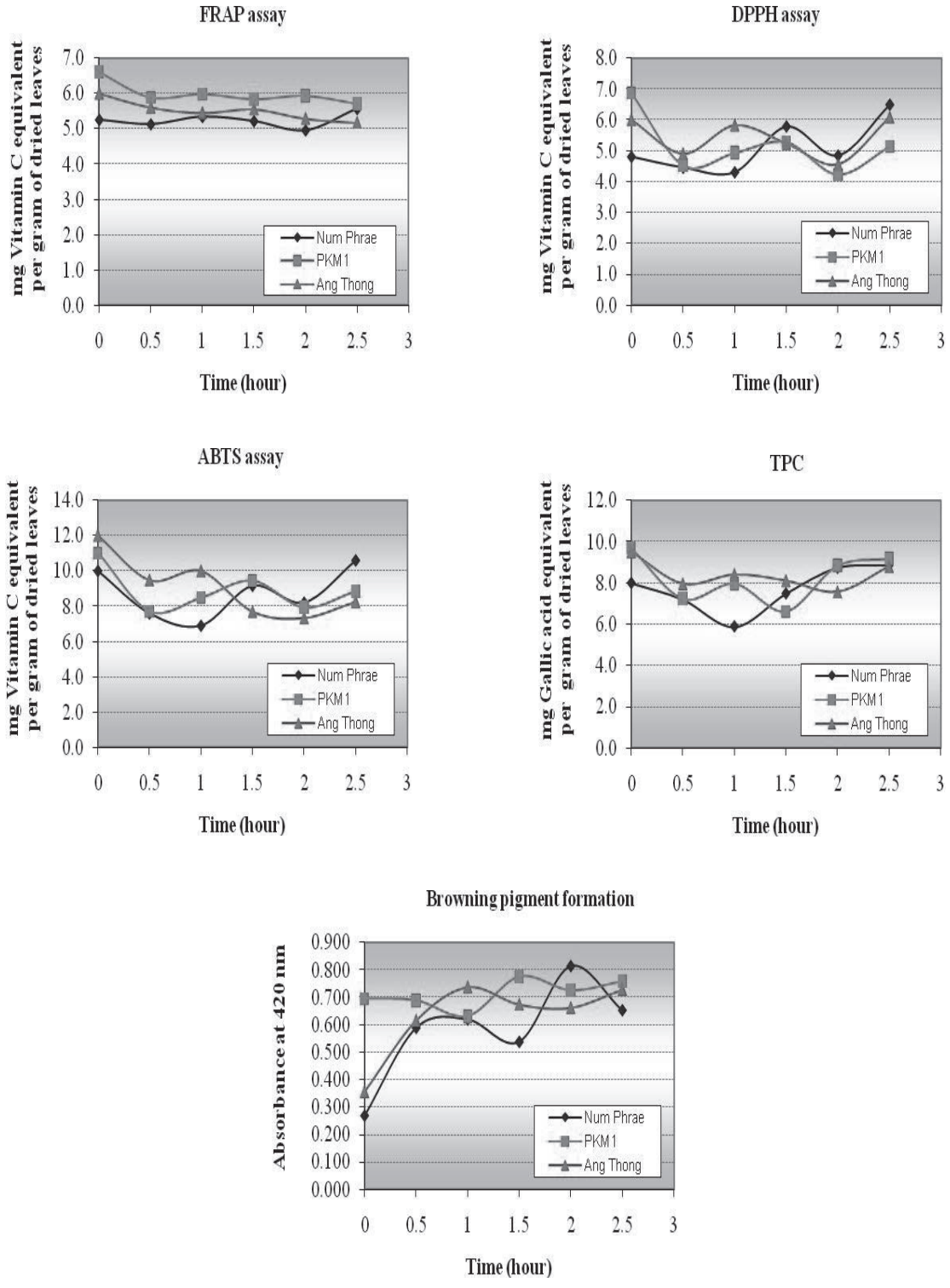

Figure 2. Antioxidant activities by FRAP, DPPH and ABTS assays, TPC and browning pigment formation of *M. oleifera* leaves during drying in hot-air oven at 100°C (Coefficient of variation = 4.44-13.94%)

ABTS assays as well as TPC appeared to decrease in the early stage of drying and then increase in the later stage. A result similar to the early stage of heating, where there is a significant decrease of antioxidant activity of *M. oleifera* leaves extract heated at 100°C for 15 min., was also reported [20].

As with the changes at 50°C, all decreases in antioxidant activities in Figure 2 could be explained by thermal oxidation and decomposition of materials including phenolic compounds [35] and other non-phenolic antioxidants such as vitamin C [5] in *M. oleifera* leaves, while all increased values could be explained by the formation of antioxidant products of thermal reactions such as non-enzymatic browning reactions [35-39], and also by the thermal degradation of insoluble and bound phenolic compounds [41]. Examples of the latter are the breaking of linkages between *p*-coumaric acid and lignin and between ferulic acid and arabinoxylans [42]. It appears that, compared with values for fresh leaves, the variation in antioxidant activities and phenolic compounds during drying at 100°C for Num Phrae variety (69-135%) were more than those for Ang Thong (61-101%) and PKM1 (61-94%) varieties.

At 100°C drying, there was a lower correlation than in the case of drying at 50°C and only between TPC and results of DPPH or ABTS assays; there was no correlation between browning pigment formation and any antioxidant activities (Table 1). This may be explained by the fact that the bivariate correlation is used to measure the direction and strength of a linear relationship between two variables [43]. However, when the two changes, i.e. thermal oxidation/ decomposition/ degradation and non-enzymatic browning reactions, occurred faster at 100°C, it might be more difficult to correlate them by a linear relationship compared to the situation at 50°C, in which the reaction rates were slower.

Compared to drying at 50°C, TPC of Num Phrae variety's leaves dried at 100 °C was higher than that in its fresh leaves (Figure 2). These phenolic compounds occurring during the later stage of drying by such thermal reactions as the degradation of insoluble and bound phenolic compounds at high temperature could also imply that the leaves of Num Phrae variety probably contain more insoluble and bound phenolic compounds than do Ang Thong and PKM1 varieties.

CONCLUSIONS

Antioxidant activities of *Moringa oleifera* leaves dried by hot-air oven at both 50°C and 100°C were found to be at least 60% that of fresh leaves. Some of the variation in antioxidant activity values were found to be significantly related to the total phenolic content and the formation of browning pigments. Similar changes in antioxidant activities were observed in the three varieties of *M. oleiferea*.

ACKNOWLEDGEMENTS

This work was a part of research projects supported by a grant from the Faculty of Engineering and Agro-Industry at Maejo University.

REFERENCES

1. F. E. M. Booth and G. E. Wickens, "Non-timber Uses of Selected Arid Zone Trees and Shrubs in Africa", Food and Agriculture Organization, Rome, **1988**.
2. J. A. Parrotta, "Healing Plants of Peninsular India", CABI Publication, New York, **2001**.

3. T. Okuda, A. U. Baes, W. Nishijima and M. Okada, "Isolation and characterization of coagulant extracted from *Moringa oleifera* seed by salt solution", *Water Res.*, **2001**, *35*, 405-410.
4. W. Wangcharoen and S. Gomolmanee, "Antioxidant capacity and total phenolic content of *Moringa oleifera* grown in Chiang Mai, Thailand", *Thai J. Agric. Sci.*, **2011**, *44*, 118-124.
5. M. Broin, "The nutritional value of *Moringa oleifera* Lam. leaves: What can we learn from figures?", (no date), http://www.moringanews.org/doc/GB/Posters/Broin_poster.pdf (Accessed: March, 2012).
6. A. Cáceres, A. Saravia, S. Rizzo, L. Zabala, E. De Leon and F. Nave, "Pharmacological properties of *Moringa oleifera* 2: Screening for antispasmodic, antiinflammatory and diuretic activity", *J. Ethnopharmacol.*, **1992**, *36*, 233-237.
7. S. Faizi, B. S. Siddiqui, R. Saleem, S. Siddiqui, K. Aftab and A. H. Gilani, "Isolation and structure elucidation of new nitrile and mustard oil glycosides from *Moringa oleifera* and their effect on blood pressure", *J. Nat. Prod.*, **1994**, *57*, 1256-1261.
8. S. L. Udupa, A. L. Udupa and D. R. Kulkarni, "Studies on anti-inflammatory and wound healing properties of *Moringa oleifera* and *Aegle marmelos*", *Fitoterapia*, **1994**, *65*,119-123.
9. I. C. Ezeamuzie, A. W. Ambakederomo, F. O. Shode and S. C. Ekwebelem, "Antiinflammatory effects of *Moringa oleifera* root extract", *Pharm. Biol.*, **1996**, *34*, 207-212.
10. K. S. Rao and S. H. Misra, "Antiinflammatory and antihepatotoxic activities of the rats of *Moringa pterygosperma*, Gaertn.", *Ind. J. Pharm. Sci*., **1998**, *60*, 12-16.
11. S. K. Pal, P. K. Mukherjee and B. P. Saha, "Studies on the antiulcer activity of *Moringa oleifera* leaf extract on gastric ulcer models in rats", *Phytother. Res.*, **1995**, *9,* 463-465.
12. A. Murakami, Y. Kitazono, S. Jiwajinda, K. Koshimizu and H. Ohigashi, "Niaziminin, a thiocarbamate from the leaves of *Moringa oleifera*, holds a strict structural requirement for inhibition of tumor-promoter-induced Epstein-Barr virus activation", *Planta Med*., **1998**, *64*, 319-323.
13. P. Tahiliani and A. Kar, "Role of *Moringa oleifera* leaf extract in regulation of thyroid hormone status in adult male and female rats", *Pharmacol. Res*., **2000**, *41*, 319-323.
14. S. Ghasi, E. Nwobodo and J. O. Ofili, "Hypocholesterolemic effects of crude extract of leaf of *Moringa oleifera* Lam in high-fat diet fed Wistar rats", *J. Ethnopharmacol*., **2000**, *69*, 21-25.
15. L. K. Mehta, R. Balaraman, A. H. Amin, P. A. Bafna and O. D. Gulati, "Effect of fruits of *Moringa oleifera* on the lipid profile of normal and hypercholesterolemic rabbits", *J. Ethnopharmacol.,* **2003**, *86*, 191-195.
16. A. V. Rao, P. U. Devi and R. Kamath, "In vivo radioprotective effect of *Moringa oleifera* leaves", *Indian J. Exp. Biol*., **2001**, *39,* 858-863.
17. P. Chumark, P. Khunawat, Y. Sanvarinda, S. Phornchirasilp, N. P. Morales, L. Phivthong-ngam, P. Ratanachamnong, S. Srisawat and K. U. Pongrapeeporn, "The in vitro and ex vivo antioxidant properties, hypolipidaemic and antiatherosclerotic activities of water extract of *Moringa oleifera* Lam. leaves", *J. Ethnopharmacol*. , **2008**, *116*, 439-446.
18. D. Jaiswal, P. K. Rai, A. Kumar, S. Mehta and G. Watal, "Effect of *Moringa oleifera* Lam. leaves aqueous extract therapy on hyperglycemic rats", *J. Ethnopharmacol*., **2009**, *123*, 392-396.

19. S. Iqbal and M. I. Bhanger, "Effect of season and production location on antioxidant activity of *Moringa oleifera* leaves grown in Pakistan", *J. Food Comp. Anal.*, **2006**, *19*, 544-551.
20. S. Arabshahi-D, D. V. Devi and A. Urooj, "Evaluation of antioxidant activity of some plant extracts and their heat, pH and storage stability", *Food Chem.*, **2007**, *100*, 1100-1105.
21. B. N. Singh, B. R. Singh, R. L. Singh, D. Prakash, R. Dhakarey, G. Upadhyay and H. B. Singh, "Oxidative DNA damage protective activity, antioxidant and anti-quorum sensing potentials of *Moringa oleifera***",** *Food Chem. Toxicol.*, **2009**, *47*, 1109-1116.
22. S. Sreelatha and P. R. Padma, "Antioxidant activity and total phenolic content of *Moringa oleifera* leaves in two stages of maturity", *Plant Foods Hum. Nutr.*, **2009**, *64*, 303-311.
23. A. R. Verma, M. Vijayakumar, C. S. Mathela and C. V. Rao, "In vitro and in vivo antioxidant properties of different fractions of *Moringa oleifera* leaves", *Food Chem. Toxicol.*, **2009** , *47*, 2196-2201.
24. R. L. Zheng and Z. Y. Huang, "Reactive oxygen species" in "Free Radicals in Medical and Agricultural Science" (Ed. R. L. Zheng and Z. Y. Huang), China Higher Education Press and Springer Press, Beijing, **2001**, Ch.2.
25. B. Halliwell, "Free radicals, antioxidants, and human disease: Curiosity, cause, or consequence?", *Lancet*, **1994**, *344*, 721-724.
26. J. Moskovitz, M. B. Yim and P. B. Chock, "Free radicals and disease", *Arch. Biochem. Biophys.*, **2002**, *397*, 354-359.
27. R. Tsao and M. H. Akhtar, "Nutraceuticals and functional foods I: Current trend in phytochemical antioxidant research", *J. Food Agric. Environ.*, **2005,** *3*, 10-17.
28. N. K. Amaglo, R. N. Bennett, R. B. L. Curto, E. A. S. Rosa, V. L. Turco, A. Giuffrida, A. L. Curto, F. Crea and G. M. Timpo, "Profiling selected phytochemicals and nutrients in different tissues of the multipurpose tree *Moringa oleifera* L., grown in Ghana", *Food Chem.*, **2010**, *122*, 1047-1054.
29. L. P. Leong and G. Shui, "An investigation of antioxidant capacity of fruits in Singapore markets", *Food Chem***., 2002,** *76*, 69-75.
30. I. F. Benzie and J. J. Strain, "Ferric reducing/antioxidant power assay: Direct measure of total antioxidant activity of biological fluids and modified version of simultaneous measurement of antioxidant power and ascorbic acid concentration", *Methods Enzymol.,* **1999**, *299*, 15-27.
31. W. Brand-William, M. E. Cuelier and C. Berset, "Use of a free radical method to evaluate antioxidant activity", *LWT- Food Sci. Technol.*, **1995**, *28*, 25-30.
32. R. Re, N. Pellegrini, A. Proteggente, A. Pannala, M. Yang and C. Rice-Evans, "Antioxidant activity applying an improved ABTS radical cation decolorization assay", *Free Rad. Biol. Med.*, **1999**, *26*, 1231-1237.
33. A. Waterhouse, "Folin-Ciocalteau micro method for total phenol in wine", (no date), http://waterhouse.ucdavis.edu/phenol/folinmicro.htm (Accessed: May, 2005).
34. ADOGA, "Official Standards and Methods of the American Dehydrated Onion and Garlic Association (ADOGA) for Dehydrated Onion and Garlic Products", American Dehydrated Onion and Garlic Association, San Francisco, **1987**, pp.1-13.
35. L. Manzocco, S. Calligaris, D. Mastrocola, M. C. Nicoli and C. R. Lerici, "Review of non-enzymatic browning and antioxidant capacity in processed foods", *Trends Food Sci. Technol.,* **2000**, *11*, 340-346.

36. K. Yanagimoto, K. G. Lee, H. Ochi and T. Shibamoto, "Antioxidative activity of heterocyclic compounds formed in Maillard reaction products", *Int. Congress Series*, **2002**, *1245*, 335-340.
37. Y. Yilmaz and R. Toledo, "Antioxidant activity of water-soluble Maillard reaction products", *Food Chem.*, **2005**, *93*, 273-278.
38. Y. Osada and T. Shibamoto, "Antioxidative activity of volatile extracts from Maillard model systems", *Food Chem*., **2006**, *98*, 522-528.
39. S. Benjakul, W. Visessanguan, V. Phongkanpai and M. Tanaka, "Antioxidative activity of caramelisation products and their preventive effect on lipid oxidation in fish mince", *Food Chem.,* **2005**, *90*, 231-239.
40. W. Wangcharoen and W. Morasuk, "Effect of heat treatment on the antioxidant capacity of garlic", *Maejo Int. J. Sci. Technol*., **2009**, *3*, 60-70.
41. M. N. Maillard and C. Berset, "Evolution of antioxidant activity during kilning: Role of insoluble bound phenolic acids of barley and malt", *J. Agric. Food Chem*., **1995**, *43*, 1789-1793.
42. M. Al-Frasi, C. Alasalvar, A. Morris, M. Baron and F. Shahidi, "Comparison of antioxidant activity, anthocyanins, carotenoids, and phenolics of three native fresh and sun-dried date (*Phoenix dactylifera* L.) varieties grown in Oman", *J. Agric. Food Chem*., **2005**, *53*, 7592-7599.
43. Anonymous, "Correlation", (no date), https://facultystaff.richmond.edu/~choyt/.../lecture10_correlation.doc (Accessed: April, 2012).

Maejo Int. J. Sci. Technol. **2013**, *7*(03), 364-376

Maejo International Journal of Science and Technology

ISSN 1905-7873
Available online at www.mijst.mju.ac.th

Full Paper

New taxa and a key to *Pertusaria* species (Pertusariaceae, lichenised Ascomycota) in Thailand

Sureeporn Jariangprasert

Faculty of Science, Maejo University, Chiang Mai 50290, Thailand

E-mail: s_vipoosunti @mju.ac.th; tel: 053-873586; fax: 053-878225

Received: 5 November 2012 / Accepted: 9 September 2013 / Published: 10 September 2013

Abstract: Four corticolous *Pertusaria* taxa from Thailand are described as new, viz. *P. flavodigitata* Jariang., *P. khuntanensis* Jariang., *P. pertusella* Müll. Arg. var. *sorediata* Jariang. and *P. phukaensis* Jariang. A key of *Pertusaria* in Thailand is presented.

Keywords: *Pertusaria*, Pertusariaceae, Thailand

INTRODUCTION

Since 2000, revisional study of the lichen genus *Pertusaria* (Pertusariaceae) in Thailand has resulted in 103 taxa, of which 73 are new to Thailand and 34 are new taxa [1-3]. Additional four taxa are here described as new.

MATERIALS AND METHODS

Many specimens were collected during an extensive survey of *Pertusaria* in Thailand. The morphology and anatomy of the specimens were studied with an Olympus SZ3 stereomicroscope and an Olympus CH-2 compound microscope. Chemical analysis was carried out by both thin layer chromatography [4, 5] and high performance liquid chromatography [6, 7].

NEW TAXA

Pertusaria flavodigitata Jariang. *sp. nov.*

Similis ***Pertusaria parmatica*** Archer & Elix *sed acidum sticticum continens vice acidum salazinicum, Apothecia ignota*

Type: **Thailand**, **Tak province**, Mueang district, Mae Taw subdistrict, Lansang National Park, between Tak province and Mae Sod district, along the road to Musoe Dam and Musoe Lhueang Agricultural Station, on the trail to Pha Daeng Unit, on bark of Fagaceae, 980 m, primary evergreen, seasonal hardwood forest, Jariangprasert 3829, 20 November 2002; holotype: QBG.

Etymology: From the Latin *flavus* = yellow and *digitatus* = finger-like; referring to the colour of the thallus under ultraviolet light and the appearance of the isidia.

Morphology and anatomy: Thallus grayish-green, corticolous, surface shiny, slightly wrinkled, isidiate, soredia absent. Isidia concolorous with the thallus, crowded, cylindrical to branched, 0.1 mm diameter, 0.1-0.6 mm long. Apothecia and pycnidia not seen.

Chemistry: K-, C-, KC-, Pd-, UV+ bright yellow; lichexanthone (major-minor), ±atranorin (minor), stictic acid (major), gracilliformin (minor), constictic acid (minor), cryptostictic acid (trace) and peristictic acid (trace).

Ecology: This species is corticolous on trees of Fagaceae and Theaceae in seasonal evergreen, hardwood forest.

Notes: *Pertusaria flavodigitata* (Figure 1A) is characterised by the isidiate thallus which fluorescence bright yellow under ultraviolet light. It is distinguished from the chemically similar, fertile Australian species, *P. isidiosa* Archer by the lack of both apothecia and 2′-*O*-methylperlatolic acid [8]. This new species resembles the isidiate, *P. parmatica* Archer & Elix from Papua New Guinea, but differs chemically. Both species give a bright yellow fluorescence under ultraviolet light, but *P. parmatica* contains salazinic acid rather than stictic acid.

Additional specimens examined (Paratypes)—**Thailand: Phitsanuloke province,** Phuhin Rongkla National Park, close to a water tank, next to Poo Paeng Ma guest house, behind a check point, on a tree trunk, 1,110 m, Jariangprasert 5599, 3 March 2004 (QBG); **Loei province**, Nahaew district, Nahaew National Park, on the way to check point 2, 1,408 m, on bark of Theaceae, in seasonal evergreen, hardwood forest, Jariangprasert 5386, 7 March 2004 (RAMK).

Pertusaria khuntanensis Jariang. *sp. nov.*

Similis ***Pertusaria parameana*** Jariang. *sed acidum 4-O-demethylplanaicum et acidum 2′-O-methylanziaicum continente differt*

Type: **Thailand**, **Lampang-Chiangmai provinces**, Khun Tan National Park, 99º 14’ E, 18º 25’ N, 600 m, deciduous dipterocarp forest, on a tree trunk, Wolseley & Boonpragob 3223, 11 Jan 1993; holotype: BM.

Etymology: From the Latin *ensis*, place of the origin and *Khun Tan* National Park.

Morphology and anatomy: Thallus grey-green to brown-green, corticolous, surface rough, subtuberculate, isidia and soredia absent. Apothecia verruciform, conspicuous, apothecia solitary, rounded confluent apothecia flattened-hemispherical, 1-4 apothecia per verrucum and contorted, constricted at the base, 0.5-1.6 mm. diameter. Ostioles black, conspicuous, protruding, solitary, sometimes fused and sunken in central concave apothecia, 1-6 per apothecia. Asci amyloid with distinctive ocular chambers, hymenium non-amyloid. Ascospores (2)-3-(4) per ascus, ellipsoid, smooth, 44-54 µm wide, 100-156 µm long, striated thick-wall, 10-14 µm.

Chemistry: K+ y, C+ rose red (transient), KC+ rose red, Pd-, UV+ reddish-orange; 4,5-dichlorolichexanthone (minor), 4-*O*-demethylplanaic acid (major), 2'-*O*- methylanziaic acid (minor).

Additional specimens examined (Paratypes)—**Thailand: Lampang province**, Mueang Bahn district, Jae Sawn National park, on mountain ridge, opposite a waterfall, primary, evergreen, seasonal, hardwood forest, on bark of Fagaceae, 900 m, Jariangprasert 3223.1, 6 November 2002 (QBG).; **Chiang Mai province**, Chiang Dao district, Doi Chiang Dao National Park, 680 m, on bark of *Shorea obtusa* Wall. ex Bl. (Dipterocapaceae), Jariangprasert 4180, 3 December 2002 (QBG).

Notes: *Pertusaria khuntanensis* (Figure 1B) is characterised by (2)-3-(4) smooth ascospores per ascus and the presence of 4,5-dichlorolichexanthone, 4-*O*-demethylplanaic acid and 2'-*O*-methylanziaic acid. 4-*O*-Demethylplanaic acid has not previously been reported in *Pertusaria*. It was reported in *Lecidea lithophila* (Ach.) Ach. and *L. plana* (Lahm in Körb.) Nyl. [9]. *Pertusaria khuntanensis* Jariang. and *P. phusoidaoensis* Jariang. [3] contain 2'-*O*-methylanziaic acid but *P. phusoidaoensis* lacks 4-*O*- demethylplanaic acid. The subtuberculate thallus surface and contorted, centrally sunken apothecia resemble those of *P. parameeana* Jariang. and *P. phusoidaoensis* Jariang. However, they differ chemically; *P. parameeana* Jariang. contains 4,5-dichlorolichexanthone and 2-*O*-methylperlatolic acid [2].

Pertusaria pertusella Müll. Arg. var. *sorediata* Jariang. *sp. nov.*

a var. ***pertusella*** *sed sorediata*

Type: **Thailand**, **Tak province**, Mueang district, Mae Taw subdistrict, Lansang National Park, between Tak province and Mae Sod district, on the way to Musoe Dam and Musoe Lhueang Agricultural Station, on a tree bark, 980 m, on mountain ridge adjacent to deciduous hardwood and bamboo forest of Phadaeng Sanctuary Unit, Jariangprasert 3760, 20 November 2002; holotype: QBG.

Etymology: The varietal name is derived from the presence of soredia.

Morphology and anatomy: Thallus grayish-green, corticolous, surface cracked and verrucose, sorediate, lacking isidia. Soralia conspicuous, concolorous with the thallus, scattered, hemispherical, 0.2-0.6 mm diameter. Apothecia verruciform, conspicuous, hemispherical, not constricted at the base, solitary, 0.3-0.7 mm diameter. Ostioles black, conspicuous, surrounded with grey translucent tissue or cortex. Ascospores 2 per ascus, fusiform, smooth, 140-168 µm long, 32-40 µm wide.

Chemistry: 2,4-dichlorolichexanthone (major), 2,5-dichlorolichexanthone (major), 2,4,5-trichlorolichexanthone (minor), 2-chlorolichexanthone (major), stictic acid (minor).

Additional specimens examined—Thailand:: **Tak province**, Mueang district, Mae Taw subdistrict, Lansang National Park, between Tak province and Mae Sod district, on the way to Musoe Dam and Musoe Lhueang Agricultural Station, on a tree bark, 980 m., on mountain ridge to Phadaeng Sanctuary Unit, Jariangprasert 3831, 3840, 20 November 2002 (RAMK, topotype); **Phetchaburi province**, Kaengkrachan National Park, Kao Pa Noen Tung, at milepost 80, left-hand side before reaching the palace, 1,000 m, on a tree bark in moist montane evergreen forest, Jariangprasert 2533, 12 June 2002 (QBG).

Notes: *Pertusaria pertusella* var. *sorediata* (Figure 1C) is characterised by having 2 smooth ascospores per ascus and the presence of 2,4-dichlorolichexanthone, 2,5-dichlorolichexanthone, 2,4,5-trichlorolichexanthone, 2-chlorolichexanthone and stictic acid. Both the chemistry and the

ascospores of the new variety resemble *P. pertusella* var. *pertusella* from Indian and Nepal, which has no soralia [8, 10]. The chemistry is identical to that of *P. lansangensis* Jariang. & Archer which was found at the same locality, but is differentiated by the smooth ascospores walls, rough in *P. lansangensis* [11]. Mature asci were rarely found. The ascospores are distinguished by the smooth walls and their acute, rather than round, ends as found in most *Pertusaria* species.

Pertusaria phukaensis* Jariang. *sp. nov.

Pertusaria hirtella Singh & Sinha *similis, a qua ascis bisporis et acido norstictico deficienti differt*

Type: **Thailand, Nan province**, Pua district, Phuka National Park, around the head office, on Sterculiaceae tree bark, 1,300 m, Jariangprasert 5512.1, 23 March 2004; holotype: QBG.

Etymology: From the Latin *ensis*, place of origin and *Phuka* National Park.

Morphology and anatomy: Thallus grey-green, corticolous, surface slightly roughened, shining, containing tiny crystals, isidia and soredia absent. Apothecia verruciform, conspicuous, concolorous with the thallus, irregularly hemispherical, not constricted at base, solitary or sometimes 2-3 confluent, 0.5-1.0 mm diameter. Ostioles large, black, conspicuous, surrounded by grey tissue, level with the apothecia surface, 1-4 per apothecium. Hymenium densely interspersed with numerous oil droplets. Ascospores (2-)3-4(-5-6) per ascus, ellipsoid, ascospores smooth, 88-104 µm long, 32-40 µm wide.

Chemistry: atranorin (major).

Notes*: Pertusaria phukaensis* (Figure 1D) is characterised by having large, black ostioles, verruciform apothecia with 3-4 smooth ascospores per ascus, and the presence of atranorin as the only lichen compound detected. *Pertusaria* taxa containing only atranorin are uncommon. This compound usually occurs with orcinol *p*-depsides, e.g. perlatolic acid in *P. granulata* (Ach.) Müll. Arg. [12], with both confluentic acid and perlatolic acid in *P. indica* Srivastawa & Awasthi [13], and with confluentic acid in *P. gorokorana* Elix & Archer [14]. At present this new species is known only from the type specimen.

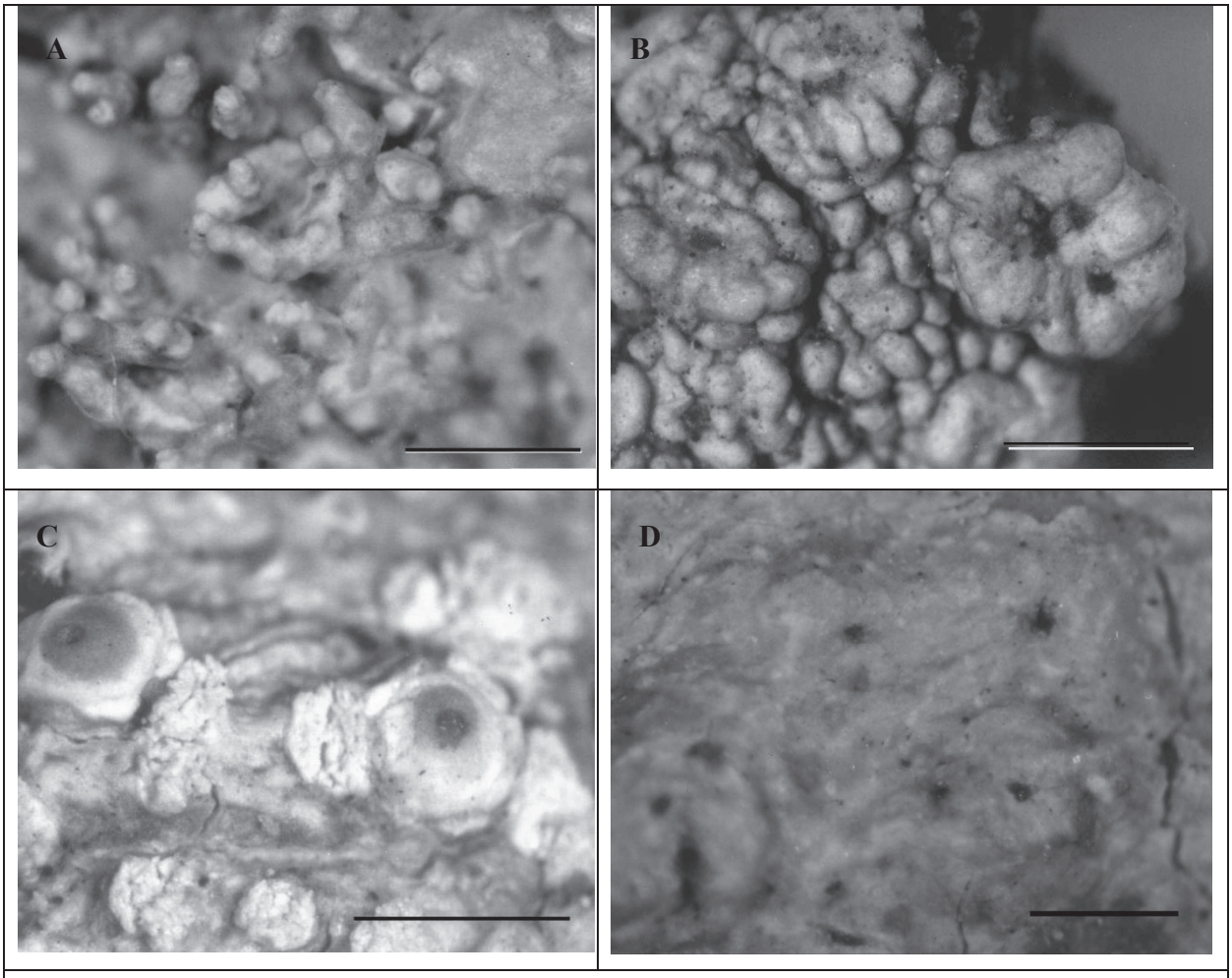

Figure 1. (A) *Pertusaria flavodigitata* Jariang. (holotype in QBG); (B) *P. khuntanensis* Jariang. (holotype in BM); (C) *P. pertusella* Müll. Arg. var. *sorediata* Jariang. (holotype in QBG); (D) *P. phukaensis* Jariang. (holotype in QBG). Scale bar = 1.0 mm

KEY TO TAXA OF *PERTUSARIA* IN THAILAND

1. Apothecia absent, thallus isidiate or sorediate **……2**
2. Thallus isidiate **……GROUP A**
2. Thallus sorediate **……GROUP B**
1. Apothecia present, thallus rarely isidiate or sorediate **……3**
3. Apothecia disciform **……GROUP C**
3. Apothecia verruciform **……4**
4. Ascospore walls rough **……GROUP D**
4. Ascospore walls smooth **……5**
5. Ascospores 2-3 (rarely 4) per ascus **……GROUP E**
5. Ascospores 4 or 8 per ascus **……6**
6. Ascospores 4 per ascus **……GROUP F**
6. Ascospores 8 per ascus **……7**

7. Ascospores uniseriate **…..…….....GROUP G**
7. Ascospores irregularly biseriate **....…….....GROUP H**

Group A: thalli isidiate

1. Thallus UV+ xanthones present**...……..……..……2**
2. Thallus UV+ yellow, lichexanthone and stictic acid present**……....*P. flavodigitata*** Jariang.
2. Thallus UV+ orange, 4,5-dichlorolichexanthone present **……..……..……..3**
3. 2′-*O*-Methylperlatolic acid present **…….……...…..*P. pilosula*** Archer & Elix
3. 2′-*O*-Methylperlatolic acid absent **…….……..……...…...4**
4. Skyrin and methyl barbatate present **...…….……....*P. montpittensis*** Archer
4. Skyrin and methyl barbatate absent**.……...……*P. angabangensis*** Archer & Elix
1. Thallus UV-, xanthones absent **……..…….……..……....…...5**
5. Stictic acid present **..……...……..……...……..……...6**
6. 2′-*O*-Methylperlatolic acid present**.……..*P. pilosula*** Archer & Elix var**. *abditiva*** Jariang.
6. 2′-*O*-Methylperlatolic acid absent **...……..……..……...……..……7**
7. Hypostictic acid present **...……..…*P. hypostictica*** Jariang.
7. Hypostictic acid absent **……..……...……*P. muricata*** David
5. Stictic acid absent **……...……...…...……..…….……8**
8. Isidia K+ red, norstictic acid present **...…….....*P. ramulifera*** Magn.
8. Isidia K-, norstictic acid absent **...…..……....……..…9**
9. Thallus Pd+ orange, protocetraric acid present**……...…..*P. umbricola*** Archer & Elix
9. Thallus Pd+ yellow, psoromic acid present**.……....*P. wauensis*** Elix & Archer

Group B: thalli sorediate

1. Thallus UV-, xanthones absent **……..……..…..…..…….....2**
2. Lichen chemical substances absent**.....*P. albescens*** (Huds.) Choisy & Wern.
2. Lichen substances present **.....3**
3. Soralia KC+ red purple, picrolichenic acid present **…….……*P. amara*** (Ach.) Nyl.
3. Soralia KC-, picrolichenic acid absent **……..……...……...……4**
4. Thallus Pd+ yellow, psoromic acid present**……...*P. psoromica*** Archer & Elix
4. Thallus Pd-, psoromic acid absent **……....……..……...…5**
5. Soralia K+purple, hypothamnolic acid present**.……....*P. bengalensis*** Vain.
5. Soralia K-, 2′-*O*-methylperlatolic acid present**.……..…..*P. uttaraditensis*** Jariang.
1. Thallus UV+ yellow or orange, xanthones present **...……..……...…..……6**
6. Thallus UV+ yellow, lichexanthone present **...……..……...……7**
7. Soralia K+ yellow, *β*-orcinol depsides present **...……...……..……..8**
8. Haemathamnolic acid present**.……...……...…*P. moreliensis*** Lesd.
8. Thamnolic acid present**..……..……*P. scaberula*** Archer
7. Soralia K-, confluentic acid present**.....*P. confluentica*** Jariang.
6. Thallus UV+ orange, di-and trichloroxanthones present with stictic acid**..*P. puffina*** Archer & Elix

Group C: apothecia disciform

1. Thallus UV-, lichexanthone absent **……...……..……...……..……...2**
2. Thallus without lichen secondary metabolites **..……...……..…..……3**

3. Apothecia fertile, fatty acids present……..…….…....***P. ophthalmiza*** (Nyl.) Nyl.
3. Apothecia rarely fertile, fatty acids absent.....….***P. albescens*** (Huds.) Choisy & Wern.
2. Thallus with lichen secondary metabolites ..……...……...……..….**4**
4. Thallus K+ red, norstictic acid present ……...……...……..……**5**
5. Thallus corticolous, ascospores 2 per ascus..……..……...…...***P. asiana*** Vain.
5. Thallus saxicolous, ascospores unknown .....***P. erubescens*** (Hook. f. & Tayl.) Nyl.
4. Thallus K- or K+ yellow, norstictic acid absent ..……..……..…...……..…**6**
6. Thallus C+ rose-pink, lecanoric acid present..……..……..***P. velata*** (Turner) Nyl.
6. Thallus C-, lecanoric acid absent …..……..……..……..……**7**
7. Thallus KC-, picrolichenic acid absent, thamnolic acid present….***P. scutellifera*** Archer & Elix
7. Thallus KC+ purple, picrolichenic acid present, thamnolic acid absent.....***P. patellifera*** Archer
1. Thallus UV+ yellow, lichexanthone present ……..……..…**8**
8. Lichexanthone only present …..……...…...***P. asterella*** Aptroot
8. Lichexanthone and other compounds present ..……...……..……**9**
9. Thallus K+ purple, hypothamnolic acid present .....…….……...…***P. tropica*** Vain.
9. Thallus K- or K+ yellow, hypothamnolic acid absent .....…….**10**
10. Thallus KC+ purple, picrolichenic acid present with derivatives.....…..**11**
11. Thamnolic acid present .....……..……..….***P. subventosa*** Malme
11. Thamnolic acid absent……...***P. clarkeana*** Archer
10. Thallus KC-, picrolichenic acid absent ……...……**12**
12. Thallus K-, Pd-, squamatic acid present……..... ***P. xantholeuca*** Müll. Arg.
12. Thallus K+ yellow, Pd+ orange, squamatic acid absent ……..……..…**13**
13. Haemathamnolic acid present……..……..***P. commutata*** Müll. Arg.
13. Thamnolic acid present…….....……..……***P. miscella*** Archer

Group D: ascospore walls rough

1. Thallus not isidiate or sorediate ……...……...……..……..**2**
2. Thallus UV+ yellow, lichexanthone present...***P. tetrathalamia*** (Fee) Nyl. var***. plicatula*** Müll. Arg.
2. Thallus UV- or UV+ orange, lichexanthone absent ..……..……..……..…...**3**
3. Thallus UV-, xanthones absent ……...……..……..……..….**4**
4. Thallus K+ red, norstictic acid present with barbatic and divaricatic acids …….***P. allothwaitesii*** Jariang. & Archer
4. Thallus K+ yellow, stictic acid present ……..***P. cicatricosa*** Müll. Arg. var***. deficiens*** Archer & Streimann
3. Thallus UV+orange, xanthones present ……..……..……..……..**5**
5. Orcinol *para*-depsides present ..……...……..……...……..……**6**
6. Thallus K-, stictic acid absent ……..….***P. litchicola*** Jariang. & Archer
6. Thallus K+ yellow, stictic acid present..……..…….***P. pallida*** Archer & Elix
5. Orcinol *para*-depsides absent ..……...……...……..……..……..……**7**
7. Protocetraric acid present, stictic acid absent..……....***P. thwaitesii*** Müll. Arg.
7. Protocetraric acid absent, stictic acid present ……...……..……..……..**8**
8.2,4-Dichloro-,2,5-dichloro and 2,4,5-trichloroxanthones present...***P. cicatricosa*** Müll. Arg.

8. 4,5-Dichlorolichexanthone present **……9**

9. Apothecia forming irregular lumps, ostioles black, ascospores dominantly cylindrical, 88-158 x 34-56 μm **…….……*P. tetrathalamia*** (Fée) Nyl.

9. Apothecia solitary, hemispherical, ostioles hyaline, ascospores dominantly ellipsoid, 74-152 x 26-56 μm **……*P. macounii*** (Lamb) Dibben

1. Thallus isidiate or sorediate **……..……..…….10**

10. Thallus isidiate **……..…….11**

11. 2′-*O*- methylperlatolic acid absent**…….....…….*P. takensis*** Jariang. & Archer

11. 2′-*O*- methylperlatolic acid present**…….....*P. microstoma*** Müll. Arg. var. ***isidiata*** Jariang.

10. Thallus sorediate **…..……*P. lansangensis*** Jariang. & Archer

Group E: ascospore walls smooth, 2-3 rarely 4 per ascus

1. Thallus isidiate or sorediate**.....2**

2. Thallus isidiate**.…….……*P. allomicrostoma*** Jariang.

2. Thallus sorediate**.....……*P. pertusella*** Müll. Arg. var. ***sorediata*** Jariang.

1. Thallus not isidiate or sorediate **……..…….……..……3**

3. Thallus without lichen chemical substances**.…….....……*P. subnegans*** Vain.

3. Thallus with lichen chemical substances**…….……..…..……..4**

4. Thallus UV-, xanthones absent **.....5**

5. Thallus K+ red, norstictic acid present**.....……*P. glomerata*** (Ach.) Schaer.

5. Thallus K- or K+ yellow, norstictic acid absent **……..…..……..6**

6. Thallus K+ yellow, stictic acid present **.....……..…….....7**

7. Planaic acid present **.....…….……8**

8. 2′-*O*-Methylperlatolic acid present (with 2-*O*-methylperlatolic acid, planaic acid, methyl 2-*O*-methylperlatolate and methylplanaiate)**…..…..*P. subcopelandii*** Jariang.

8. Methyl 2′-*O*-methylstenosporate present (with 2-*O*-methylperlatolic acid, planaic acid, methyl 2-*O*-methylperlatolate and methyl planaiate)**.....*P. methylstenosporica*** Jariang.

7. Planaic acid absent**…..…….*P. ramuensis*** Archer & Elix

6. Thallus K-, stictic acid absent **……..…….…..…..……9**

9. Confluentic acid present**……..……..*P. orientalis*** Jariang.

9. Confluentic acid absent, 2′-*O*-methylstenosporic acid present with 2′-*O*-methylperlatolic acid, planaic acid, methyl 2-*O*-methylperlatolate and methylplanaiate**.…*P. archeri*** Jariang.

4. Thallus UV+ yellow or orange, xanthones present**…..…….10**

10. Thallus UV+ yellow, lichexanthone present (with confluentic and stictic acids)**……**

…..……..……..*P. inthanonensis* Jariang.

10. Thallus UV+ orange, lichexanthone absent**..…….……..…11**

11. Thallus KC+rose-red, 2'-*O*-methylanziaic acid present**..…..……..12**

12. 4-*O*-demethylplanaic acid present**..……*P. khuntanensis*** Jariang.

12. 4-*O*- demethylplanaic acid absent**…..……..….*P. phusoidaoensis*** Jariang.

11. Thallus K+ or K-, 2'-*O*-methylanziaic acid absent **..……..…….……..……..13**

13. Thallus K+ red or K-, stictic acid absent **..……..…….……14**

14. Thallus K+ red, norstictic acid present (with 4,5-dichloroliche xanthone)**……**

…..…….....*P. neoknightiana* Jariang.

14. Thallus K-, norstictic acid absent **15**

15. Orcinol *para*-depsides absent **16**

16. Dichloro- and trichloroxanthones present...***P. xanthonaria*** Archer & Elix

16. Dichlorolichexanthone only present.....***P. irregularis*** Müll. Arg.

15. Orcinol *para*-depsides present **17**

17. 2-*O*-Methylperlatolic acid present **18**

18. Thallus corticolous.....***P. parameeana*** Jariang.

18. Thallus saxicolous.....***P. nahaeoensis*** Jariang. & Archer

17. 2-*O*-Methylperlatolic acid absent **19**

19. 2,2′-Di-*O*-methylstenosporic acid present with 2′-*O*-methyl stenosporic acid.....***P. subplanaica*** Archer & Elix var. ***tetraspora*** Jariang & Archer

19. 2,2′-Di-*O*-methylstenosporic acid and 2′-*O*-methylstenosporic acid absent planaic acid present.....***P. siamensis*** Jariang.

13. Thallus K+ yellow, stictic acid present **20**

20. Orcinol *para*-depsides present **21**

21. Confluentic acid present.....***P. cinchonae*** Müll. Arg.

21. Confluentic acid absent **22**

22. 2′-*O*-Methylperlatolic acid present (with ±2-chlorolichexanthone, planaic and 2-*O*-methylperlatolic acids, methyl 2′-*O*-methylperlatolate and methylplanaiate).....***P. novaguineae*** Archer & Elix

22. 2-*O*-Methylperlatolic acid present (with 4,5-dichlorolichexanthone)..... ***P. loeiensis*** Jariang.

20. Orcinol *para*-depsides absent.....**23**

23. 4,5-Dichlorlichexanthone present.....**24**

24. Ostioles fused.....***P. pustulata*** (Ach.) Duby

24. Ostioles rarely fused.....***P. pertusa*** (Weigel) Tuck.

23. 2,4-Dichloro-, 2,5-dichloro- and 2,4,5,-trichlorolichexanthone present...**25**

25. Ostioles hyaline, ascospores 2, rarely 3 per ascus...***P. pertusella*** Müll. Arg.

25. Ostioles black, ascospores 3-4, rarely 2 per ascus...***P. ceylonica*** Müll. Arg.

Group F: ascospore walls smooth, 4 per ascus

1. Thallus UV+ yellow, lichexanthone present.....**2**

2. 2,2′-Di-*O*-methylstenosporic acid present..... ***P. alboaspera*** Archer & Elix var. ***tetraspora*** Jariang.

2. 2′-*O*-methylstenosporic acid, 2′-*O*-methyl divaricatic acid, and 2′-*O*-methylperlatolic acid present.....***P. elixii*** Jariang.

1. Thallus UV- or UV+ orange, lichexanthone absent.....**3**

3. Thallus UV-, xanthones absent **4**

4. Thallus K-, stictic acid absent, atranorin present.....***P. phukaensis*** Jariang.

4. Thallus K+ yellow, stictic acid present.....***P. radiata*** Oshio

3. Thallus UV+ orange, xanthones present **5**

5. Orcinol *para*-depsides absent.....**6**

6. Stictic acid present **.....*P. leioplaca*** Sch.

6. Stictic acid absent **.....7**

7. Thiophaninic acid present **.....*P. endochroma*** Müll. Arg.

7. Thiophaninic acid absent**.....*P. nebulosa*** Archer

5. Orcinol *para*-depsides present **.....8**

8. Stictic acid absent **.....*P. kansriae*** Jariang.

8. Stictic acid present **.....9**

9. Planaic acid present**.....*P. bonariensis*** Malme

9. Planaic acid absent **.....10**

10. Ostioles black; 2-*O*-methylperlatolic acid present with 2-chlorolichexanthone, 2-*O*-methylisohyperlatolic, 2-*O*-methylhyperlatolic and 2-*O*-methylsuperlatolic acids**.....*P. follmanniana*** Archer & Elix

10. Ostioles hyaline; 2-*O*-methylperlatolic acid absent; 4,5-dichlorolichexanthone present with 2′-*O*-methylstenosporic, 2′-*O*-methyldivaricatic and 2′-*O*-methylperlatolic acids **.....*P. thailandica*** Jariang.

Group G: ascospores 8 per ascus, uniseriate

1. Thallus UV-, K- or K+, xanthones absent**.....2**

2. Thallus K- ; 2-*O*-methylperlatolic acid present**..... *P. mattogrossensis*** Malme

2. Thallus K+ yellow, stictic acid present**.....3**

3. 2-*O*-Methylsuperlatolic acid present with superlatolic and isohyperlatolic acids**.....*P. krabiensis*** Jariang.

3. 2′-*O*-Methylperlatolic acid present**.....*P. phulhuangensis*** Jariang.

1. Thallus UV+ yellow or orange, xanthones present **.....4**

4. Thallus UV+ yellow, lichexanthone present**.....*P. leucostigma*** Müll. Arg.

4. Thallus UV+ orange, lichexanthone absent **.....5**

5. Ostioles yellow; thiophaninic acid and 2-*O*-methylperlatolic acid present**.....*P. xylophyes*** Archer

5. Ostioles black; thiophaninic acid absent; 4,5-dichlorolichexanthone, 2,2′-di-*O*-methylstenosporic, 2′-*O*-methylperlatolic, 2′-*O*-methylstenosporic, planaic and 2,2′-di-*O*-methyldivaricatic acids present**.....*P. subplanaica*** Archer & Elix

Group H: ascospores 8 per ascus, irregularly uniseriate-biseriate

1. Thallus lacking lichen chemical substances**.....*P. subrigida*** Müll. Arg.

1. Thallus containing lichen chemical substances**.....2**

2. Thallus UV-, xanthones absent **.....3**

3. Thallus K+ red, norstictic acid present**.....*P. norstictica*** Archer

3. Thallus K- or K+ yellow, norstictic acid absent, stictic and 2,2′-di-*O*-methylstenosporic acids present**.....*P. alboaspera*** Archer & Elix var. ***disflavens*** Jariang.

2. Thallus UV+ yellow or orange, xanthones present **.....4**

4. Thallus UV+ yellow, lichexanthone present **.....5**

5. Orcinol *para*-depsides absent **.....*P. phaeostoma*** Müll. Arg.

5. Orcinol *para*-depsides present **.....6**

6. Thallus K-, stictic acid absent **.....7**

7. Protocetraric acid present **.....….*P. nanensis*** Jariang. & Archer
7. 2′-*O*-Methylstenosporic acid present**....*P. alboaspera*** Archer & Elix var. *deficiens* Jariang.
6. Thallus K+ yellow, stictic acid present **……..…….8**
8. 2,2′-Di-*O*-methylstenosporic acid present**.....….*P. alboaspera*** Archer & Elix
8. 2′-*O*-Methylstenosporic present**....…….…....*P. platycarpa*** Jariang.
4. Thallus UV+ orange, lichexanthone absent **……..……..……..…...…..9**
9. Thiophaninic acid present **……..……..……...……..…….10**
10. Stictic acid absent **..……..……...……11**
11. Thallus saxicolous**……...*P. petrophyes*** Knight
11. Thallus corticolous**.....…..….....….*P. thiophaninica*** Archer
10. Stictic acid present **……..……..……..……...12**
12. Orcinol *para*-depsides present **……..……..…13**
13. 2,2′-Di-*O*-methylstenosporic, planaic and isoplacodiolic acids present**……..**
...……..…*P. omkoiensis* Jariang. & Archer
13. Perlatolic and hyperlatolic acids present**……..*P. hylocola*** Jariang. & Archer
12. Orcinol *para*-depsides absent**……..…….14**
14. Depsides present (4-*O*-methylisocryptochlorophaeic acid) **……...**
……..….*P. paradoxica* Archer & Elix
14. Depsides absent**……..……..……..…….15**
15. Hypostictic acid absent**……..……..*P. texana*** Müll. Arg.
15. Hypostictic acid present**……..……..…….*P. leioplacella*** Nyl.
9. Thiophaninic acid absent **……..……..……..……..……..……...16**
16. 4,5-Dichlorolichexanthone absent **...……..……..……..……...…17**
17. Stictic acid absent **……..……...……..…18**
18. Divaricatic acid, 2-chlorolichexanthone, methyl 2,2′-di-*O*-methyl divaricatate and methyl 2-*O*-methyldivaricatate present**...…..*P. orarensis*** Archer & Elix
18. Arthothelin, 6-*O*-methylarthothelin, di- and trichlorinated norlichexanthones present **……..…….*P. howeana*** Archer & Elix
17. Stictic acid present**……..……..……..…..……..19**
19. Di- and trichloro xanthones present**…….....*P. lordhowensis*** Archer & Elix
19. 2-Chlorolichexanthone present**..……..……*P. limbata*** Vain.
16. 4,5-Dichlorolichexanthone present **……..……..……..……...20**
20. Stictic acid absent **……..……...……..21**
21. Orcinol *para*-depsides absent **.....….....*P. mundula*** Müll. Arg.
21. Orcinol *para*-depsides present**.....22**
22. 2,2′-Di-*O*-methylstenosporic acid present**…....*P. bokluensis*** Jariang.
22. 2′-*O*-Methylperlatolic acid present**.....……*P. gibberosa*** Müll. Arg.
20. Stictic acid present **……..……..……...23**
23. Ostioles black**……..……*P. sommerfeltii*** Flk.
23. Ostioles not black **...……...……..……24**
24. Orcinol *para*-depsides absent **.....25**

25. Ostioles protruding, ascospores 72-92 x 32-40 µm**…….....*P. leiocarpella*** Müll. Arg.

25. Ostioles surrounded with hyaline tissue, ascospores 90-114 x 28-36 µm

……..……..……..…….....*P. stenostoma* Vain.

24. Orcinol *para*-depsides present **.....26**

26. 2,2′-Di-*O*-methylstenosporic acid present with 2,2′-di-*O*-methyldivaricatic, 2′-*O*-methylstenosporic, planaic acids and 2′-*O*-methylstenosporate**……..**

……..….*P. subplanaica* Archer & Elix var. ***stictica*** Jariang.

26. 2,2′-Di-*O*-methylstenosporic acid present; 2,2′-di-*O*-methyldivaricatic, methyl 2′-*O*-methylstenosporic, planaic acids and methyl 2′-*O*-methylstenosporate absent**.....*P. kansriae*** Jariang. var. ***stictica*** Jariang.

ACKNOWLEDGEMENTS

I would like to express my thanks to Prof. J. A. Elix (Australian National University) for the high performance liquid chromatography results and editorial assistance, and Dr. A. W. Archer (National Herbarium of New South Wales) and Prof. K. Kalb (Lichenologisches Institut Neumarkt, Germany) for editorial assistance. The Biotechnology Programme, Faculty of Science, Maejo University is thanked for the use of the laboratories and equipment.

REFERENCES

1. S. Jariangprasert, "Taxonomy and ecology of the lichen family Pertusariacae in Thailand**"**, *PhD Thesis*, **2005**, Chiang Mai University, Thailand.
2. S. Jariangprasert, "New taxa of the lichen genus *Pertusaria* (Ascomycota) from Thailand", *Mycotaxon***, 2006**, *96*, 109-121.
3. J. A. Elix, S. Jariangprasert and A. W. Archer, "New *Pertusaria* (lichenized Ascomycota) from Australia and Thailand", *Telopea,* **2008**, *12,* 263-272.
4. F. J. White and P. W James, "A new guide to the microchemical techniques for the identification of lichen substances", *Brit. Lichen Soc. Bull.*, **1985**, No. *57*.
5. J. A. Elix and K. D. Ernst-Russell, "A Catalogue of Standardized Thin Layer Chromatographic Data and Biosynthetic Relationships for Lichen Substances", Australian National University, Canberra, **1993**.
6. J. A. Elix, M. Giralt and J. H. Wardlaw, "New chloro-deosides from the lichen *Dilemelaenaradiata*", *Biblio. Lichenol.*, **2003,** Band *86*.
7. G. B. Feige, H. T. Lumbsch and J. A. Elix, "The identification of the lichen substances by a standardized high-performance liquid chromatography method", *J. Chromatog.*, **1993,** *646*, 417-427.
8. A. W. Archer, "New species and new reports of *Pertusaria* (lichenised Ascomycotina) from Australia and New Zealand with a key to the species in Australia", *Mycotaxon,* **1991,** *41*, 223-269.
9. C. F. Culberson and H. Hertel, "Chemical and morphological analysis of the *Lecidea lithophila* –plana group (Lecideaceae)", *Bryologist*, **1979**, *82*, 189-197.
10. A. W. Archer, "Additional new species and new reports of *Pertusaria* (lichenised Ascomycotina) from Australia", *Mycotaxon*, **1992**, *44*, 13-20.

11. S. Jariangprasert, A. W. Archer and V. Anusarnsunthorn, "Further new species in the genus *Pertusaria* (lichenized Ascomycota) from Thailand", *Mycotaxon,* **2004,** *89*, 123-129.
12. D. D. Awasthi, "A key to the microlichens of India, Nepal and Sri Lanka", *Biblio. Lichenol.*, **1991,** Band *40*.
13. D. D. Awasthi and P. Srivastava, "New species of *Pertusaria* (lichenized fungi) from India", *Bryologist***, 1993,** *96*, 210-215.
14. J. A. Elix, A. Aptroot and A. W. Archer, "The lichen genus *Pertusaria* (lichenised Ascomycotina) in Papua New Guinea and Australia: Twelve new species and thirteen new reports", *Mycotaxon***, 1997**, *64*, 17-35.

Maejo International Journal of Science and Technology

ISSN 1905-7873
Available online at www.mijst.mju.ac.th

Full Paper

Effect of organic fertiliser residues from rice production on nitrogen fixation of soya (*Glycine max* L. Merrill), Chiang Mai 60 variety

Nattida Luangmaka*, Somchai Ongprasert and Jiraporn Inthasan

Division of Soil Resources and Environment, Faculty of Agricultural Production, Maejo University, Chiang Mai 50290, Thailand

*Corresponding author, e-mail: l_pucca31@hotmail.com

Received: 18 February 2013 / Accepted: 23 September 2013/ Published: 23 September 2013

Abstract: A field study was undertaken on the residual effect of organic fertilisers applied to the preceding rice cropping on nitrogen fixation of soya in a rice-soya cropping system. The experiment was conducted on a farmer's lowland paddy in Mae Rim district, Chiang Mai province, Thailand. Organic fertiliser treatments assigned were: 1) control (no fertiliser), 2) animal manure of cattle (AM), 3) compost (CP), 4) azolla (AZ), 5) AM + CP, 6) AM + AZ, 7) CP + AZ and 8) AM + CP + AZ. Soya seeds were planted without rhizobial inoculation in December 2011, four months after the application of organic fertilisers. Nodule weight, total shoot nitrogen accumulation and relative ureide index at various growth stages were recorded as the indices of nitrogen fixation. Results of the study demonstrate that the residues from the application the organic fertilisers of narrow C/N ratios during the land preparation for rice cropping four months before soya cultivation promoted nitrogen fixation by native rhizobia.

Keyword: soya, nitrogen fixation, ureides, organic fertiliser residue

INTRODUCTION

Soya planted areas in Thailand declined from 480 to 93 thousand hectares, reducing output from 0.63 to 0.15 million tons during 1989-2012 [1]. The domestic production was therefore far below the domestic feed and soya bean oil industry demand. Approximately, one half of soya bean production is produced from paddy rice - soya cropping system. However, the soya bean production from such paddy-based production system has been dramatically waning due to better economic returns from rice-rice and rice-corn cropping systems as a result of the government's price intervention in rice and corn markets. To maximise the yields of rice and corn, farmers have used chemical fertilisers more intensively and this may lead to unsustainability of the

systems. On the other hand, organic rice-soya production system in which organic fertilisers are applied during land preparation for rice cropping has been promoted by many parties. The indirect benefit from such practice of enhancing nitrogen fixation in soya cropping is expected besides the direct benefit in giving nutrients for rice. This experiment is aimed at studying the benefit from the residue of organic fertiliser application in paddy rice cropping of enhancing nitrogen fixation of soya grown after rice as there is still no definite conclusion as to the extent of the fixation occurring in this system.

MATERIALS AND METHODS

The on-farm experiment was conducted at lowland paddy fields of a farmer at Mae Rim district, about 35 km north of Chiang Mai city. Soya (var. Chiang Mai 60 from Chiang Mai Field Crop Research Centre, Chiang Mai) was grown without rhizobial inoculation as a second crop after paddy rice during December 2011 - April 2012. Organic fertilisers of narrow C:N ratios were applied: 1) control (no fertiliser), 2) animal manure (AM): 6.25 tons ha^{-1}, 3) compost (CP): 6.25 tons ha^{-1}, 4) azolla (AZ): 12.5 tons ha^{-1}, 5) AM + CP: 3.125 + 3.125 tons ha^{-1}, 6) AM + AZ : 3.125 + 12.5 tons ha^{-1}, 7) CP + AZ : 3.125 + 12.5 tons ha^{-1}, and 8) AM + CP + AZ: 3.125 +3.125 + 12.5 tons ha^{-1}. All organic fertilisers were applied during land preparation for rice transplanting in July 2011. Their compositions were reported as follows: 1.82%N, 0.82%P, 0.43%K, 1.82%Ca and 0.56%Mg (AM); 1.09%N, 0.48%P, 1.2%K, 2.20%Ca and 0.17%Mg (CP); 3.52%N, 0.27%P, 1.19%K, 1.77%Ca and 2.81%Mg (AZ). The experimental design was a randomised complete block with 4 replications. Each experimental unit of soya was grown in a 4 x 4 m plot with 25 x 25 cm plant spacing. Fallow irrigation technique was managed during soya cultivation. Root sap samples were collected (10 plants/sample) by plastic syringe and transferred into a glass tube with 95% ethanol at 1:1 ratio. The stages at which the sap samples were collected were: V4 (vegetative growh stage, fourth node), R2 (full bloom), R4 (full pod) and R6 (full seed). All the xylem sap samples were kept at -4^{o}C until analysis [2]. The samples were analysed for ureide-N, nitrate-N and amino-N by ureide technique and the relative ureide index (%RUI) was calculated from the molar concentration of ureide, amino and nitrate using the following equation [3, 4]:

$$\%\ RUI = \left[\frac{4 \times Ureide}{4 \times Ureide + Amino + Nitrate} \right] X\ 100$$

Nitrogen fixation (Nfix) was calculated from %RUI using the following equations [3, 4]:

a) %Nfix = 7.7+0.64%RUI for V1-V5 stages
b) %Nfix = 4.8+ 0.83%RUI for R1-R2 stages
c) %Nfix = 21.3+ 0.67%RUI for R3-R6 stages

Shoot and nodule samples were also collected at V4, R2, R4 and R6 stages. All plant samples were oven-dried at 70-73^{o}C for 48 hours and weighed. The nitrogen content in shoot was determined by Kjeldahl digestion and distillation method [5]. Total nitrogen accumulations in shoot at various growth stages were then calculated [5]. Nitrogen uptake from soil was the difference between nitrogen accumulated and nitrogen fixed at R6 stage.

RESULTS AND DISCUSSION

Nodule Dry Weight

The nodule dry weight of soya was lowest in the control treatment with 58, 87, 168 and 143 mg plant^{-1} at V4, R2, R4 and R6 respectively ($P<0.05$) (Table 1). At V4 stage, the CP and AZ applications provided the highest nodule dry weight at 104 mg plant^{-1}. Generally, the AZ treatment gave higher nodule dry weight than other treatments ($P<0.05$). Interestingly, at the R4 and R6 growth stages, the nodule mass observed in AM+AZ treatment was at 235 and 212 mg plant^{-1} respectively. The effect of organic fertiliser residue in this experiment is comparable to the former results (117-270 mg plant^{-1}) at V5-R6 stages based on nodule dry weight of the same variety [6]. Other experiments, however, reported nodule dry weight as varying with soya cultivar and environmental conditions [7-9]. From the present experiment, addition of AZ in paddy rice field resulted in the highest nodule dry weight of soya compared to other treatments. This is consistent with a report on rice experiment that showed high organic matter with a high-rate application of AZ [10].

Table 1. Soya nodule dry weight (mg plant^{-1}) at different stages of growth

Treatment	V4	R2	R4	R6
Control	58^{d}	87^{b}	168^{c}	143^{d}
AM	82^{c}	121^{a}	169^{c}	145^{d}
CP	62^{d}	120^{a}	169^{c}	146^{d}
AZ	60^{d}	126^{a}	213^{b}	178^{c}
AM+CP	93^{b}	121^{a}	231^{a}	200^{b}
AM+AZ	84^{c}	123^{a}	235^{a}	212^{a}
CP+AZ	104^{a}	124^{a}	234^{a}	211^{a}
AM+CP+AZ	76^{c}	124^{a}	232^{a}	211^{a}
CV (%)	7.0	3.6	2.3	4.0
F-test	0.05	0.01	0.01	0.05

Note: Means with different letters in each column are significantly different.

Relative Ureide Index

The %RUI was affected most by both AZ and CP+AZ applications at R2, R4 and R6 stages. The data in Table 2 shows that the values of %RUI at V4, R2 and R4 stages were highest at 61, 87 and 82% respectively ($P<0.05$) when CP+AZ was applied. However, the %RUI in CP+AZ treatment was not significantly different from AZ application (86% and 82% at R2 and R4 respectively). At R6 stage, AZ at 12.5 tons ha^{-1} gave the highest %RUI (76%, $P<0.01$). The control treatment gave the lowest % RUI at all growth stages.

Total Shoot Nitrogen Accumulation

The content of shoot N uptake of soya appeared to be associated with shoot dry weight (Table 3). The lowest shoot N uptake was found in the control at every stage of growth. Application of AM+CP+AZ gave the highest shoot N uptake at V4, R2 and R4 stages while at R6 stage, the highest shoot N uptake (85 kg N ha^{-1}) was recorded on applying AZ at a rate of 12.5

tons ha^{-1}. In general, the total shoot N-uptake is substantially increased with the use of various organic fertilisers [11-13].

Table 2. %RUI of soya at different stages of growth

Treatment	V4	R2	R4	R6
Control	38^{d}	77^{b}	61^{c}	44^{d}
AM	56^{ab}	85^{a}	73^{b}	63^{bc}
CP	44^{cd}	86^{a}	78^{ab}	53^{cd}
AZ	45^{cd}	86^{a}	82^{a}	76^{a}
AM+CP	59^{a}	85^{a}	81^{a}	64^{bc}
AM+AZ	56^{ab}	84^{a}	79^{ab}	66^{ab}
CP+AZ	61^{a}	87^{a}	82^{a}	64^{bc}
AM+CP+AZ	49^{bc}	85^{a}	80^{a}	67^{ab}
CV (%)	8.4	1.5	3.4	7.4
F-test	0.01	0.01	0.05	0.05

Note: Means with different letters in each column are significantly different.

Table 3. Nitrogen accumulation (kg ha^{-1}) in soya at different stages of growth

Treatment	V4	R2	R4	R6
Control	23^{d}	29^{c}	36^{e}	48^{d}
AM	35^{c}	42^{b}	51^{d}	80^{a}
CP	35^{c}	42^{b}	50^{d}	63^{bc}
AZ	40^{ab}	46^{a}	55^{bc}	85^{a}
AM+CP	37^{bc}	42^{b}	53^{cd}	66^{b}
AM+AZ	37^{bc}	40^{b}	55^{bc}	60^{c}
CP+AZ	40^{ab}	47^{a}	58^{b}	63^{bc}
AM+CP+AZ	42^{a}	47^{a}	61^{a}	68^{b}
CV (%)	7.4	5.2	4.9	5.8
F-test	0.05	0.05	0.05	0.05

Note: Means with different letters in each column are significantly different.

Nitrogen Fixation and Nitrogen Uptake from Soil

All organic residues from organic paddy rice had a significant effect on nitrogen fixation (Figure 1) which was highest for AZ (53.9 kg N ha^{-1}). Compatible with other data, the control treatment provided the lowest nitrogen fixation at only 17.5 kg N ha^{-1} ($P<0.05$). Soil nitrogen uptake was determined by total plant nitrogen accumulated minus fixed nitrogen. AM gave the highest amount of nitrogen uptake from soil (32.2 kg ha^{-1}) but there was no significant level between control, CP and AM treatments. CP + AZ treatment gave the lowest amount of nitrogen uptake from soil ($P<0.05$).

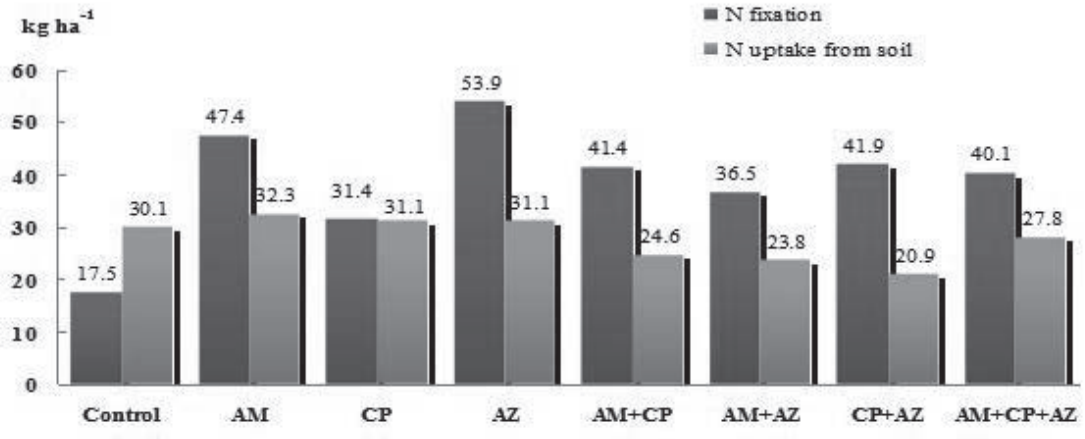

Figure 1. Nitrogen fixation and nitrogen uptake from soil (kg ha^{-1})

The amount of nitrogen uptake appeared to correspond with %RUI, which peaked at R2 stage and then slightly decreased at R4 and R6 stages. Generally, %RUI is high during the stage of flowering to the beginning of seed production [4, 11, 14]. AZ application in paddy rice field was observed to contribute to the highest nitrogen fixation in soya grown after paddy rice. Other organic fertilisers also provided higher nitrogen fixation than did control treatment. This result is supported by research work which reported high levels of nitrogen fixation when soya was grown in conditions without chemical fertilisers or with inoculated rhizobium strains [6, 11-13]. The extent of nitrogen fixation in the present experiment (17.5-53.9 kgN ha^{-1}), however, was less than that obtained in temperate areas (100 kgN ha^{-1}) [15], which may be attributable to the difference in physical and environmental conditions between the temperate and tropical zones.

All of the organic matter used in this experiment had a C:N ratio of less than 24:1, comparable to those used in other studies [16-17]. The C:N ratio can affect the microbial activity in the decomposition of organic matter and mineralisation process [17-18]. Organic fertilisers such as cow manure, hay, compost and azolla were shown to have high concentrations of Cd, Zn, Ni, Fe, Mo and Cr [19-21]. The availability of some elements such as Fe, Mo and Ni could suggest high nitrogen fixation, nodulation forming and seed yield [22-24].

The average efficiency of nitrogen fixation was 57.4% (Table 4). CP +AZ gave the highest efficiency at 67.0%, although this was not significantly different from the AZ treatment. However, all organic fertiliser applications gave an efficiency of at least 50%, which was higher than that obtained in control treatment. The residues from the organic fertilisers could enhance the activity of endophytic bacteria and the rhizobium population around the rhizosphere zone between rice and soya [25]. Table 5 shows soya seed yields subsequently obtained. Apparently, the control treatment provided the lowest yield level and the addition of all organic fertilisers proved to enhance the soya seed yield, with AM+CP+AZ giving the highest yield (1,463 kg ha^{-1}). The average yield was 1,310 kg ha^{-1}, which was coparable to one at 1,656 kg ha^{-1} obtained in a former study performed in the same district in 1999 to increase the efficiency of soya production with chemical fertilisers on the same variety [26].

Table 4. Nitrogen fixing efficiency of soya (% of total N uptake at R6 stage)

Treatment	N fixing efficiency
Control	36.8 %
AM	59.5 %
CP	50.2 %
AZ	63.5 %
AM+CP	62.7 %
AM+AZ	60.6 %
CP+AZ	67.0 %
AM+CP+AZ	59.0 %

Table 5. Soya seed yield (kg ha^{-1})

Treatment	Yield (kg ha^{-1})
Control	981^{b}
AM	1294^{a}
CP	1225^{ab}
AZ	1331^{a}
AM+CP	1256^{a}
AM+AZ	1238^{ab}
CP+AZ	1369^{a}
AM+CP+AZ	1463^{a}
CV (%)	10.61
F-test	0.01

Note: Means with different letters in each column are significantly different.

CONCLUSIONS

The application of organic fertilisers before paddy rice land preparation significantly enhanced the relative ureide index and nitrogen uptake of the following soya crop at all studied stages. The advantage came from high microbial nitrogen fixation compared to control as shown in the R6 stage. The residues from the application of organic fertilisers of narrow C:N ratios during land preparation for rice cropping four months before growing soya thus clearly promote nitrogen fixation by native rhizobia. Application of organic fertilisers such as animal manure, compost, azolla or their combinations is therefore confirmed and suggested as a good practice of sustainable management of rice-soya cropping system in lowland paddies.

ACKNOWLEDGEMENTS

The financial support for this work from the National Research Council of Thailand (NRCT) is gratefully acknowledged.

REFERENCES

1. Department of Agricultural Extension, "Soybean 2555" (in Thai), http://www.agriman.doae.go.th/home/ news/Year%202012/034_ Soybean.pdf (Accessed: September 2012).
2. W. R. Fehr, C. E. Caviness, D. T. Burmood and J. S. Pennington, "Stages of development descriptions for soybeans, Glycine max (L.) Merrill", *Crop Sci.,* **1971**, *11*, 929-931.
3. M. B. Peoples, A. W. Faizah, B. Rerkasem and D. F. Herridge, "Methods for Evaluating Nitrogen Fixation by Nodulated Legumes in the Field", Australian Centre for International Agricultural Research (ACIAR), Canberra, **1989**.
4. D. F. Herridge and M. B. Peoples, "Uride assay for measuring nitrogen fixation by nodulated soya calibrated by ^{15}N methods", *Plant Physiol*., **1990**, *93,* 495-503.
5. J. E. Lepo and S. M. Ferrenbach, "Measurement of nitrogen fixation by direct means", in "Methods for Evaluating Biological Nitrogen Fixation" (Ed. F. J. Bergersen), Jonhn Wiley & Sons, Chichester, **1990**, pp.67-111.
6. A. Shutsrirung, P. Sutigoolabud, C. Santasup, K. Senoo, S. Tajima, M. Hisamatsu and A. Bhromsiri, "Symbiotic efficiency and compatibility of native rhizobia in northern Thailand with different soya cultivars", *Soil Sci. Plant Nutri*., **2002**, *48,* 491-499.
7. J. A. Thompson, A. Bhromsiri, A. Shutsrirung and S. Lillakan, "Native root-nodule bacteria of traditional soybean-growing areas of northern Thailand", *Plant Soil*, **1991**, *135*, 53-65.
8. D. F. Herridge and S. K . A. Danso, "Enhancing crop legume N_2 fixation through selection and breeding", *Plant Soil*, **1995**, *174*, 51-82.
9. Y. Gan, I. Stulen, H. van Keulen and P. J. C. Kuiper, "Effect of N fertilizer top-dressing at various reproductive stages on growth, N_2 fixation and yield of three soya (*Glycine max* (L.) Merr.) genotypes", *Field Crops Res.*, **2003**, *80*, 147-155.
10. P. Swatdee, S. Choonluchanon, B. Topark-Ngarm, P. Pakkong, S. Supamtee and P. Sudto, "Application of azolla for rice production in the north-east of Thailand", Proceedings of Conference of Biotecnology and Biology Diversity, **1993,** Bangkok, Thailand.
11. D. F. Herridge, B. Palmer, D. P. Nurhayti and M. B. Peoples, "Evaluation of the xylem ureide method for measuring N_2 fixation in six tree legume species", *Soil Biol. Biochem*., **1996**, *28*, 281-289.
12. L. C. Purcell, R. Serraj, T. R. Sinclair and A. De, "Soybean N_2 fixation estimates, ureide concentration, and yield responses to drought", *Crop Sci.*, **2004**, *44,* 484-492.
13. P. Schweiger, M. Hofer, W. Hartl, W. Wanek and J. Vollmann, "N_2 fixation by organically grown soya in Central Europe: Method of quantification and agronomic effects", *Eur. J. Agron*., **2012**, *41*, 11-17.
14. D. F. Herridge and M. B. Peoples, "Timing of xylem sampling for ureide analysis of nitrogen fixation", *Plant Soil*, **2002**, *238*, 57-67.
15. A. Oberson, S. Nanzer, C. Bosshard, D. Dubois, P. Mäder and E. Frossard, "Symbiotic N_2 fixation by soya in organic and conventional cropping systems estimated by ^{15}N dilution and ^{15}N natural abundance", *Plant Soil*, **2007**, *290*, 69-83.
16. R. Kourik, "Designing and Maintaining Your Edible Landscape Naturally", Matamorhic Press, London, **1986**.
17. N. C. Brady and R. R. Weil, "The Nature and Properties of Soil", 13th Edn., Prentice Hall, Upper Saddle River (NJ), **2002**, Ch 15.

18. K. Fog, "The effect of added nitrogen on the rate of decomposition of organic matter", *Biol. Rev.*, **1988**, *63*, 433-462.
19. M. Sela, E. Tel-Or, E. Fritz and A. Huttermann, "Localization and toxic effects of cadmium, copper, and uranium in azolla", *Plant Physiol.*, **1988**, *88*, 30-36.
20. R. Parnes, "Fertile Soil: A Grower's Guide to Organic and Inorganic Fertilizers", 2nd Edn., Ag Access Corporation, Davis (CA), **1990**.
21. H. H. Zahran, A. H. Abo-Ellil and E. A. Al Sherif, "Propagation, taxonomy and ecophysiological characteristics of the azolla-anabaena symbiosis in freshwater habitats of beni-suef governorate (Egypt)", *Egyptian J. Biol.*, **2007**, *9*, 1-12.
22. D. Mishra and M. Kar, "Nickel in plant growth and metabolism", *Bot. Rev.*, **1974**, *40*, 395-452.
23. R. Cammack, "Splitting molecular hydrogen", *Nature*, **1995**, *373,* 556-557.
24. D. Werner and W. E. Newton, "Nitrogen Fixation in Agriculture, Forestry, Ecology, and the Environment", Springer, Dordrecht, **2005**.
25. N. Teaumroong, "Nitrogen Fixing Bacteria" (In Thai), ChulaPress, Bangkok, Thailand, **2011**.
26. N. Hirunburana, "A pilot program for increasing the efficiency of soya production in the northern region of Thailand" (in Thai), Final Report, **1999**, Faculty of Agriculture, Chiang Mai University, Thailand.

Maejo International Journal of Science and Technology

ISSN 1905-7873
Available online at www.mijst.mju.ac.th

Full Paper

Clinical study of chitosan-derivative-based hemostat in the treatment of split-thickness donor sites

Wanida Janvikul [1,*], Boonlom Thavornyutikarn [1], Wasana Kosorn [1] and Pairoj Surattanawanich [2]

[1] National Metal and Materials Technology Centre, Pathumthani 12120, Thailand
[2] Department of Surgery, Angthong Hospital, Angthong 14000, Thailand

* Corresponding author, email: wanidaj@mtec.or.th

Received: 26 October 2012 / Accepted: 23 September 2013 / Published: 27 September 2013

Abstract: The hemostatic efficacy of a chitosan-derivative-based prototype was clinically evaluated in the treatment of split-thickness skin-graft donor sites in 17 patients, in comparison with two commercial materials. The test materials were placed randomly on the wound sites for 8 min. to stop the bleeding; the treated wounds were uncovered afterwards for evaluation. The total amount of blood loss in each treated wound was determined by measuring the blood absorbed in each used dressing. The bleeding area in each treated wound after an 8-min. treatment, was determined by wound image analysis. The amounts of blood loss measured from the wound sites treated with each material for 8 min. were found insignificantly different. However, from the visual observation and wound image analysis, the amount of blood ooze and the bleeding area after being left uncovered for 30, 60 and 90 sec. were significantly detected to be at a miniumum in wounds treated with the chitosan-derivative-based prototype, implying that the prototype could stop the bleeding most effectively.

Keywords: clinical study, chitosan-derivative-based hemostat, wound dressing, split-thickness donor sites

INTRODUCTION

Recently, there has been a great deal of interest in the development of new hemostatic materials to achieve hemostasis when conventional methods fail or cannot be used [1]. In general, hemostatic agents used for the control of hemorrhage must be non-cytotoxic, biocompatible and resorbable (if required). One of the developed hemostatic products is HemCon® Bandage (HemCon Medical Technologies, Oregon, USA), which is essentially composed of chitosan and a non-absorbable backing in a vacuum-sealed pouch [2].

Chitin and chitosan are abundant biopolymers derived from renewable resources in nature [3]. They were reported to accelerate a wound healing process [4-5] and hemostasis [6-8]. In our previous study, carboxymethylchitosan, a water-soluble chitosan derivative, was found to possess a greater *in vitro* hemostatic effect than chitosan [9]. Carboxymethylchitosan was also clinically found to promote the wound healing process in the treatment of partial-thickness wounds [10].

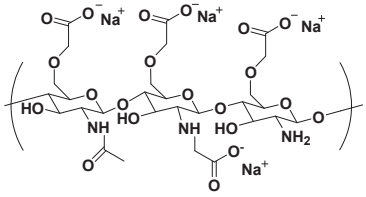

Carboxymethylchitosan

The preparation of carboxymethylchitosan-based hemostat, a chitosan-derivative-based prototype (CDP), was attempted in our laboratory. Both *in vitro* and *in vivo* hemostatic ability of the developed prototype was assessed in comparison with that of a commercial material, SPONGOSTAN® [11]. The results showed that both materials could significantly decrease the clotting time of pure whole blood ($p < 0.05$); their *in vitro* hemostatic ability appeared comparable. However, in the animal trial, the CDP could stop the bleeding from the transected rat tails more effectively than SPONGOSTAN® Standard; the average bleeding time of the wounds treated with the prototype was much shorter and the amount of blood loss was also lower.

The objective of this study is to clinically evaluate the hemostatic efficacy of this chitosan-derivative-based hemostatic prototype, in comparison with that of two commercial materials, SPONGOSTAN® Standard and Algisite-M, in the treatment of split-thickness skin-graft donor sites.

MATERIALS AND METHODS

Preparation of Chitosan-Derivative-Based Hemostat

Typically, 6 wt% carboxymethylchitosan aqueous solution was poured into moulds of a given dimension and subsequently lyophilised to produce sponge-like pads. The water-soluble pads were then individually immersed in a gently stirred 10% aqueous calcium chloride solution for 30 min. to form water-insoluble pads. Afterwards, the pads were removed and successively washed with distilled water. The resulting pads were then freeze-dried to yield the CDP, which was sterilised by ethylene oxide gas prior to use.

SPONGOSTAN® Standard (a resorbable gelatin sponge) and Algisite-M (a calcium-alginate dressing) were obtained from Department of Surgery, Angthong Hospital.

Patients

Seventeen patients (4 females and 13 males), aged 25-71 years, enrolled in this study between June 2008 - December 2009. The principal conditions and diseases to be treated with split-thickness skin grafts were avulsion wounds (13 patients) and necrotising fasciitis (4 patients). Informed consent forms (Document No. AT.0027.202.5/001) were signed by the patients upon their enrollment in the trial, which was approved by the Independent Ethics Committee of Angthong Hospital.

Hemostatic Efficacy Assessment

Total amount of blood loss by gravimetric method

In brief, three test materials (CDP, SPONGOSTAN® Standard and Algisite-M, size 1x1 in., as shown in Figure 1) and dry gauze dressing (size 1x1 in.) were initially weighed. Split skin grafts were harvested from the thighs using a Zimmer® dermatome. The normal cut width and depth were 1.5 in. and 0.1 mm respectively. The three test materials were randomly placed on the wound sites. Pre-weighed gauze was placed on top of each test material. To secure the whole materials, they were gently held by hand (without a press), as illustrated in Figure 2. After 8 min., the wound sites were uncovered and photographed. Then, they were re-photographed at 8.5, 9 and 9.5 min. for the observation of blood ooze. Finally, the used test materials and gauze were weighed for the determination of blood loss.

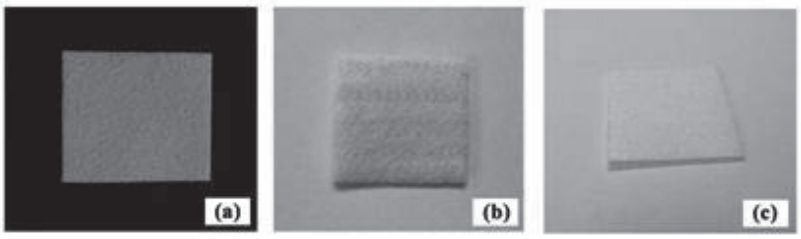

Figure 1. Test materials: (a) CDP; (b) Algisite-M; (c) SPONGOSTAN® Standard

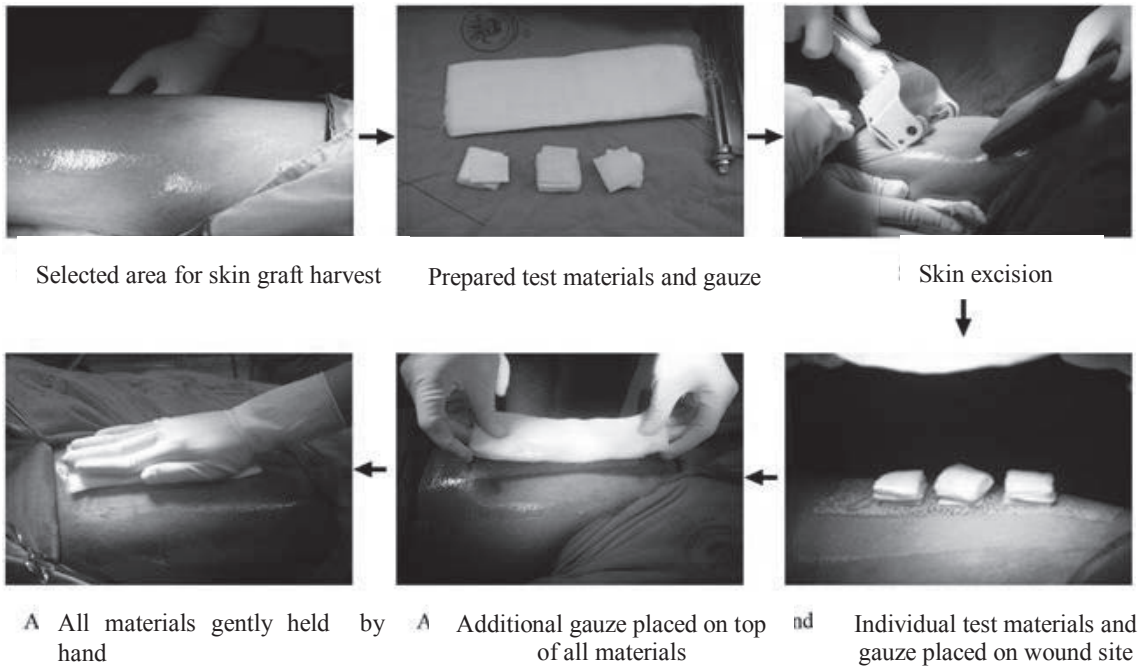

Figure 2. Clinical hemostatic evaluation on donor site

Percentage of bleeding area by image analysis

The photographs of the wound sites taken at 8, 8.5, 9 and 9.5 min. were re-created for the determination of bleeding area by an image analyser. The duplicated images were manually marked with two different colours for bleeding and non-bleeding areas.

Statistical analysis

The results were expressed as mean±standard deviation. The acquired data were statistically analysed using Scheffe's test and paired t-test, and p-values<0.05 were considered significant.

RESULTS AND DISCUSSION

Hemostatic Efficacy: Total Amount of Blood Loss

The total amount of blood loss, the amount of blood found in each test material and gauze, from each wound site is shown in Table 1. All the acquired data were statistically analysed using Scheffe's test. The average amounts of blood absorbed in the test materials were in the following order: SPONGOSTAN® Standard < Algisite-M < CDP, although there were no significant differences between the groups (p=0.348). For the average amount of blood absorbed in the gauze placed on top of each test material, the order was: $gauze_{CDP} < gauze_{SPONGOSTAN® Standard} < gauze_{Algisite-M}$, although there were also no significant differences between the groups (p=0.376). The total amounts of blood loss were insignificantly different between the groups (p=0.702). The amount of blood found in each test material was different from that found in the gauze due to different blood absorbability of each material.

Table 1. Amounts of blood loss from wound sites after being treated with test materials for 8 min.

Test material	Material weight (g)	Material thickness (mm)	Amount of blood found in test material (g)	Amount of blood found in gauze (g)	Total amount of blood loss (g)
CDP	0.063±0.007	1.57	0.273±0.165	0.143±0.124	0.416±0.254
SPONGOSTAN® Standard	0.063±0.015	1.50	0.218±0.075	0.193±0.161	0.411±0.226
Algisite-M	0.096±0.012	0.78	0.256±0.074	0.217±0.175	0.473±0.232

Note: The data were collected from 17 patients who underwent a skin grafting process.

The differences in blood absorbability of the test materials can be attributed to both the physical appearance and the chemical characteristic of each material. Algisite-M is a non-woven calcium-alginate dressing which absorbs blood readily but does not hold it as much as the other two test materials. The dressing seems to swell least when wet, mainly owing to the three dimensional network formed by the complexation of carboxylate anions of the alginate with bivalent calcium ions. On the other hand, SPONGOSTAN® Standard is a resorbable gelatin sponge which absorbs blood most slowly among all the three evaluated samples. Once wet, however, it can hold blood more effectively than Algisite-M. The carboxymethylchitosan-based prototype absorbs and holds blood most readily due to its chemical structure; the carboxymethylchitosan molecules present in the prototype are lightly cross-linked [10]. In addition, the blood absorbability of this material is facilitated by its porous structure.

As a consequence, CDP possesses the greatest blood absorbability among the test materials. This is practically attractive as the gauze dressed on top of the material can then be used in a relatively smaller quantity. In addition, good blood absorption leads to a dry wound surface; a favourable close contact between the wound site and the material is consequently

achieved. As a result, blood coagulation can occur more readily. In addition, the negatively charged surface with carboxylate groups of the carboxymethylchitosan could induce the contact activation of clotting proteins and initiate the clotting cascade, resulting in a fast formation of fibrins [9]. This is evidently supported by the results obtained from the wound image analysis, which is discussed below.

Hemostatic Efficacy: Percentage of Bleeding Area

From a preliminary clinical study, the bleeding still continued after the wound sites had been treated for 5 min. Blood ooze was markedly observed after the wound sites were uncovered for 30 sec. Hence, in this study, the wounds were treated for 8 min. As a result, the wound surfaces appeared nearly dry, especially the ones treated with CDP and SPONGOSTAN® Standard (Figure 3a). In addition, blood ooze seemed to be less after they had remained uncovered for 30 sec. Unlike wounds treated with these two materials, the wound covered with Algisite-M was still slightly bleeding (Figure 3b).

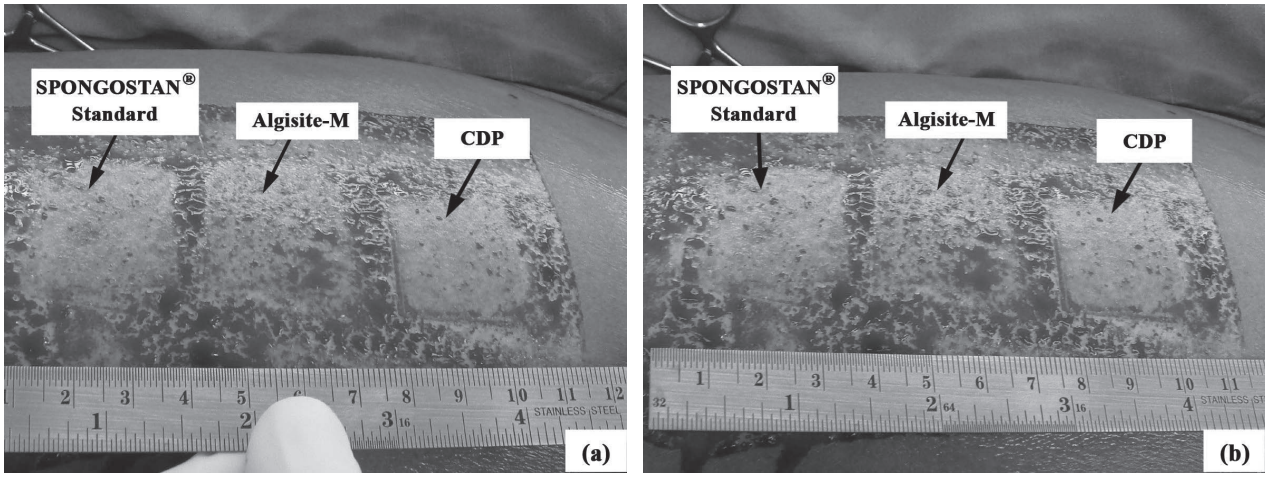

Figure 3. Wound appearances after being treated with test materials for: (a) 8 min.; (b) 8.5 min.

The photographs of the treated wound sites of five patients taken at 8 min. and 8.5 min. were re-created for quantification of the amount of blood ooze. The duplicated images were marked with different colours (Figure 4) for bleeding and non-bleeding areas, which were subsequently analysed by image analysis to determine the percentage of bleeding area. Table 2 shows the calculated percentages of bleeding area of the wounds at 8 min. and 8.5 min. after the treatment together with the bleeding area increment of the wounds at 8.5 min. It clearly suggests that the CDP almost completely stopped the bleeding from the wounds after 8 min. of treatment. Blood ooze scarcely occurred afterwards; extremely small increases in the percentage of bleeding area were observed in the wounds that remained uncovered for 30 sec. after the treatment. On the contrary, small bleeding was still continuing in the wounds treated with the other two materials; considerably larger percentages of bleeding area increment were observed in the wounds after being uncovered for 30 sec.

To acquire more information about blood ooze in the wounds after the 8-min. treatment, the treated wound sites were left uncovered longer in another five patients. The wound sites were photographed consecutively after the 8-min. treatment and then at 30, 60 and 90 sec. afterwards to

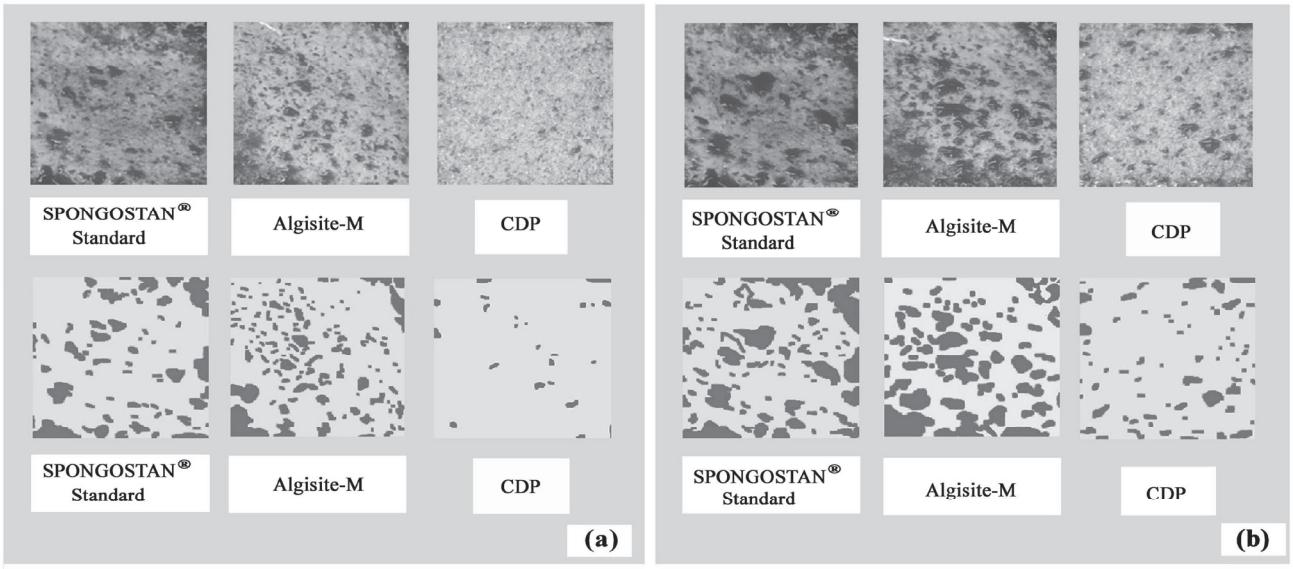

Figure 4. Photographs of wound sites and their duplicated images marked with different colours for bleeding (red) and non-bleeding (yellow) areas: (a) wounds after 8-min. treatment; (b) wounds after a further uncovering for 30 sec.

determine the amount of blood ooze at each time point. The percentages of bleeding area of the wounds were computed using image analysis with the same procedure as described previously. Table 3 shows the calculated percentages of bleeding area after the 8-min. treatment and bleeding area increments of the wounds after a further uncovering for 30, 60 and 90 sec. The bleeding area increments of the wounds are also comparatively shown in Figure 5. All the wound sites covered with CDP had the least percentages of bleeding area in all cases. Furthermore, in most cases, CDP appeared to stop the bleeding most effectively as blood ooze was observed to increase the least when the treated wounds were uncovered for a prolonged period.

The calculated percentages of bleeding area of wound sites after the 8-min. treatment and a further uncovering for 90 sec. (data from Table 3) were further statistically analysed using a paired t-test. Comparisons were performed between CDP and SPONGOSTAN® Standard, and also between CDP and Algisite-M. As shown in Table 4, the percentages of bleeding area of wound sites treated with CDP were significantly lower than those of wounds treated with SPONGOSTAN® Standard. All the *p*-values were lower than 0.05: p=0.015 at 8.5 min., p=0.010 at 9 min. and p=0.007 at 9.5 min. The wounds treated with CDP and SPONGOSTAN® Standard for 8 min., however, were found insignificantly different in terms of percentage of bleeding area (p=0.052). A slightly different analytical result was obtained in the statistical comparison between CDP and Algisite-M. The percentages of bleeding area of wound sites left uncovered for 90 sec. after being treated with CDP were significantly lower than those of wounds treated with Algisite-M. All the *p*-values were lower than 0.05: p=0.003 at 8.5 min., p=0.025 at 9 min. and p=0.015 at 9.5 min. The percentages of bleeding area of wounds treated with CDP and Algisite-M for 8 min. were also found significantly different in these five patients (p=0.003), which might be partially due to the low absorbability of Algisite-M. These statistically analysed results confirm that, among these three evaluated materials, CDP can stop the bleeding from the split-thickness skin-graft donor sites most effectively.

Table 2. Percentages of bleeding area of wound sites after 8-min. treatment and after further uncovering for 30 sec.

Case number	Sex	Age (years)	Test material	Bleeding area (%)		Bleeding area increment (%) [a]
				At 8 min.	At 8.5 min.	At 8.5 min.
1	M	54	CDP	8.38	8.53	0.15
			SPONGOSTAN® Standard	4.08	8.22	4.14
			Algisite-M	20.57	36.52	15.95
2	F	25	CDP	6.06	7.56	1.50
			SPONGOSTAN® Standard	32.41	47.13	14.72
			Algisite-M	13.55	24.75	11.20
3	F	60	CDP	1.00	1.23	0.23
			SPONGOSTAN® Standard	2.27	2.84	0.57
			Algisite-M	1.14	2.78	1.64
4	M	57	CDP	2.63	8.20	5.57
			SPONGOSTAN® Standard	23.15	33.73	10.58
			Algisite-M	18.66	33.42	14.76
5	M	30	CDP	2.45	4.86	2.41
			SPONGOSTAN® Standard	6.47	11.41	4.94
			Algisite-M	11.15	14.84	3.69

Note: The data were collected from 5 patients who underwent a skin grafting process.
[a] By subtracting percentage of bleeding area at 8 min. from percentage of bleeding area at 8.5 min.

Table 3. Percentages of bleeding area of wound sites after 8-min. treatment and after further uncovering for 30, 60 and 90 sec.

Case number	Sex	Age (years)	Tested material	Bleeding area (%)				Bleeding area increment (%)		
				At 8 min.	At 8.5 min.	At 9 min.	At 9.5 min.	At 8.5 min.[a]	At 9 min.[b]	At 9.5 min.[c]
1	M	65	CDP	0.29	1.02	1.02	1.10	0.73	0.73	0.81
			SPONGOSTAN® Standard	1.75	5.91	6.26	6.49	4.16	4.51	4.74
			Algisite-M	3.02	6.63	7.72	7.99	3.61	4.70	4.97
2	M	71	CDP	0.00	0.21	0.57	0.61	0.21	0.57	0.61
			SPONGOSTAN® Standard	3.07	5.01	5.93	6.16	1.94	2.86	3.09
			Algisite-M	6.39	8.17	8.92	9.51	1.78	2.53	3.12
3	M	71	CDP	0.28	0.73	0.91	1.00	0.45	0.63	0.72
			SPONGOSTAN® Standard	0.54	5.62	6.73	8.74	5.08	6.19	8.20
			Algisite-M	1.66	7.26	8.51	8.65	5.60	6.85	6.99
4	M	34	CDP	0.75	1.02	1.02	1.10	0.27	0.27	0.35
			SPONGOSTAN® Standard	3.08	8.71	9.67	9.87	5.63	6.59	6.79
			Algisite-M	3.50	8.17	9.50	10.09	4.67	6.00	6.59
5	F	40	CDP	9.23	11.51	13.37	15.41	2.28	4.14	6.18
			SPONGOSTAN® Standard	17.07	31.54	32.17	33.75	14.47	15.10	16.68
			Algisite-M	19.89	26.99	35.74	39.33	7.10	15.85	19.44

Note: The data were collected from 5 patients who underwent a skin grafting process.

[a] By subtracting percentage of bleeding area at 8 min. from percentage of bleeding area at 8.5 min.

[b] By subtracting percentage of bleeding area at 8 min. from percentage of bleeding area at 9 min.

[c] By subtracting percentage of bleeding area at 8 min. from percentage of bleeding area at 9.5 min.

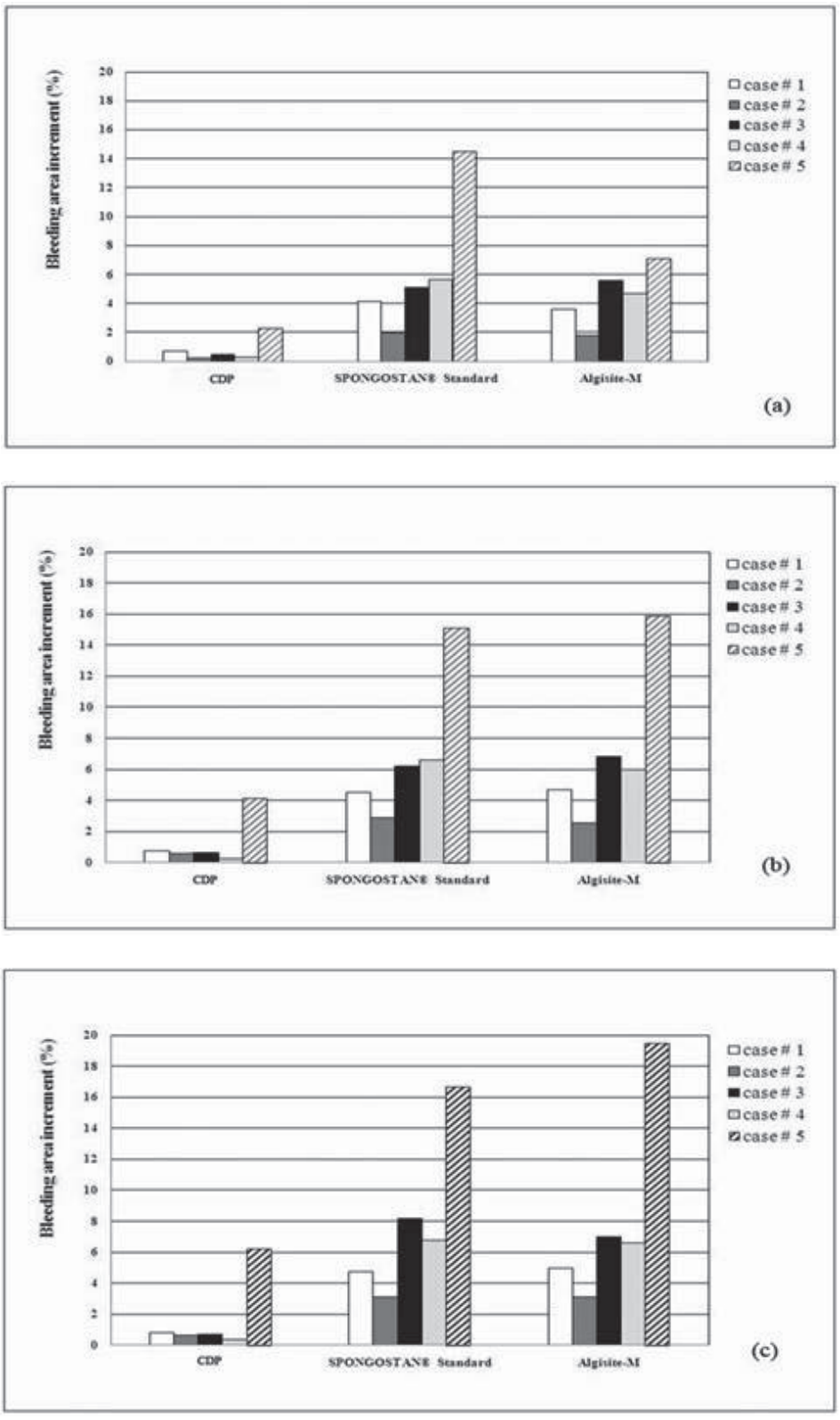

Figure 5. Bleeding area increments of wounds left uncovered for: (a) 30 sec.; (b) 60 sec.; (c) 90 sec.

Table 4. Statistical comparisons of percentages of bleeding area of wound sites treated with CDP and SPONGOSTAN® Standard, and of those treated with CDP and Algisite-M (n=5)

Paired sample comparison	*p*-Value
CDP versus SPONGOSTAN® Standard (8 min.)	0.052
CDP versus SPONGOSTAN® Standard (8.5 min.)	0.015*
CDP versus SPONGOSTAN® Standard (9 min.)	0.010*
CDP versus SPONGOSTAN® Standard (9.5 min.)	0.007*
CDP versus Algisite-M (8 min.)	0.003*
CDP versus Algisite-M (8.5 min.)	0.003*
CDP versus Algisite-M (9 min.)	0.025*
CDP versus Algisite-M (9.5 min.)	0.015*

*Considered significant

CONCLUSIONS

The results of this clinical study clearly demonstrate that after an 8-min. treatment CDP can stop the bleeding from the split-thickness skin-graft donor sites more effectively than SPONGOSTAN® Standard and Algisite-M. The amount of blood ooze as well as percentage of bleeding area is significantly at a minimum in wounds treated with CDP after being left uncovered for 30, 60 and 90 sec. Even so, more trial with a greater number of enrolled patients must be conducted in order to acquire more supportive results on the hemostatic efficacy of CDP before the prototype can get approved for clinical use in general.

ACKNOWLEDGEMENTS

This study was financially supported by the National Metal and Materials Technology Centre, Thailand. The authors would like to thank the nurses at the Department of Surgery, Angthong Hospital, for their assistance throughout this clinical study.

REFERENCES

1. J. Granville-Chapman, N. Jacobs and M. J. Midwinter, "Pre-hospital haemostatic dressings: A systematic review", *Injury*, **2011**, *42*, 447-459.
2. M. A. Brown, M. R. Daya and J. A. Worley, "Experience with chitosan dressings in a civilian EMS system", *J. Emerg. Med.*, **2009**, *37*, 1-7.
3. K. Kurita, "Chitin and chitosan: Functional biopolymers from marine crustaceans", *Mar. Biotechnol. New York*, **2006**, *8*, 203-226.

4. C. A. Stone, H. Wright, T. Clarke, R. Powell and V. S. Devaraj, "Healing at skin graft donor sites dressed with chitosan", *Br. J. Plast. Surg.*, **2000**, *53*, 601-606.
5. A. K. Azad, N. Sermsintham, S. Chadrkrachang and W. F. Stevens, "Chitosan membrane as a wound-healing dressing: Characterization and clinical application", *J. Biomed. Mater. Res. B Appl. Biomater.*, **2004**, *69*, 216-222.
6. J. L. Sondeen, A. E. Pusateri, V. G. Coppes, C. E. Gaddy and J. B. Holcomb, "Comparison of 10 different hemostatic dressings in an aortic injury", *J. Trauma*, **2003**, *54*, 280-285.
7. Y. Okamoto, R. Yano, K. Miyatake, I. Tomohiro, Y. Shigemasa and S. Minami, "Effect of chitin and chitosan on blood coagulation", *Carbohydr. Polym.*, **2003**, *53*, 337-342.
8. P. L. Kang, S. J. Change, I. Manousakas, C. W. Lee, C. H. Yao, F. H. Lin and S. M. Kuo, "Development and assessment of hemostasis chitosan dressings", *Carbohydr. Polym.*, **2011**, *85*, 565-570.
9. W. Janvikul, P. Uppanan, B. Thavornyutikarn, J. Krewraing and R. Prateepasen, "*In Vitro* comparative haemostatic studies of chitin, chitosan, and their derivatives", *J. Appl. Polym. Sci.*, **2006**, *102*, 445-451.
10. A. Angspatt, B. Taweerattanasil, W. Janvikul, P. Chokrungvaranont and W. Sirimaharaj, "Carboxymethylchitosan, alginate and tulle gauze wound dressing: A comparative study in the treatment of partial-thickness wounds", *Asian Biomed.*, **2011**, *5*, 413-416.
11. W. Janvikul, P. Uppanan, W. Kosorn, D. Phulsuksombati and R. Prateepasen, "Evaluation of efficacy of chitosan derivative based hemostat: *In vitro* and *in vivo* studies", Proceedings of 2nd International Symposium on Biomedical Engineering, **2006**, Bangkok, Thailand, pp.281-283.

Maejo Int. J. Sci. Technol. **2013**, *7*(03), 396-407

Maejo International Journal of Science and Technology

ISSN 1905-7873
Available online at www.mijst.mju.ac.th

Full Paper

A novel algorithm for the conversion of shuffle regular expressions into non-deterministic finite automata

Ajay Kumar* **and Anil Kumar Verma**

Department of Computer Science and Engineering, Thapar University, Patiala, Punjab-147004, India

* Corresponding author, e-mail: (ajayloura@gmail.com)

Received: 19 September 2012 / Accepted: 7 October 2013 / Published: 14 October 2013

Abstract: Regular expressions with shuffle operators are widely used in diverse fields of computer science. The work presented here investigates the shuffling of regular expressions and their conversion into non-deterministic finite automata. The aim of the paper is to design a novel algorithm for constructing ε-free non-deterministic finite automata from the shuffling of regular expressions. Non-deterministic finite automata generated using the proposed approach requires, in the worst case, 2^{m+s+1} states. This is a significant improvement over other existing approaches in the literature, where the number of states reaches $2^{2(m+u+k+s)-C}$ in the worst case.

Keywords: regular expression, parallel regular expression, non-deterministic finite automaton, shuffle operator

INTRODUCTION

Regular expressions (REs) are used in various applications such as compiler designs, XML schema languages, text processors, and as a programming tool for multifarious scripting languages such as PERL and PHP [1-4]. REs used in these applications require standard operators (union, concatenation and Kleene closure). Extended REs [5] consist of shuffle, intersection and counting operators, in addition to standard operators. Although the use of these additional operators do not increase the expressive power of REs, succinctness occurring due to the addition of these operators is difficult to handle with the standard operators [5]. Extended REs are used in diverse applications such as XML schema languages [6], text processors and programming languages [7]. A semi-extended RE [5] consists of union, concatenation, Kleene closure and intersection operators. REs with union, concatenation, Kleene closure and counting operators are used in different areas such as egrep, PERL and XML schema [5].

A shuffle operator is used in the modelling of process algebra, concurrent systems and critical section problems [2, 8-9]. A parallel RE (PRE) consists of disjunction (+), concatenation (.), Kleene closure (*) and shuffle (Ш) operators [2]. Shuffle operators appear in diverse forms

of computer science such as process algebra, multipoint communications, XML schema Relax NG and concurrency of processes [6, 9-11].

PRELIMINARY CONCEPTS

For the rest of the paper, $\sum$ denotes an alphabet depicting a non-empty set of symbols [3]. A string $s=a_1a_2...a_n$ is a finite sequence of symbols taken from the alphabet. The position of symbol a_i is equal to *i*. The length of a string *s* (denoted by $|s|$) represents the number of occurrence of symbols presented in *s*. $\sum^*$ [3] depicts a set of all strings generated from $\sum$. An empty string (denoted by ε) is a string which has no symbols. The null language (denoted by ϕ) does not contain any string. A language *L* is a subset of $\sum^*$ [3]. A language can be classified into regular, context-free, context-sensitive and recursive enumerable. A regular language can be represented by an RE or a finite automaton (FA).

RE *a,* where $a \in \sum$, depicts a regular language $\{a\}$. ε and ϕ are the REs describing null string (ε) and null language (ϕ) respectively. If r_1 and r_2 are REs depicting the languages L_1 and L_2 respectively, then union, concatenation and Kleene closure are described by the REs $r_1 + r_2$, $r_1 r_2$ and r_1^* respectively. Union, concatenation and Kleene closure rules can be finitely applied many times [3].

FA is a quintuple [3] $M = (Q, \sum, \delta, q_0, F)$, where Q is the set of states, $\sum$ is an alphabet, δ is a transition function $\delta \subseteq Q \times \{\sum \cup \varepsilon\} \times Q$, $q_0 \in Q$ is the starting state and $F \subseteq Q$ is the set of final states. Deterministic finite automaton (DFA) can be represented by a partial function $(\delta : Q \times \sum \to Q)$. Non-deterministic finite automaton (NFA) may or may not involve ε-transitions; ε*-free* NFA does not contain any ε-transitions and its transition function can be represented by $\delta \subseteq Q \times \sum \times Q$.

Shuffling [3] of two strings *x* and *y* comprises all strings *z* such that each position of *z* is assigned either to *x* or *y* for each string *z*. If we concatenate the symbols of the positions prescribed to *x* from left to right, we obtain the string *x*. Similarly, if we concatenate the symbols of the positions prescribed to *y* from left to right, we obtain the string *y*. Formally, shuffling can be defined by $a\alpha \amalg b\beta = a(\alpha \amalg b\beta) \bigcup b(a\alpha \amalg \beta)$ for $(a, b \in \sum) \wedge (\alpha, \beta \in \sum^*)$. For example, given $\alpha = 01$ and $\beta = ab$, then $\alpha \amalg \beta = \{01ab, 0a1b, 0ab1, ab01, a0b1, a01b\}$. Shuffling of two languages L_i and L_j can be defined by $L_i \amalg L_j = \{w \mid w = w_1 \amalg w_2, (\exists w_1 \in L_i) \wedge (\exists w_2 \in L_j)\}$.

A PRE can be described using a parallel finite automaton (PFA) [12], which consists of 7-tuple $(Q, q_0, N, \sum, F, \delta, \gamma)$, where $Q \subseteq 2^N$ is a finite set of states, q_0 is the starting state, N is a finite non-empty set of nodes, $\sum$ is an alphabet, $F \subseteq N$ is a set of final nodes, δ is a state transition function defined by $Q \times (\sum \cup \lambda) \to 2^Q$, and γ is a node transition function defined by $2^N \times (\sum \cup \lambda) \to 2^{2 \wedge N}$. A λ-transition represents the joining of two languages with a shuffle operator.

A shuffle RE (SRE) is a confined form of PRE, in which the shuffle operators explicitly occur between REs. Conversion of an SRE to an RE or a DFA has been studied widely with respect to the concurrency aspects.

LITERATURE REVIEW

Estrade *et al.* [2] investigated the explicitly PRE, proposed an algorithm for the conversion of SREs to NFAs using PFA as an intermediate step and designed a tool kit FLAT in the PERL language. Figure 1 delineates the PFA corresponding to SRE $r = (10) \text{Ш } 0^*$ using Estrade *et al.*'s methodology. Biegler *et al.* [13] reasserted that shuffle decomposition is not unique over the finite sets. Gelade [5] proved that a double exponential size is required for the conversion of PREs to REs. Hovland [14] proposed a membership algorithm for an RE with unordered concatenation, which is a limited form of shuffle operator, for example $(acb \,\&\, ge) = \{acbge, geacb\}$, where & represents the unordered concatenation. Standard generalised markup language [14] allows the use of unordered concatenation. Gelade *et al.* [15] worked on REs with numerical constraints and a shuffle operator. They depicted the overview of complexity for the decision problems of XML schema languages, namely DTDs, RELAX NG, and XSDs. Berstel et al. [16] studied different kinds of language classified based on the shuffle operations and proved partial results for the star-free commutative language.

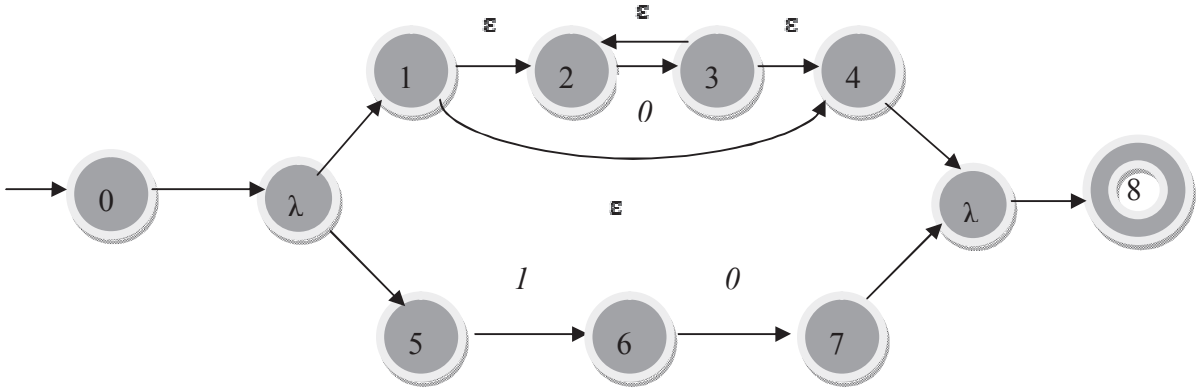

Figure 1. PFA for $r = (10) \text{Ш } 0^*$ using Estrade *et al.*'s methodology

SREs can be used for depicting the number of processes competing for the critical section [8]. Each critical section of a process can be described by a symbol. For example, critical sections of three processes can be represented by a, $(ab)^*$ and b^*. For a single CPU, the SRE describes the probabilistic ways of scheduling. An equivalent RE commensurate with the SRE renders the way for tasks to be completed. In the case of resource reduction in the modelling of concurrent systems, partial serialisation can be useful [2]. In this paper, we propose a novel algorithm for the conversion of SREs into ε-free NFAs without using intermediate steps.

Methodologies exist in the literature for the conversion of REs into NFAs, namely Thompson's construction [17], partial derivatives [18] and follow automata [19]. Estrade *et al.* [2] worked on the conversion of SRE into NFA using PFA as an intermediate state. SRE-to-PFA conversion can be achieved by using modified Thompson's construction. PFA with n states can be converted into an NFA requiring 2^n states in the worst case [2]. However, an RE can be converted into DFA directly with fewer states than the trivial Thompson's construction. The motivation for this research stems from the scope for the conversion of an SRE into a DFA by extending the direct conversion method.

PROPOSED APPROACH

In the direct method of conversion of REs into DFAs [1, 20], a syntax tree is constructed for the augmented RE. *Firstpos*, *lastpos* and *nullable* are determined using the rules given in Table 1. Additional rules for the shuffle operator are described with those for the direct conversion of RE into DFA [1, 20]. *Followpos* are determined using the rules given in Table 2. *Firstpos*, *lastpos*, *followpos* and *nullable* are determined for the nodes of the syntax tree, and using these *followpos*, an equivalent DFA can be generated.

Table 1. Rules for *firstpos(r), lastpos(r)* and *nullable*

RE	Firstpos(r)	Lastpos(r)	Nullable
$r = \phi$	ϕ	ϕ	*false*
$r = \varepsilon$	ϕ	ϕ	True
$r = a$	$position(a)$	$position(a)$	*false*
$r = r_i + r_j$	$firstpos(r_i) \cup firstpos(r_j)$	$lastpos(r_i) \cup lastpos(r_j)$	$nullable(r_i) \vee nullable(r_j)$
$r = r_i r_j$	**If** $\varepsilon \in L(r_i)$ $firstpos(r_i) \cup firstpos(r_j)$ **Else** $firstpos(r_i)$	**If** $\varepsilon \in L(r_j)$ $lastpos(r_i) \cup lastpos(r_j)$ **Else** $lastpos(r_j)$	$nullable(r_i) \wedge nullable(r_j)$
$r = r_i^*$	$firstpos(r_i)$	$lastpos(r_i)$	*true*
$r = r_i \text{ Ш } r_j$	$firstpos(r_i) \cup firstpos(r_j)$	$lastpos(r_i) \cup lastpos(r_j)$	$nullable(r_i) \wedge nullable(r_j)$

Table 2. Computation of *followpos*

RE	Followpos
$r_i r_j \in r$	**For** $p \in lastpos(r_i)$ $followpos(p) \leftarrow followpos(p) \cup firstpos(r_j)$
$r_i^* \in r$	**For** $p \in lastpos(r_i)$ $followpos(p) \leftarrow followpos(p) \cup firstpos(r_i)$

SRE r with s shuffle operators can be dispensed to $s+1$ sub-regular expressions $r_1, r_2, \ldots, r_{s+1}$ such that:

1. $r = r_1 \text{ Ш } r_2 \text{ Ш} \ldots \text{ Ш} r_{s+1}$
2. $r_1, r_2, \ldots, r_{s+1}$ are the REs.

An augmented SRE can be obtained by adding # before each shuffle operator and at the end of SRE r. A syntax tree (similar to that shown in Figure 2) is constructed for the augmented SRE such that the symbols and #'s appear at leaf nodes and operators appear as the internal nodes. For all leaf nodes, except a node labelled with #, *followpos* are calculated. *Followpos*(#) is taken as null set.

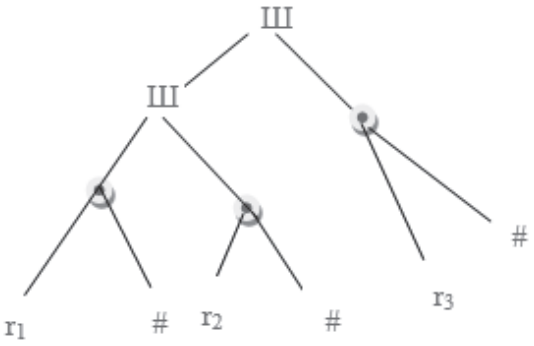

Figure 2. Syntax tree for augmented SRE

Followpos for each sub-regular expression is calculated severally. Consider SRE $r = r_i \text{ Ш } r_j$ having a single shuffle operator. *Firstpos*, *lastpos* and *followpos* of r_i and r_j are calculated severally. The starting state of the NFA is the union of *firstpos*(r_i) and *firstpos*(r_j). *Lastpos* of the root node is determined by taking the union of all positions labelled with #. State q_i is a final state if $lastpos(root) \subseteq q_i$. Using the definition of shuffle, the resulting NFA must include all strings generated from the shuffling of r_i and r_j. The final state of the NFA accepts all strings generated from r_i Ш r_j. At any instant of time during the processing of string *w*, consider q_i is the current state. On reading symbol *a*, from the sub-REs r_i and r_j, the following two cases can occur after reading symbol *a* as shown in Figure 3.

- Reading of symbol *a* from r_i:
  $q_j \leftarrow followpos((position(r_i)\ labelled\ with\ \ a)\ in\ \ q_i) \cup (positions(r_j)\ in\ \ q_i)$
- Reading of symbol *a* from r_j:
  $q_k \leftarrow followpos((position(r_j)\ labelled\ with\ \ a)\ in\ \ q_i) \cup (positions(r_i)\ in\ \ q_i)$

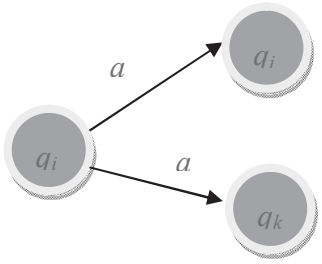

Figure 3. Reading symbol *a* from r_i Ш r_j

Similarly, there is a possibility of reading symbol *a* on states q_j and q_k from sub-expressions r_j and r_i respectively. Hence, if $(symbols(r_i) \cap symbols(r_j) \neq \phi) \wedge (r_i \text{ Ш } r_j \in r)$, then an NFA is generated from *r* using the proposed approach. Repeating this procedure, all possible shuffled strings can be generated. The final state of the NFA will accept all strings which are obtained by r_i Ш r_j. In general, SRE *r* consists of (*s+1*) sub-REs *(r_1, r_2, r_3, ..., r_{s+1})*, such that $r = r_1$ Ш r_2 Ш r_3 Ш ... Ш r_{s+1}. At any instant of time during the processing of a string *w*, consider q_i is the current state. Symbol *a* can be taken from sub-REs r_x, r_y and r_z of the state q_i. The following cases can occur after reading symbol *a*:

- Reading symbol a from r_x:
  $q_j \leftarrow followpos((position(r_x)\ labelled\ with\ a)\ in\ q_i) \cup (q_i - positions(r_x))$
- Reading symbol a from r_y:
  $q_k \leftarrow followpos((position(r_y)\ labelled\ with\ a)\ in\ q_i) \cup (q_i - positions(r_y))$
- Reading symbol a from r_z:
  $q_l \leftarrow followpos((position(r_z)\ labeled\ with\ a)\ in\ q_i) \cup (q_i - positions(r_z))$

Further, reading of symbol a from the sub-expression r_y and r_z on state q_j is possible. Similarly, there is a possibility of reading symbol a on states q_k and q_l. Repeating this procedure, all possible shuffled strings can be generated from the sub-regular expressions $r_1, r_2, \ldots, r_{s+1}$. The final state will accept all strings of the SRE r. If a common symbol appears in different sub-REs of r involved in shuffling, then DFA cannot be generated directly from SRE r. Algorithms for the conversion of SRE into NFA are depicted in Schemes 1-3.

Algorithm 1: SRE_ NFA (p, NFA)

Input: SRE p

Output: ε -free NFA equivalent to SRE p

1. Generate augmented SRE p.
2. Construct a syntax tree for augmented SRE p. // Syntax tree construction
3. *Calculate_Follow(p).* *// Call to Procedure Calculate_follow*
4. *Create_*NFA*(firstpos,lastpos, followpos).* *// Call to Procedure Create_*NFA

Scheme 1. Algorithm for the conversion of SRE into ε -free NFA

Notations used in the algorithm *Calculate_Follow(p)* are as follows. Consider c_1 and c_2 are the left and right child during traversal of a node delineated by union, concatenation and shuffle operators. Consider c_1 is the only child of a node delineated by Kleene closure. Let a indicate symbol from $\sum$. Position(n) depicts the position of the symbol embarked at RE n. Using Brueggemann-Klein's methodology [20], *firstpos, lastpos* and *followpos* are determined for all nodes except for shuffle operator. The rules for determination of *firstpos, lastpos, nullable* and *followpos* are depicted in Tables 1-2. The same are represented by the procedure *Calculate_Follow*(p) as shown in the Scheme 2.

The reading of a symbol of a state is processed by two steps. In the first step we find the *followpos* of the current symbol from a sub-RE. In the second step we add the positions of other sub-REs involved in a shuffling of the current state to the result of the first step. This process is repeated for each $q \in Q$ and each $a \in \sum$. The initial and final states are determined using the *firstpos* and *lastpos* of the root node respectively. The complete procedure is specified in Scheme 3.

Algorithm 2: *Calculate_Follow*(p)

Input: Syntax tree for the SRE r

Output: *Firstpos*, *lastpos* and *followpos*

1. **Repeat** steps 2 to 6 for each node n during the post-order traversal of the syntax tree do
2. **If** $(n = 'a' \vee n = '\#')$ then // Leaf node
   $firstpos(n) \leftarrow position(n)$
   $lastpos(n) \leftarrow position(n)$

   End If
3. **If** $n = '+'$ then // Union node
   $firstpos(n) \leftarrow firstpos(c_1) \cup firstpos(c_2)$
   $lastpos(n) \leftarrow lastpos(c_1) \cup lastpos(c_2)$

   End If
4. **If** $n = '.'$ then // Concatenation node
   $firstpos(n) \leftarrow firstpos(c_1)$
   $lastpos(n) \leftarrow lastpos(c_2)$
   If $c_1 = '*'$ then // nullable at left child is true
   $firstpos(n) \leftarrow firstpos(n) \cup firstpos(c_2)$

   End If
   If $c_2 = '*'$ then // nullable at right child is true
   $lastpos(n) \leftarrow lastpos(n) \cup lastpos(c_1)$

   End If
   For each $i \in lastpos(c_1)$ do
   $followpos(i) \leftarrow followpos(i) \cup firstpos(c_2)$

   End For

   End If
5. **If** $n = '*'$ then // Kleene closure
   $firstpos(n) \leftarrow firstpos(c_1)$
   $lastpos(n) \leftarrow lastpos(c_1)$
   For each $i \in lastpos(n)$ do
   $followpos(i) \leftarrow followpos(i) \cup firstpos(n)$

   End For

   End If
6. **If** $n = ' ш '$ then // Shuffle operator
   $firstpos(n) \leftarrow firstpos(c_1) \cup firstpos(c_2)$
   $lastpos(n) \leftarrow lastpos(c_1) \cup lastpos(c_2)$

   End If

Scheme 2. Procedure for computing *firstpos*, *lastpos* and *followpos* of the SRE p

Algorithm 3: *Create*_NFA (*firstpos, followpos, lastpos*)
Input: *Firstpos*, *lastpos* and *followpos* of SRE *p*
Output: NFA equivalent to SRE *p*

1. $q_0 \leftarrow firstpos(root)$
   $s \leftarrow$ *number of shuffle operator in p*
2. $Q \leftarrow q_0$ and make q_0 as unmarked.
3. **Repeat** steps 4-9, while there is an unmarked state $q \in Q$ do
4. Choose an unmarked state *q* and mark it.
5. $\Pr evlast \leftarrow 0$ //indicates the last position of the sub-expression recently processed
   $i \leftarrow 1$
6. **Repeat** steps 7-9 while $(i \le s+1)$ // Reading of *a* on the current sub-expression
7. $currentlast \leftarrow i^{th}$ value of $lastpos(root)$
   $T \leftarrow \phi$
   For $(\forall pos \in q)$ do
   If $(\Pr evlast < pos \le currentlast)$
   $T \leftarrow T \cup pos$
   End If
   End For
   $N \leftarrow q - T$ // Remaining positions of the other sub-expressions
8. **For** $\forall a \in \sum$ do
   $Newstate \leftarrow \phi$
   For $\forall t \in T$ do
   If $(symbol(t) = a)$ then
   $Newstate \leftarrow Newstate + followpos(t)$
   End If
   End For
   If $Newstate \neq \phi$
   $Newstate \leftarrow Newstate \cup N$
   $Tran[q, a] \leftarrow Newstate$
   If $Newstate \notin Q$ then
   $Q \leftarrow Q \cup Newstate$
   Make *Newstate* as unmarked state.
   End If
   End If
9. $prevlast \leftarrow currentlast$
   $i \leftarrow i+1$
10. $q_0 = \{q \mid q = firstpos(root)\}$ //Starting state
    $F = \{q_f \mid q_f \in Q \wedge lastpos(root) \subseteq q_f\}$ //Final state

Scheme 3. Algorithm for generating equivalent NFA from SRE *p*

The complete procedure for the conversion of SRE to NFA is expounded by the following numerical example.

Example. Given $r = (a(a+b)^*) \text{Ш} (a^*b^*)$

Augmented $r = (a_1(a_2+b_3)^*)\#_4 \text{Ш} (a_5^*b_6^*)\#_7$

Figure 4 delineates the syntax tree for the augmented SRE. The *firstpos* of a node is depicted on the left side of the node in blue colour and the *lastpos* of a node is depicted on the right side of the node in green colour.

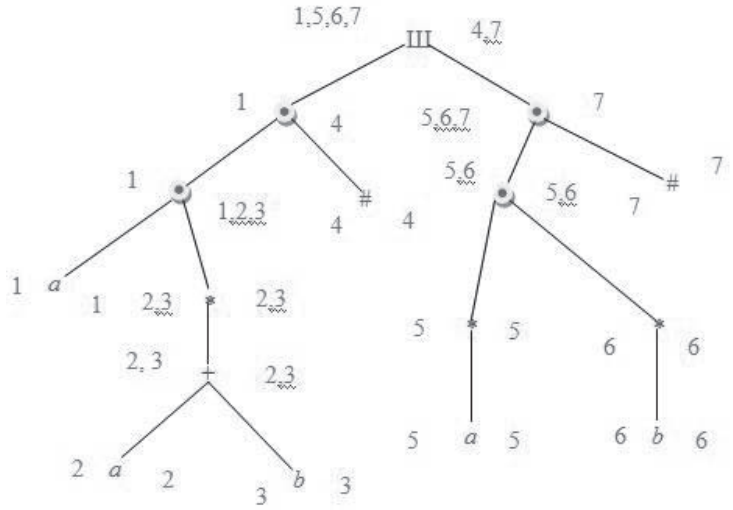

Figure 4. Syntax tree for $r = (a(a+b)^*) \text{Ш} (a^*b^*)$

The following values are determined using algorithm 2:

$$followpos(1) = \{2,3,4\}$$
$$followpos(2) = \{2,3,4\}$$
$$followpos(3) = \{2,3,4\}$$
$$followpos(5) = \{5,6,7\}$$
$$followpos(6) = \{6,7\}$$
$$followpos(4) = followpos(7) = \phi$$

Figure 5 delineates the NFA $M = (\{q_0, q_1, F_0, F_1\}, \{a,b\}, \delta, q_0, \{F_0, F_1\})$ corresponding to SRE *r*.

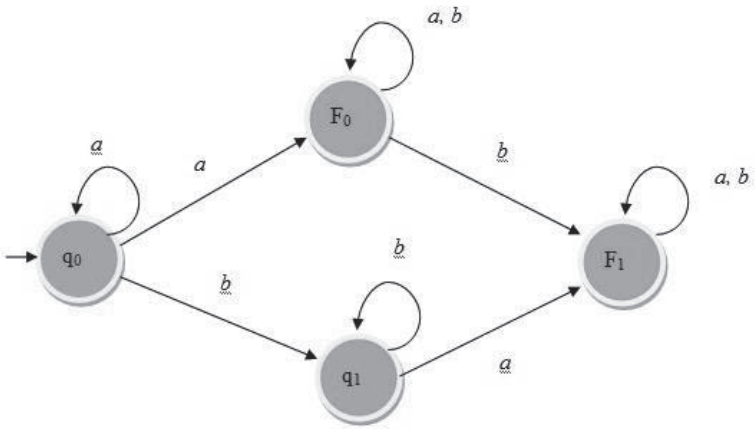

Figure 5. NFA for $r = (a(a+b)^*) \text{Ш} (a^*b^*)$

DESCRIPTIONAL COMPLEXITY OF THE OBTAINED NFA

In this section, analysis is carried out on state complexity of the NFA obtained using Estrade *et al.* methodology [2] and the proposed approach. It is well known that a PFA with n states can be converted into an NFA with 2^n states. This leads to the following theorems:

Theorem 1. If C is the number of occurrence of the concatenation operator in SRE r, then the NFA obtained using Estrade *et al.*'s methodology [2] requires $2^{2|r|-3C}$ states in the worst case.

Proof: Estrade *et al.*'s methodology converts r to a PFA using the modified Thompson's construction [8]. The number of states of the PFA using the modified Thompson's construction is equal to $2|r|-3C$. A PFA with n states can be converted to an NFA using the subset construction that requires 2^n states in the worst case [2]. Hence, a PFA with $2|r|-3C$ states can be converted to an NFA using a subset construction requiring $2^{2|r|-3C}$ states in the worst case. □

Theorem 2. If m denotes the number of instances of symbols and s denotes the number of shuffle operators in the SRE r, then a ε-free NFA can be constructed using the proposed algorithm requiring 2^{m+s+1} states in the worst case.

Proof. In the proposed algorithm, the syntax tree is constructed such that all symbols and #'s appear as leaf nodes. Each state can be constructed using the positions assigned to the leaf nodes. The total number of leaf nodes in the syntax tree is $(m+s+1)$. The maximum 2^{m+s+1} states can be constructed using the positions of the syntax tree. Hence, using the proposed algorithm, the worst case state complexity of the NFA is 2^{m+s+1}. □

Theorem 3. The state complexity of the proposed algorithm is less than the state complexity of Estrade *et al.*'s methodology [2] for the conversion of an SRE to an NFA.

Proof. SRE r with m, u, k, s and c represent instances of symbols, union, Kleene closure, shuffle and concatenations respectively. The worst-case state complexity of the proposed algorithm and of Estrade *et al.*'s methodology are 2^{m+s+1} and $2^{2(m+u+k+s)-C}$ respectively. That the proposed algorithm will generate an NFA with fewer states can be proved by the relation:

$$m+s+1<2(m+u+k+s)-C \Rightarrow 1<m+2u+2k+s-C$$

Each concatenation operation is performed between two symbols. Similarly, n concatenation can be performed with at least $(n+1)$ symbols, which means $m-C\geq 1$.

Hence, the relation $1\leq m+2u+2k+s-C$ always holds and the worst-case state complexity of the proposed algorithm is always less than that of Estrade *et al.*'s methodology. □

The worst-case state complexity of the ε-NFA is $2^{2|r|-3C}$ using Estrade *et al.*'s methodology [2]. The pattern matching will decelerate if the NFA consists of ε-transitions. Using the proposed algorithm, a ε-free NFA is generated.

The worst case-state complexity of the NFA is 2^{m+s+1}. Table 3 describes the differences between the proposed approach and Estrade *et al.*'s methodology [2].

Table 3. Comparison between the proposed algorithm and Estrade *et al.*'s methodology

Criterion	Proposed algorithm	Estrade *et al.*'s methodology
Worst-case state complexity	2^{m+s+1}	$2^{2\|r\|-3C}$
Output	ε -free NFA	ε -NFA
Conversion chain	SRE $\rightarrow$ NFA $\rightarrow$ DFA	SRE $\rightarrow$PFA$\rightarrow$ NFA $\rightarrow$ DFA

CONCLUSIONS AND FUTURE SCOPE

An algorithm has been designed for the conversion of SREs into ε -free NFAs without using any intermediate steps. Using the proposed approach, a svelte NFA is generated. The number of states of the NFA generated using the proposed approach is equal to 2^{m+s+1} states in the worst case, which is a significant improvement over the existing approaches in the literature. Another advantage of this approach is that the ε -free NFAs is produced. Pattern matching is delayed if the NFA consists of ε -transitions. Further, if $\forall(r_i \amalg r_j) \in r \wedge ((symbols(r_i) \bigcap symbols(r_j)) \neq \phi)$, then it is implausible to generate a DFA directly from the SRE. This approach will be useful in the field of process algebra and concurrent aspects. In the future, this work can be extended to the conversion of PREs into REs. The reduction of time and state complexity for the conversion of SREs into NFAs can also be carried out.

REFERENCES

1. A. V. Aho, R. Sethi and J. D. Ullman, "Compilers: Principles, Techniques and Tools", 19th Edn., Pearson Education, Singapore, **2005.**
2. B. D. Estrade, A. L. Perkins and J. M. Harris, "Explicitly parallel regular expressions", Proceedings of 1st International Multi-symposiums on Computer and Computational Sciences, **2006,** Hangzhou, China, pp.402-409.
3. J. E. Hopcroft, R. Motwani and J. D. Ullman, "Introduction to Automata Theory, Languages, and Computation", 12th Edn., Pearson Education, Singapore, **2005.**
4. P. D. Stotts and W. Pugh, "Parallel finite automata for modeling concurrent software systems", *J. Syst. Softw.*, **1994,** *27*, 27-43.
5. W. Gelade, "Succinctness of regular expressions with interleaving, intersection and counting", *Theor. Comput. Sci.*, **2010,** *411*, 2987-2998.
6. J. Clark and M. Murata, "RELAX NG Specifications", **2001**, http://www.oasis-open.org/committes/relax-ng/spec-20011203.html (Date of access: Dec. 2001).
7. L. Wall, T. Christiansen and J. Orwant , "Programming Perl",3rd Edn., O'Reilly Media, Sebastopol (CA), **2000**.
8. B. D. Estrade, "An investigation of equivalent serialized forms of parallel finite automata", *MS Thesis,* **2005**, University of Southern Mississippi, USA.
9. M. Nivat, "Behaviours of synchronized systems of processes", L.I.T.P. Report No. 81-64, University of Paris 7, France, **1981**.

10. K. Iwama, "Unique decomposability of shuffled strings: A formal treatment of asynchronous time-multiplexed communication", Proceedings of 15th Annual ACM Symposium on Theory of Computing, **1983,** Boston, USA, pp.374-381.
11. J. C. M. Baeten and W. P. Weijland, "Process Algebra (Cambridge Tracts in Theoretical Computer Science)", Cambridge University Press, Cambridge, **1990**.
12. V. K. Garg, "Modeling of distributed systems by concurrent regular expressions", Proceedings of 2nd International Conference on Formal Description Techniques for Distributed Systems and Communication Protocols, **1989,** Vancouver, Canada, pp.313-327.
13. F. Biegler, M. Daley, M. Holzer and I. McQuillan, "On the uniqueness of shuffle on words and finite languages", *Theor. Comput. Sci.*, **2009,** *410*, 3711-3724.
14. D. Hovland, "The membership problem for regular expressions with unordered concatenation and numerical constraints", Proceedings of 6th International Conference on Language and Automata Theory and Applications, **2012**, Coruna, Spain, pp.313-324.
15. W. Gelade, W. Martens and F. Neven, "Optimizing schema languages for XML: Numerical constraints and interleaving", *SIAM J. Comput.*, **2009**, *38*, 2021-2043.
16. J. Berstel, L. Boasson, O. Carton, J.-E. Pin and A. Restivo, "The expressive power of the shuffle product", *Inform. Comput.*, **2010**, *208*, 1258-1272.
17. K. Thompson, "Regular expression search algorithm", *Commun. ACM,* **1968,** *11*, 419-422.
18. V. Antimirov, "Partial derivatives of regular expressions and finite automaton constructions", *Theor. Comput. Sci.*, **1996,** *155*, 291-319.
19. L. Ilie and S. Yu, "Follow automata", *Inform. Comput.*, **2003,** *186*, 140-162.
20. A. Brueggemann-Klein, "Regular expressions into finite automata", *Theor. Comput. Sci.*, **1993,** *120*, 197-213.

Maejo International Journal of Science and Technology

ISSN 1905-7873
Available online at www.mijst.mju.ac.th

Full Paper

Modified approach to PROMETHEE for multi-criteria decision-making

Miroslav Radojicic [1], Malisa Zizovic [2], Zoran Nesic [1,*] and Jasmina Vesic Vasovic [1]

[1] Technical Faculty, University of Kragujevac, Svetog Save 65, 32000 Cacak, Serbia
[2] Business Faculty, Singidunum University, Danijelova 32, 11000 Belgrade, Serbia

*Corresponding author, e-mail: zornes2002@yahoo.com

Received: 25 October 2012 / Accepted: 21 October 2013 / Published: 24 October 2013

Abstract: This paper presents a modification of PROMETHEE for multi-criteria decision-making. The authors of PROMETHEE have defined six generalised preference functions in order to express their preferences for particular criteria. A modified approach to PROMETHEE is based on the Universal preference function which replaces the six proposed functions and generates an unlimited number of other preference functions. By applying this method, we can express all the complexity of selecting preference functions in the problems of optimisation by PROMETHEE.

Keywords: multi-criteria decision-making, universal preference function, PROMETHEE

INTRODUCTION

Practical managerial problems set diverse requirements, which are often of different relative importance and are differently sensitive to changes of input and output variables. Therefore, managerial decision-making requires the use of multiple criteria methods. A number of different criteria provide a comprehensive insight in accordance with the requirements set by decision-makers. The criteria may appear in different units and can often be of different relative importance and with different requirements for maximisation or minimisation.

A method by the name of PROMETHEE (Preference Ranking Organisation Method for Enrichment Evaluations) has been developed by Brans and Vincke [1] and Brans *et al.* [2]. The authors of PROMETHEE developed four variants of this method: PROMETHEE I provides a partial ranking alternative, PROMETHEE II provides a complete order, PROMETHEE III gives an interval order and PROMETHEE IV is used for a continuous set of alternatives. These methods have been constantly improved [3].

Some of the important directions of multi-criteria methods are the inclusion of fuzzy mathematical programming [4-8] and the formation of integrated hybrid models and other

methods of multi-criteria decision-making [9-12]. By combining different methods of multiple criteria, many authors highlight the importance of multi-criteria methods [13-16].

The development of methodology of multi-criteria decision-making has resulted in the formation of a large number of models and different approaches [17-20]. Multi-criteria methods are used by many authors as the basis for different approaches to the formation of new models: an interactive aggregation-desegregation approach [21], visualisation methods [22-23], a multiple-criteria decision analysis (MCDA) model based on multi-graded dominance relations [24], a method based on stochastic dominance degrees [25], and many others. PROMETHEE is one of the MCDA methods frequently applied in a wide range of multi-criteria decision-making processes [26-31].

The novelty of this paper is in the implementation of expanded modified access to PROMETHEE by the introduction of Universal preference function, which enables the definition of a practically unlimited number of functions that can be used as the preference function. The modification is reflected in the expansion of the possibilities of expressing the intensity of preferences within the criteria, according to which a comparison is performed. These extensions make it easier for the decision-makers to determine the intensity of subjective preferences, speed and preference limits. This allows a greater dispersion of the values of preference index of compared alternatives in the range 1 to 0. In this way, the ranking procedure in the case of close rank positions, without clear quantitative preference, is facilitated.

METHODS

The following multi-criteria problem is being considered:

$$\text{Max } \{k_1(a), k_2(a), ..., k_p(a) \mid a \in A\} \quad (1)$$

where A is a finite set of possible alternatives $\{a_1, a_2, a_3, .., a_n\}$ and $\{k_1, k_2, ..., k_p\}$ is a set of selected evaluation criteria. The data for problem-solving are usually recorded in an evaluation table (Table 1).

Table 1. Evaluation table

Alternative	**Criteria**					
	$\mathbf{k_1}$	$\mathbf{k_2}$	**...**	$\mathbf{k_j}$	**...**	$\mathbf{k_p}$
$\boldsymbol{a_1}$	$k_1(a_1)$	$k_2(a_1)$	...	$k_j(a_1)$	...	$k_p(a_1)$
$\boldsymbol{a_2}$	$k_1(a_2)$	$k_2(a_2)$	...	$k_j(a_2)$	...	$k_p(a_2)$
...	...	...	...	...	...	...
$\boldsymbol{a_j}$	$k_1(a_j)$	$k_2(a_j)$	...	$k_j(a_j)$	...	$k_p(a_j)$
...	...	...	...	...	...	...
$\boldsymbol{a_n}$	$k_1(a_n)$	$k_2(a_n)$	...	$k_j(a_n)$	...	$k_p(a_n)$

The preference structure in this case is based on pairwise comparisons. The authors of this method [1] introduced the functions of preferences. They are mathematical functions by which decision-makers can express preferences for certain criteria. P(a, b) is a preference function of alternative a in relation to alternative b, which is defined by:

$$P(x) = \begin{cases} P(a,b) & x \geq 0 \\ P(b,a) & x \leq 0 \end{cases}, \quad x = k(a) - k(b) \quad (2)$$

where $0 \le P(a, b) \le 1$ and $P(a,b) \ne P(b,a)$. The potential preferences can be expressed using the following relations:

$P(a, b) = 0$	no preference, indifference	
$P(a, b) \sim 0$	weak preference	$k(a) > k(b)$
$P(a, b) \sim 1$	strong preference	$k(a) >> k(b)$
$P(a, b) = 1$	strict preference	$k(a) >>> k(b)$

Graphically, the preference function (2) can be presented as follows (Figure 1):

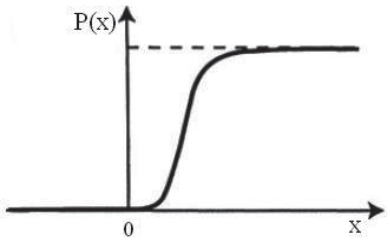

Figure 1. General form of preference function

The authors of PROMETHEE [1] introduced six generalised preference functions defined by expressions (3-8). The parameters p and q are the limits of preferences. Graphical interpretation of these functions is presented in Figure 2.

Type I. Usual criterion: $$P(x) = \begin{cases} 0, & x \le 0 \\ 1, & x > 0 \end{cases} \quad (3)$$

Type II. Quasi-criterion: $$P(x) = \begin{cases} 0, & x \le p \\ 1, & x > q \end{cases} \quad (4)$$

Type III. Criterion with linear preference: $$P(x) = \begin{cases} 0, & x < 0 \\ \dfrac{x}{p}, & 0 \le x \le p \\ 1, & x > p \end{cases} \quad (5)$$

Type IV. Level criterion: $$P(x) = \begin{cases} 0, & x \le q \\ \dfrac{1}{2}, & q < x \le p \\ 1, & x > p \end{cases} \quad (6)$$

Type V. Criterion with linear preference and indifference area:

$$P(x) = \begin{cases} 0, & x \le q \\ \dfrac{(x-q)}{(p-q)}, & q < x \le p \\ 1, & x > p \end{cases} \quad (7)$$

Type VI. Gaussian criterion: $$P(x) = \begin{cases} 0, & x \le 0 \\ 1 - e^{\frac{-x^2}{2\sigma^2}}, & x > 0 \end{cases} \quad (8)$$

Depending on the particular problem, the decision-maker has the option to choose one of the six general types of preference function. In addition to the visual approach, which is provided to the decision-makers, preference functions enable the expressing of different importance of criteria in certain areas of multi-criteria space. Faster growth of a function means a greater

expression of preferences in individual segments. Expression of preferences is one of the most sensitive elements in the process of multi-criteria decision-making. Therefore, many authors pay great attention to this stage [32-35]. It is often based on knowledge and experience of the decision-makers, preference measuring methods and subjective factors.

a) Type I. Usual criterion

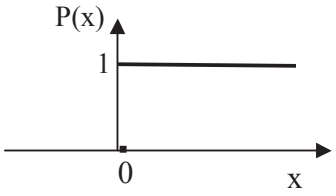

b) Type II. Quasi-criterion

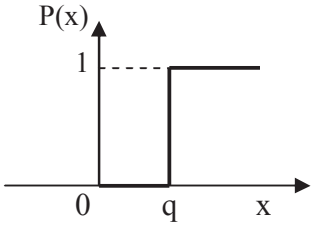

c) Type III. Criterion with linear preference

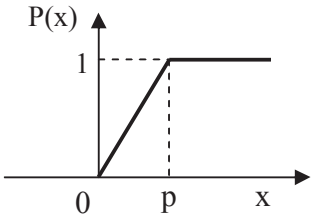

d) Type IV. Level criterion

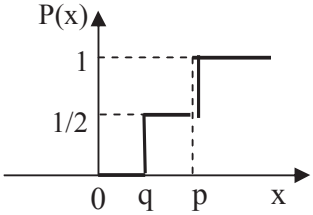

e) Type V. Criterion with linear preference and indifference area

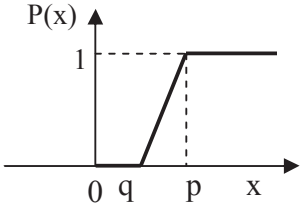

f) Type VI. Gaussian criterion

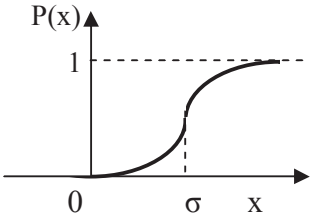

Figure 2. Generalised preference functions [1]

In further proceeding, values of preference index are calculated for each pair of compared alternatives (*a*, b) on the basis of certain preference functions and parameters:

$$IP(a,b) = \frac{1}{\sum_{i=1}^{k} Z_i} \sum_{i=1}^{k} P_i(a,b) \cdot Z_i \qquad 0 \le IP(a,b) \le 1 \tag{9}$$

where $P_i(a,\ b)$ is the preference function and Z_i is the relative importance of the i-th criterion.

Based on the preference index, the values are determined for each of the compared alternatives:

- The values of the outgoing flow $\phi^+(a)$ (synthetic measure of preference of alternatives in relation to all the others in the set of criteria K):

$$\phi^+(a) = \sum_{x \in K} IP(a,x) \tag{10}$$

- The values of the incoming flow $\phi^-(a)$ (which shows how all the other compared alternatives outperform alternative *a*):

$$\phi^-(a) = \sum_{x \in K} IP(x,a) \tag{11}$$

- The values of the net flow $\phi(a)$ (complete ranking of alternatives):

$$\phi(a) = \phi^{+}(a) - \phi^{-}(a) \tag{12}$$

This paper presents a modification of PROMETHEE by the introduction of the Universal preference function, which is a unique mathematical model that combines the generalised functions and allows the formation of an unlimited number of others. Taking into account a large number of different functions that can be generated from it, the decision-maker is provided with a significantly improved preference system. The modification of PROMETHEE is reflected in the expansion of the possibilities of expressing the intensity of preferences within the criteria, according to which a comparison is performed.

RESULTS AND DISCUSSION

Modified PROMETHEE

A modified approach to PROMETHEE is based on the Universal preference function that replaces the six proposed functions and generates an unlimited number of other preference functions. The Universal preference function is defined as:

$$P(x) = \begin{cases} m\dfrac{|x|^{\alpha}}{p^{\alpha}} & |x| \le p \\ m + \dfrac{1-m}{(q-p)^{\beta}}(|x|-p)^{\beta}, & p < |x| \le q \\ 1, & |x| > q \end{cases} \tag{13}$$

where m is a parameter, p and q are borders of preference, α and β are parameters of preference intensity changes ($0<\alpha<\infty$; $0<\beta<\infty$).

In general, preference function y=P(x) is not decreasing for $\forall x \geq 0$ and for $\forall x \in R$ $0 \leq P(x) \leq 1$. Some specific points of preference changes are as follows (Figure 3):

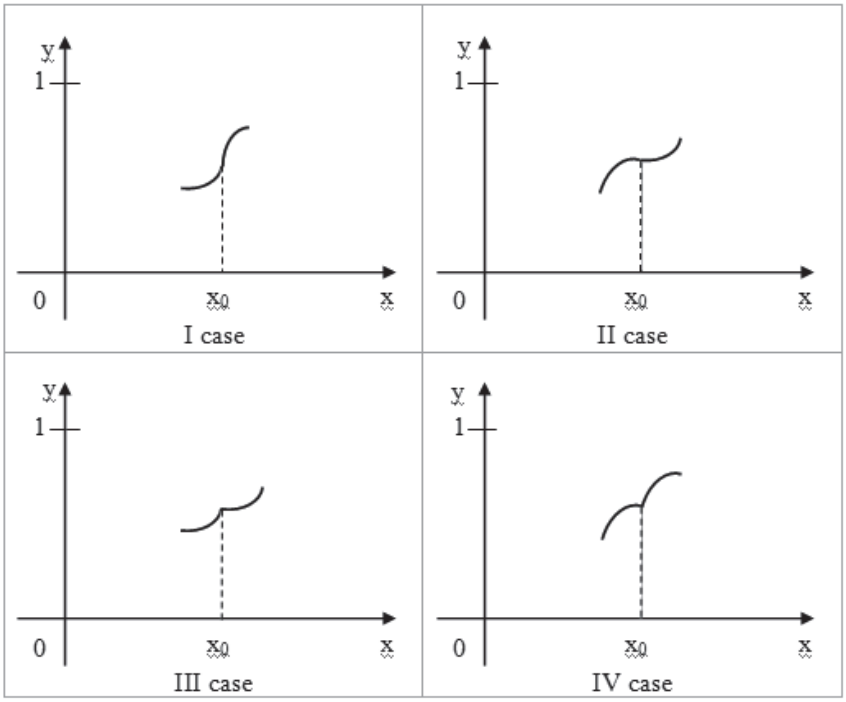

Figure 3. Some characteristic changes of preferences

The first two cases are the limits of continuous preference changes of I and II types. In the first case preference is changing at point x_0. In the second case the speed of preference is changing from decreasing to increasing. The other two types are borders with sudden changes of preferences of type I and II. In the third case the preference rate increases to the point x_0 and then increases again, while in the fourth case it decreases to the point x_0 and then again decreases. Therefore, at point x_0 the speed changes in intensity (a decrease in the first case and an increase in the second case).

The generalised preference functions are obtained from the previous function (13) as follows.

1) Usual criterion:

$$P(x) = \begin{cases} 0 & x = 0 \\ 1 & x > 0 \end{cases} \tag{14}$$

can be replaced with:

$$P(x) = \begin{cases} \dfrac{|x|^{\alpha}}{p^{\alpha}} & |x| \le p \\ 1 & |x| > p \end{cases} \tag{15}$$

which is obtained from (13) by setting m=1, p=q, $0<\alpha<\infty$. When $\alpha \to 0$ one of the six generalised criteria, Usual criterion, is obtained (Figure 4).

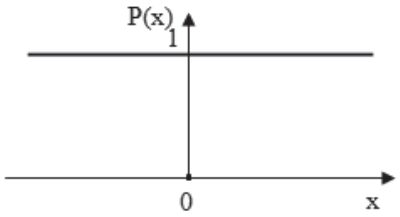

Figure 4. Graph of preference function of Usual criterion

2) Quasi-criterion:

$$P(x) = \begin{cases} 0 & x \le q \\ 1 & x > q \end{cases} \tag{16}$$

In this case when m=1, p=q, $0<\alpha<\infty$ in (13):

$$P(x) = \begin{cases} \dfrac{|x|^{\alpha}}{p^{\alpha}}, & |x| \le p \\ 1, & |x| > p \end{cases} \tag{17}$$

Letting $\alpha \to \infty$ in (17), the known generalised criterion, Quasi-criterion, is obtained (Figure 5).

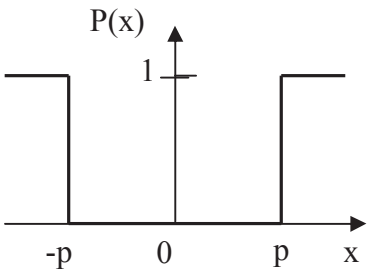

Figure 5. Graph of preference function of Quasi-criterion

3) Criterion with linear preference:

$$P(x)=\begin{cases}\dfrac{x}{p}, & x\le p\\ 1, & x>p\end{cases} \tag{18}$$

By the replacement of following parameters m=1, p=q, 0<α<∞ in (13), we get:

$$P(x)=\begin{cases}\dfrac{|x|^{\alpha}}{p^{\alpha}}, & |x|\le p\\ 1, & |x|>p\end{cases} \tag{19}$$

For α=1, the known criterion (one of the generalised criteria), Criterion with linear preference, is obtained (Figure 6a). By changing the parameter α in (19), the following modifications can be obtained. For α>1, more significant preference is obtained near the preference border defined by p (Figure 6b). For α<1, the obtained criterion emphasises the importance of the higher initial preference for any slightest differences in the criterion space (Figure 6c).

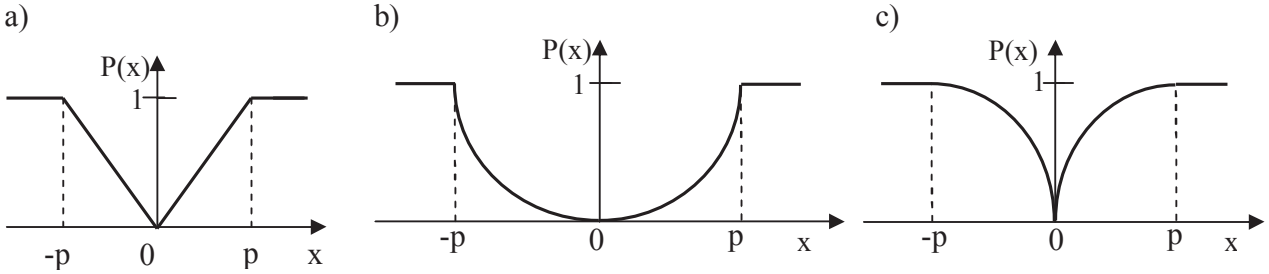

Figure 6. Graphs of preference functions of Criterion with linear preference and its modifications

4) Level criterion:

$$P(x)=\begin{cases}0 & x\le q\\ 1/2 & q<x\le p\\ 1 & x>q\end{cases} \tag{20}$$

can be replaced with:

$$P(x)=\begin{cases}\dfrac{|x|^{\alpha}}{2p^{\alpha}}, & |x|\le p\\ \dfrac{1}{2}+\dfrac{1}{2}\left(\dfrac{|x|-p}{q-p}\right)^{\beta} & p<|x|\le q\\ 1 & |x|>q\end{cases} \tag{21}$$

The function (21) is obtained directly from (13) by setting m=1/2. Letting α→∞ and β→∞ in (21), a generalised criterion, Level criterion, is obtained (Figure 7a). By changing parameter β in (21), the following modifications of Level criterion can be obtained: for β>1, indifference area is obtained up to the preference change parameter p while the prominent preference growth is obtained near the border of preference q (Figure 7b); for β=1, indifference area is obtained up to the preference change parameter p while the linear growth is obtained from the border of preference p to the border of preference q (Figure 7c); for β<1, indifference area is

obtained up to the preference change parameter p while the prominent preference growth is obtained after the parameter p (Figure 7d).

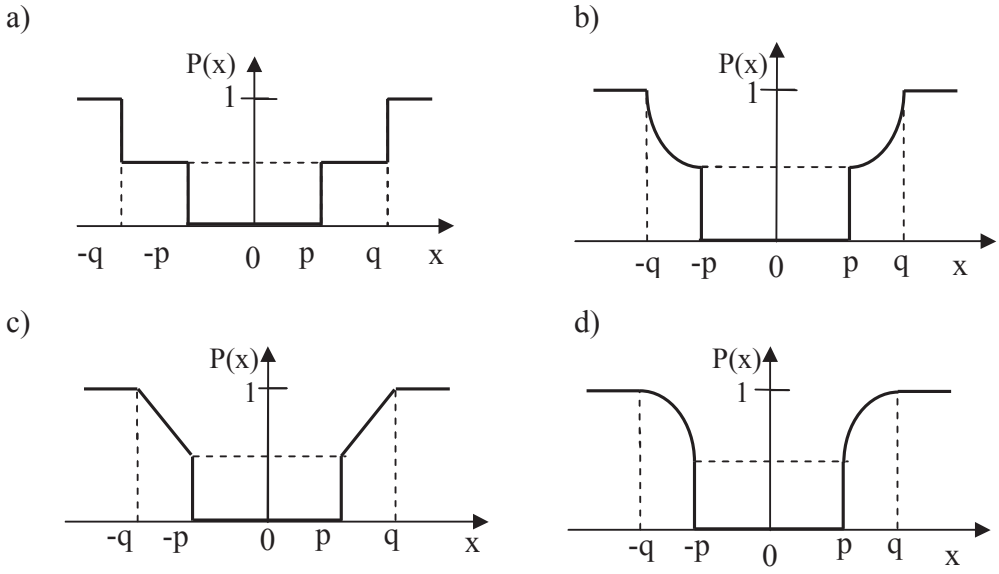

Figure 7. Graphs of preference functions of Level criterion and its modifications

5) Criterion with linear preference and indifference area:

$$P(x)=\begin{cases}0, & x\le q\\ \dfrac{(x-q)}{(p-q)}, & q<x\le p\\ 1, & x>p\end{cases} \tag{22}$$

can be replaced with:

$$P(x)=\begin{cases}0, & |x|\le p\\ \left(\dfrac{|x|-p}{q-p}\right)^{\beta} & p<|x|\le q\\ 1 & x>q\end{cases} \tag{23}$$

which was obtained from (13) by setting m=0.

Criterion with linear preference and indifference area is obtained from (23) using parameter β=1 (Figure 8a). For β >1, the function gives a distinct preference near the preference border of q (Figure 8b). For β <1, the area of indifference is obtained up to p while the prominent growth of preference is obtained for values higher than parameter p, but only in its nearest vicinity (Figure 8c).

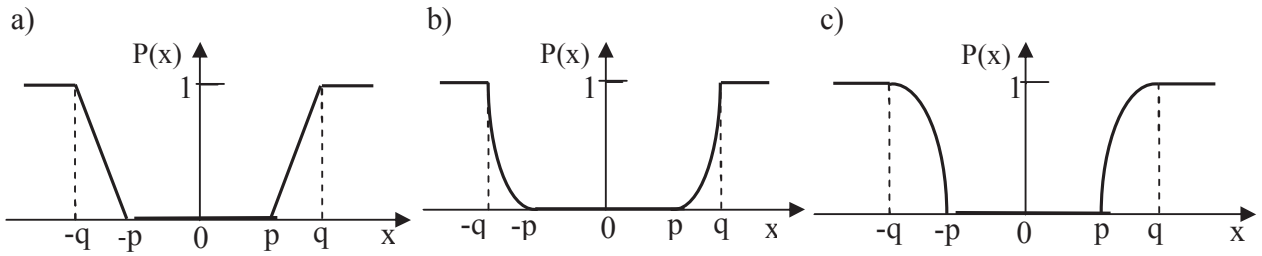

Figure 8. Graph of preference function of linear preference and indifference area and its modification

6) Gaussian criterion:

The preference function which can approximate the preferences presented by the Gaussian criterion can be obtained by using Universal preference function (13) and changing the appropriate parameters. A function which emphasises the importance and higher intensity of preference growth in the region of parameter p, which changes the preference intensity, is obtained for $\alpha>1$ and $\beta<1$ (Figure 9).

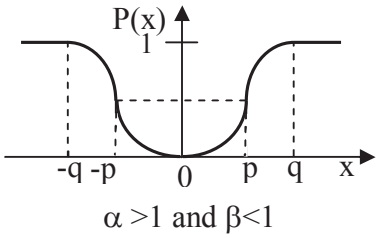

Figure 9. Characteristic appearance of Universal preference function

By changing the parameters of Universal preferential function (13), it is possible to get a number of other preference functions (presented in Figure 10). For $\alpha>1$ and $\beta>1$, the obtained function gives a distinct preference when the value of independent variable is approaching parameter p and parameter q (Figure 10a). For $\alpha<1$ and $\beta<1$, the obtained function highlights the preference for each of the smallest initial differences and for small values greater than p (Figure 10b). For $\alpha<1$ and $\beta>1$, the obtained function highlights the prominent preferences for the smallest initial differences and in the nearest vicinity of parameter q (Figure 10c).

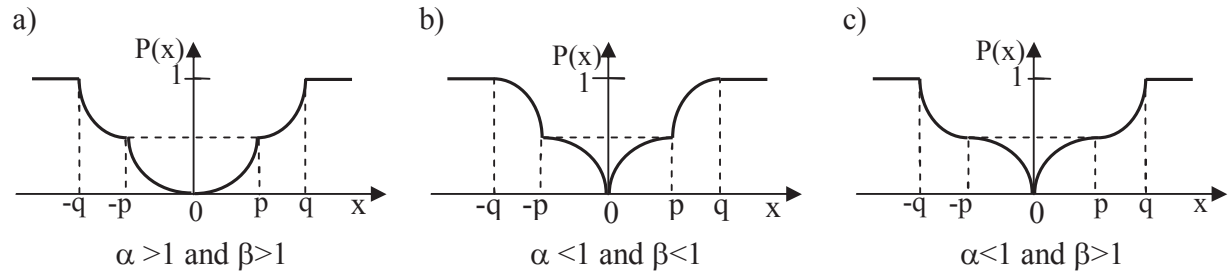

Figure 10. Some other types of preference functions

Based on Universal preference function (13) and dependent on the parameter change, it is possible to obtain different preference functions. Some of the characteristic shapes of this function, in accordance with the change of parameter α, are illustrated in Figure 11. The

influence of parameter change of α and β on possible shapes of Universal preference function is presented in Figure 12.

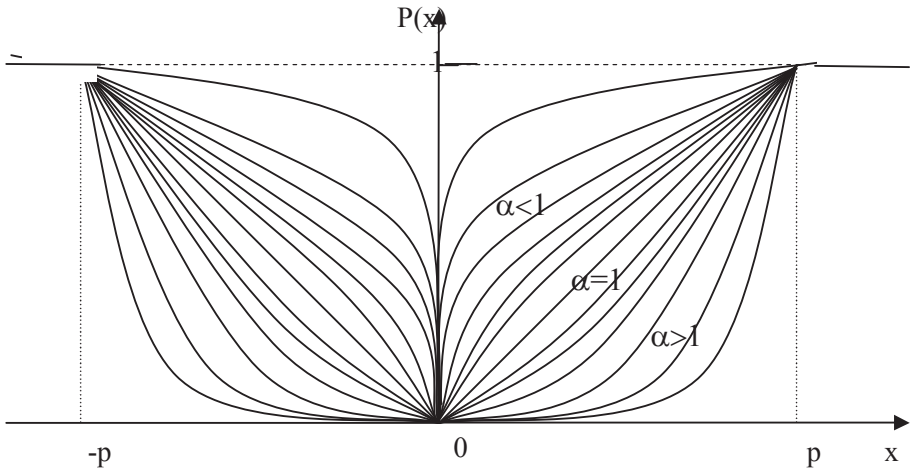

Figure 11. Different appearance options of Universal preference function in accordance with change of parameter α

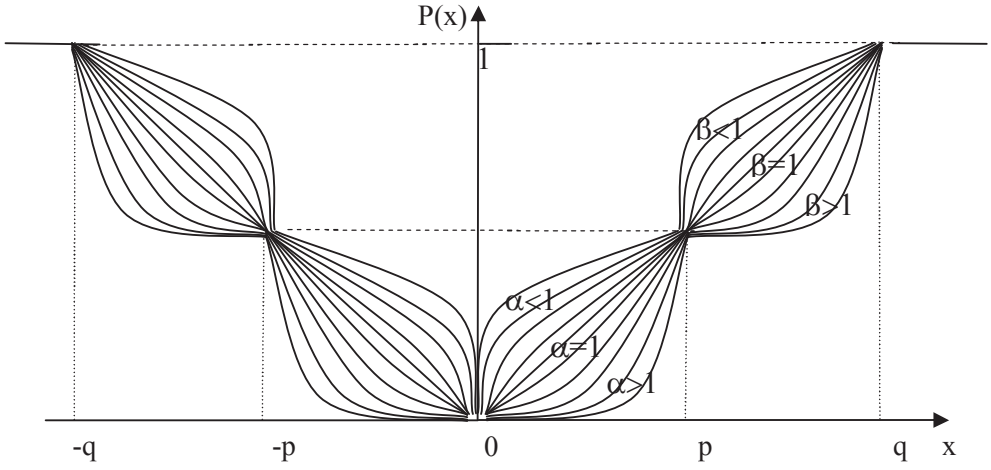

Figure 12. Some characteristic shapes of Universal preference function in accordance with the change of parameters α and β

Case Study

In order to verify the model in a case study, we have formed the basis for multi-criteria decision-making (Table 2) for the purpose of choosing the best investment project in a tool factory located in Cacak, Serbia. We compared five different design solutions (a_1, a_2, a_3, a_4, a_5) evaluated in a system of five criteria (economy, technical dependence, technology, logistics and environment) with various demands for extremisation (maximisation or minimisation).

The result was obtained by PROMETHEE II, using the usual type of generalised criterion for all the criteria (without the use of modified PROMETHEE). Values of the net flow, $\phi(a)$, for each of the considered alternatives are presented in Table 3. The resulting graph of alternatives, obtained by using the usual type of generalised criterion for all criteria, is presented in Figure 13.

Table 2. Initial values of realised example

	Criterion	Request	Alternative				
			a_1	a_2	a_3	a_4	a_5
k_1	Economy	max	200	185	180	215	250
k_2	Technical dependence	min	15	12	16	21	20
k_3	Technology	max	35	26	28	20	10
k_4	Logistics	max	82	85	94	108	105
k_5	Environment	min	4	4	3	2	5

Table 3. Values of the net flow of alternatives

Alternative	a_1	a_2	a_3	a_4	a_5
$\phi(a)$	0.2	-0.2	0.00	0.8	-0.8

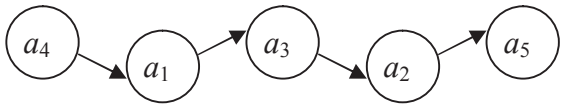

Figure 13. Graph of alternatives obtained by the usual type of generalised criterion

By using Universal preference function and by selecting the parameters, the rank of alternatives may be altered. While analysing the technological criteria in the considered example, the need for specific expression of its preference was established. In the following calculation, only one preference function (of the technological criterion) was changed while the others maintained the usual type of generalised functions. The values of the parameters of this function are: m=0.5, α=1.5, β=0.5, p=20, q=35. The illustrated preference function emphasises the importance and greater rate of preference growth around the parameter of preference change p = 20.

This function was selected with the presumption of favoured alternatives whose values belong to the range of faster function growth. Also, the alternatives whose values are farther from this range (to a greater or lesser extent) should be given lower priority. Values of the net flow, $\phi(a)$, for each of the considered alternatives in this case is shown in Table 4. The resulting graph of alternatives, obtained by using Universal preference function, is presented in Figure 14.

Table 4. Values of the net flow of alternatives obtained by using Universal preference function

Alternative	a_1	a_2	a_3	a_4	a_5
$\phi(a)$	-0.27	-0.12	-0.26	0.94	-0.29

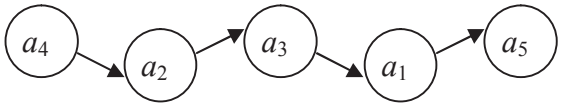

Figure 14. Graph of alternatives obtained by Universal preference function

The above example clearly shows that the alternatives are favoured in proportion to the growth of preference function. This causes a change of ranking positions of alternatives a_1 and a_2, while alternative a_4 remains in the first position regardless of the change of preferential function. The use of the proposed functions opens up a wide range of possibilities of expressing subjective preferences of decision-makers in the whole criterion space. The generation of a large number of different forms of new preferences (as previously discussed) allows the expression of preferences which would not be possible by using only six generalised criteria.

CONCLUSIONS

The Universal preference function enables a successful expression of preferences made by individual criteria, taking into account essential characteristics of different criteria. Based on the Universal preference function, it is possible to define practically unlimited number of functions that can be used as preference functions. Determining the parameters that define the proposed preference function, the decision-maker can express both certain specific problems and his/her preferences of the used criteria. By using this function, all the complexity of preference functions in optimisation problems of the PROMETHEE can be expressed. It should be emphasised that this unique feature allows the formation of all generalised criteria and at the same time the formation of many new ones.

The modification of the PROMETHEE represents the expansion of possibilities for expressing the intensity of preferences within the criteria according to which a comparison is performed. Further research trends would include statistical investigation of the results of application of the Universal preference function in multi-criteria decision-making in relation to the generalised criteria.

REFERENCES

1. J. P. Brans and Ph. Vincke., "A Preference ranking organization method (The Promethee Method for Multiple Criteria Decision Making)", *Manage. Sci.*, **1985**, *31*, 647-656.
2. J. P. Brans, Ph. Vincke and B. Mareschal, "How to select and how to rank projects: The PROMETHEE method*" Eur. J. Oper. Res.*,**1986**, *24,* 228-238.
3. J. P. Brans and B. Mareschal, "PROMETHEE V: MCDM problems with segmentation constraints", *INFOR J.*, **1992**, *30*, 85-96.
4. A. S. Fernández-Castro and M. Jiménez, "PROMETHEE: An extension through fuzzy mathematical programming", *J. Oper. Res. Soc.*, **2005**, *56*, 119-122.
5. J. Q. Wang and T. Sun, "Fuzzy multiple criteria decision making method based on prospect theory", Proceedings of International Conference on Information Management, Innovation Management and Industrial Engineering, **2008**, Taipei, Taiwan, pp.288-291.
6. X. Shen, Y. Guo, Q. Chen and W. Hu, "A multi-objective optimization evolutionary algorithm incorporating preference information based on fuzzy logic", *Comput. Optim. Appl.*, **2010**, *46*, 159-188.
7. T. C. Wang, L. Y. Chen, Y. H. Chen "Applying fuzzy PROMETHEE method for evaluating IS outsourcing suppliers", Proceedings of 5th International Conference on Fuzzy Systems and Knowledge Discovery, **2008**, Jinan Shandong, China, pp.361-365.

8. G. Tuzkaya, B. Gülsün, C. Kahraman and D. Özgen, "An integrated fuzzy multi-criteria decision making methodology for material handling equipment selection problem and an application", *Expert Syst. Appl. Int. J.*, **2010**, *37*, 2853-2863.
9. J. Ignatius, S. M. H Motlagh, M. M. Sepehri, M. Behzadian and A. Mustafa, "Hybrid models in decision making under uncertainty: The case of training provider evaluation", *J. Intell. Fuzzy Syst.*, **2010**, *21*, 147-162.
10. J. J. Wang, D. L. Yang "Using a hybrid multi-criteria decision aid method for information systems outsourcing", *Comput. Oper. Res.*, **2007**, *34*, 3691-3700.
11. D. Aloini, R. Dulmin and V. Mininno, "A hybrid fuzzy-Promethee method for logistic service selection: Design of a decision support tool", Proceedings of 9th International Conference on Intelligent Systems Design and Applications, **2009**, Pisa, Italy, pp.462-466.
12. C. Araz, P. M. Ozfirat and I. Ozkarahan, "An integrated multicriteria decision-making methodology for outsourcing management", *Comput. Oper. Res.*, **2007**, *34*, 3738-3756.
13. N. Tomic-Plazibat, Z. Aljinovic and Z. Babic, "A multi-criteria approach to credit risk assessment", Proceedings of 7th WSEAS International Conference on Mathematics and Computers in Business and Economics, **2006**, Cavtat, Croatia, pp.76-81.
14. Y. O. Yazir, C. Matthews, R. Farahbod, S. Neville, A. Guitouni, S. Ganti and Y. Coady, "Dynamic resource allocation in computing clouds using distributed multiple criteria decision analysis", Proceedings of 3rd International Conference on Cloud Computing, **2010**, Miami (FL), USA, pp.91-98.
15. S. Gilliams, D. Raymaekers, B. Muys and J. van Orshoven, "Comparing multiple criteria decision methods to extend a geographical information system on afforestation", *Comput. Electron. Agric.*, **2005**, *49*, 142-158.
16. S. Chenayah and E. Takeda, "Exploitation procedure based on eigenvector revisited: The concept of weighted preference flows in multicriteria outranking analysis", *Cybern. Syst.*, **2008**, *39*, 61-78.
17. A. Lahsasna, R. N. Ainon and T. Y. Wah, "Enhancement of transparency and accuracy of credit scoring models through genetic fuzzy classifier", *Maejo Int. J. Sci. Technol.*, **2010**, *4*, 136-158.
18. A. D. Adeyeye and F. A. Oyawale, "Optimisation of weld-metal chemical composition from welding- flux ingredients: A non-pre-emptive goal programming approach", *Maejo Int. J. Sci. Technol.*, **2010**, *4*, 347-359.
19. O. F. Ogunwolu, S. A. Oke and O. P. Popoola, "A multi-criteria model for maintenance job scheduling", *Maejo Int. J. Sci. Technol.*, **2008**, *2*, 1-12.
20. O. S. Asaolu and J. Ogbemhe, "A decision support tool for basin irrigation in northern Nigeria", *Maejo Int. J. Sci. Technol.*, **2009**, *3*, 295-305.
21. S. Zhaoxu and H. Min, "Multi-criteria decision making based on PROMETHEE method", Proceedings of International Conference on Computing, Control and Industrial Engineering, **2010**, Wuhan, China, pp.416-418.
22. Q. Hayez, B. Mareschal and Y. De Smet, "New GAIA visualization methods", Proceedings of 13th International Conference on Information Visualisation, **2009**, Barcelona, Spain, pp.247-251.
23. K. Lidouh, Y. De Smet and E. Zimanyi, "GAIA map: A tool for visual ranking analysis in spatial multicriteria problems", Proceedings of 13th International Conference on Information Visualisation, **2009**, Barcelona, Spain, pp.393-402.

24. Z. Rong, L. Bin and L. Sifeng, "A new model for complete ranking problems in MCDA based on multi-graded dominance relations", Proceedings of 6th International Conference on Fuzzy Systems and Knowledge Discovery, **2009**, Tianjin, China, pp.46-51.
25. Y. Zhang, Z. P. Fan and Y. Liu, "A method based on stochastic dominance degrees for stochastic multiple criteria decision making", *Comput. Ind. Eng.*, **2010**, *58*, 544-552.
26. W. T. Lin, "Earthquake-induced landslide hazard monitoring and assessment using SOM and PROMETHEE techniques: A case study at the Chiufenershan area in Central Taiwan", *Int. J. Geogr. Inform. Sci*, **2008**, *22*, 995-1012.
27. C. A. V. Cavalcante and A. T. de Almeida, "A multi-criteria decision-aiding model using PROMETHEE III for preventive maintenance planning under uncertain conditions", *J. Qual. Mainten. Eng.*, **2007**, *13*, 385-397.
28. D. Zhou, S. Sun and Q. Wang, "A new method for optimal configuration of weapon system", Proceedings of 4th International Symposium on Advances in Computation and Intelligence, **2009**, Huangshi, China, pp.487-493.
29. Z. S. Andreopoulou, T. Koutroumanidis and B. Manos, "The adoption of e-commerce for wood enterprises", *Int. J. Bus. Inform. Syst.*, **2009**, *4*, 440-459.
30. X. C. Ge and H. Liu, "The evaluation of education institutes' performance by using PROMETHEE", Proceedings of 1st IEEE International Conference on Information Science and Engineering, **2009**, Nanjing, China, pp.3490-3493.
31. A. Albadvi, "Formulating national information technology strategies: A preference ranking model using PROMETHEE method", *Eur. J. Oper. Res.*, **2004**, *153*, 290-296.
32. J. Ma, Q. Zhang, Z. Fan, J. Liang and D. Zhou, "An approach to multiple attribute decision making based on preference information on alternatives", Proceedings of 34th Hawaii International Conference on System Sciences, **2001**, Maui (HI), USA, Vol.3, p.3024.
33. H. Zhao, "Study on group decision making based on different preference information", Proceedings of 1st International Workshop on Database Technology and Applications, **2009**, Wuhan, China, pp.614-617.
34. Q. Li, "A method for multi-criteria decision making with linguistic preference information on criteria and alternatives", Proceedings of International Colloquium on Computing, Communication, Control, and Management, **2008**, Guangzhou, China, pp.260-264.
35. R. Lahdelma, P. Salminen, "Representing incomplete preference information by probability distributions", Proceedings of 25th IASTED International Multi-Conference: Artificial Intelligence and Applications, **2007**, Innsbruck, Austria, pp.590-597.

Maejo Int. J. Sci. Technol. **2013**, *7*(03), 422-432

Maejo International Journal of Science and Technology

ISSN 1905-7873
Available online at www.mijst.mju.ac.th

Full Paper

Realisation of low-voltage square-root-domain all-pass filters

Farooq A. Khanday* **and Nisar A. Shah**

Department of Electronics and Instrumentation Technology, University of Kashmir, Srinagar, India 190 006

* Corresponding author, email: farooqsnn20@yahoo.co.in

Received: 18 July 2012 / Accepted: 8 October 2013 / Published: 24 October 2013

Abstract: Novel low-voltage first-order and second-order square-root-domain all-pass filters derived systematically by means of transfer function decomposition and state-space synthesis techniques are proposed. The employment of only a few geometric-mean cells and grounded capacitors permits the circuits to absorb shunt parasitic capacitances, which is desirable for production in monolithic form. The circuits enjoy the features of electronic adjustment of frequency characteristics, wider dynamic range and low-voltage environment operation. The filters are employed to design high-order all-pass filters using cascade approach. First-order low-pass and second-order band-pass filters, being the inherited building blocks of the proposed low-order all-pass filters are also discussed. The behaviour of the filters is evaluated through simulations using Taiwan semiconductor manufacturing company 0.25 μm level-3 complementary metal oxide semiconductor process parameters, where the most important performance factors are considered.

Keywords: analog integrated circuits, companding filters, current-mode circuits, square-root-domain filters, all-pass filters

INTRODUCTION

The downscaling of complementary metal oxide semiconductor (CMOS) processes allows operation of analog-signal processing circuits at relatively reduced voltage levels. The principal motivation for this is to reduce power consumption of the digital circuitry in mixed-mode very large scale integration systems and to prevent gate-oxide breakdown with drop-off in its thickness. In addition, low power consumption and low supply voltages are requirements of the portable electronic equipment. In contrast to the digital circuits, the decrease in the supply voltage of contemporary integrated circuit technologies often necessitates an increase in the power consumption of conventional analog circuit processors for preservation of the same dynamic range and chip area for a given bandwidth [1]. Towards this end, several techniques have been proposed for the reduction of supply voltage in analog and mixed-signal circuits [2-5].

The technique of companding (compressing-expanding) allows, under low-voltage operating condition, construction of continuous-time analog circuits with higher dynamic range per unit power consumption. In this technique linear input signal is initially compressed before it is handled by the non-linear core system. For preservation of linear operation of the whole system, the non-linear signal produced by the core system is converted to a linear output through employment of an appropriate output stage.

In recent years many researchers have endeavoured to develop companding circuits comprising log-domain and square-root-domain (SRD) topologies [6-25]. However, in most of the integrated circuit (IC) fabrication technologies motivated by the current trend of digital CMOS processes, the more economical metal oxide semiconductor field effect transistor (MOSFET) implementation of log-domain circuits is adopted. To comply with such demand and change, log-domain circuits are designed using strong inversion MOSFETs instead of weak inversion MOSFETs as the circuits based on the latter are sensitive to threshold matching and a mere kilo-hertz-range bandwidth restriction. The problems encountered in the above method were solved by realising SRD filters [13-20]. Since MOSFETs have squared current-voltage (I-V) characteristics in a strong inversion region, derived circuits are therefore known as square-root domains. Thus, the input signal is initially compressed by a square-root operator and in order to preserve the linear operation of the whole system, the non-linear signal produced by the core system is converted back to a linear output signal by employing a squared operator at the output stage. Further, the SRD circuits reduce the fabrication cost, besides eliminating the drawbacks of having high power supply voltage, high-power consumption and low frequency of operation.

The all-pass (AP) filters are among the most important building blocks of many analog signal processing applications and therefore have received due attention. These are generally used for introducing a frequency-dependent delay while keeping the amplitude of the input signal constant over the desired frequency range. During the last few years, some log-domain AP filters were proposed [21, 22]. Some SRD-based AP filters have also been reported in the literature [23-25], although the reported designs are complex, limited to first-order and devoid of electronic tunability feature. Besides, the mathematical modelling is difficult and the effective circuit operation is dependent on transistor matching performance, thus not suitable for monolithic integration. In addition, the reported designs are suited for high voltages and are thus not the candidates for contemporary low-voltage analog and mixed IC design. Based on the above facts, two simple designs for first-order and second-order AP filters are proposed in this paper, which are systematically derived using transfer function decomposition procedure and state-space technique. Compared to various SRD filtering techniques, which require both the geometric mean (GM) cells and the squarer-divider cells for their synthesis, the SRD filter design using state-space technique has the advantage of using only GM cells, resulting in canonical circuit structures with low-power consumption. In addition, the transfer function decomposition procedure, as compared to the direct synthesis, also leads to canonical circuit structures and thus enhances the low-power consumption capability [25]. The functionality of the proposed filters is verified using personal simulation computer programme with integrated circuit emphasis simulations with Taiwan semiconductor manufacturing company 0.25μm CMOS process.

PROPOSED LOW-VOLTAGE CURRENT-MODE SRD AP FILTER DESIGN

First-Order AP Filter

A first-order AP filter transfer function can be written as:

$$H(s) = k\frac{s\tau - 1}{s\tau + 1} \tag{1}$$

where τ and k are respectively time constant and gain or loss throughout the frequency response of the filter. Equation (1) after decomposition becomes

$$H(s) = k - \frac{2k}{s\tau + 1} \tag{2}$$

The second term in the preceding equation is the transfer function of first-order low-pass (LP) filter for which the state-space equations are:

$$\begin{aligned} \dot{x} &= -\frac{x}{\tau} + 2k\frac{u}{\tau} \\ y &= x \end{aligned} \tag{3}$$

The node voltages, being state variables, permits substitution of $x = V_1$ and $u = U$ in equation (3) yielding

$$\begin{aligned} \dot{V}_1 &= -\frac{V_1}{\tau} + 2k\frac{U}{\tau} \\ y &= V_1 \end{aligned} \tag{4}$$

Multiplying with constant C on both sides of equation (4), we have

$$\begin{aligned} C\dot{V}_1 &= -C\frac{V_1}{\tau} + 2kC\frac{U}{\tau} \\ y &= V_1 \end{aligned} \tag{5}$$

For a MOSFET in saturated region, the drain current is given by

$$I_{DS} = \frac{1}{2}\mu C_{OX}\left(\frac{W}{L}\right)\left(V_{GS} - V_{TH}\right)^2 = \beta\left(V_{GS} - V_{TH}\right)^2 \tag{6}$$

where β, V_{GS} and V_{TH} are transconductance parameter, gate to source voltage and threshold voltage of the MOSFET respectively. The new currents I_1, I_U and I_o are defined as

$$\begin{aligned} I_1 &= \beta\left(V_1 - V_{TH}\right)^2 \Rightarrow V_1 = \sqrt{\frac{I_1}{\beta}} + V_{TH} \\ I_U &= \beta\left(U - V_{TH}\right)^2 \Rightarrow U = \sqrt{\frac{I_U}{\beta}} + V_{TH} \end{aligned} \tag{7}$$

$$I_o = \frac{C^2}{\tau^2\beta} \Rightarrow \tau = \frac{C}{I_o\beta} \tag{8}$$

After routine manipulation, the state-space equations become

$$\begin{aligned} C\dot{V}_1 &= 2k\sqrt{I_o I_U} - \sqrt{I_o I_1} + I_T\left(2k - 1\right) \\ y &= V_1 \end{aligned} \tag{9}$$

where

$$I_T = \frac{CV_{TH}}{\tau} = V_{TH}\sqrt{I_o\beta} \tag{10}$$

Equation (9) is the complete derivation of the first-order LP filter. An examination of equation (9) reveals that it can be transformed into a circuit through interconnection of two square-root circuits, a load capacitor, some current mirrors, two additional DC-biased current sources and two n-type MOSFETs. From equation (9), it is clear that for the implementation of the proposed LP filter, a square-root circuit or GM cell is needed. According to our literature survey, among the various GM cells, the most commonly used one is given in Figure 1 [26] as it has a low-voltage requirement. The complete circuit diagram of the proposed first-order AP filter constructed as per equations (2) and (9) is as shown in Figure 2.

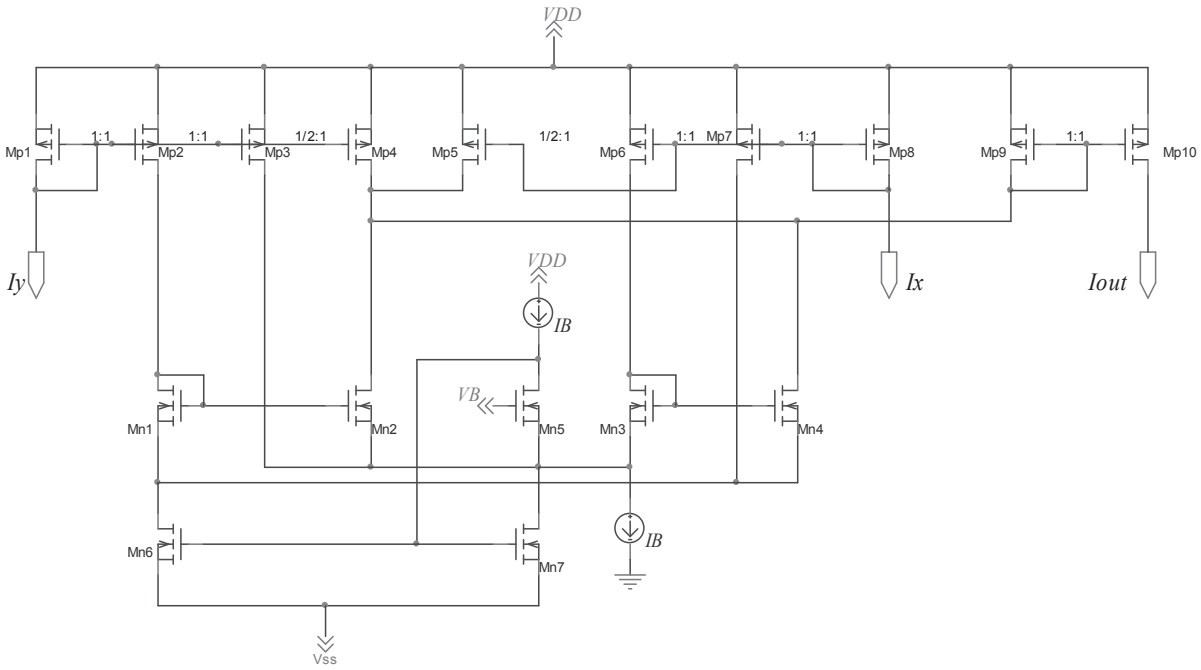

(a)

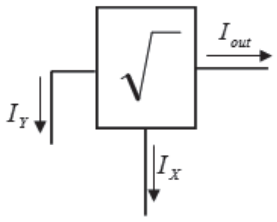

$$I_{out} = \sqrt{I_X I_Y}$$

(b)

Figure 1. (a) Low-voltage current GM cell; (b) The employed symbols

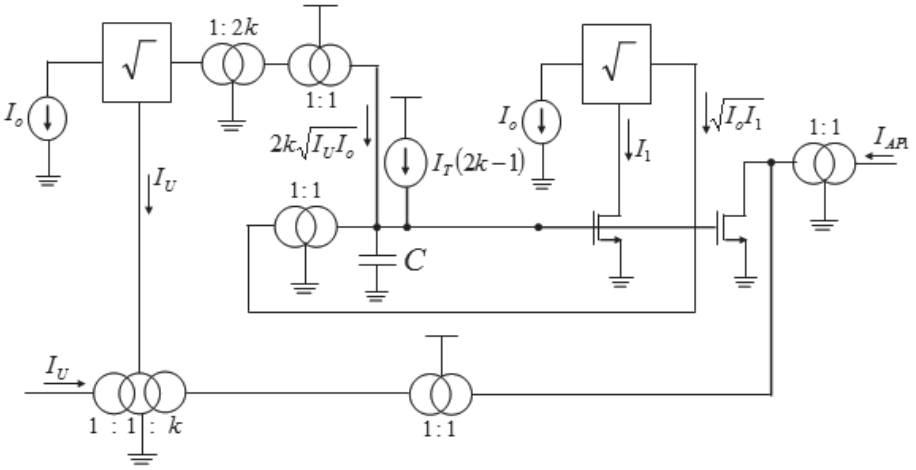

Figure 2. Proposed low-voltage SRD design of first-order AP filter

Second-Order AP Filter

The transfer function for second-order AP filter can be written as:

$$H(s) = k\frac{s^2\tau^2 - \frac{s\tau}{Q} + 1}{s^2\tau^2 + \frac{s\tau}{Q} + 1} \tag{11}$$

This after decomposition becomes

$$H(s) = \frac{Y(s)}{U(s)} = k - \frac{2k\frac{s\tau}{Q}}{s^2\tau^2 + \frac{s\tau}{Q} + 1} \tag{12}$$

The transfer function of the second-order band-pass filter is represented by the second term of the preceding equation. By following a similar procedure as introduced the pervious section, the complete derivation of the second-order band-pass filter is

$$\begin{aligned} C\dot{V}_1 &= -\sqrt{I_o I_2} - I_T \\ C\dot{V}_2 &= \sqrt{I_o I_1} - \frac{\sqrt{I_o I_2}}{Q} + 2k\frac{\sqrt{I_o I_U}}{Q} + I_S \\ y &= V_2 \end{aligned} \tag{13}$$

where

$$I_S = I_T\left(1 + \frac{2k}{Q} - \frac{1}{Q}\right) \tag{14}$$

Equation (13) can be implemented in circuit form through the use of three GM cells, two grounded capacitors, several current mirrors, three additional DC-biased current sources and three n-type MOSFETs. The proposed second-order AP filter obtained by means of equations (12) and (13) is as depicted in Figure 3. Moreover, a high-order AP filter can be implemented by

cascading low-order (first-order and second-order) AP filters and the same has been verified with the help of simulated results.

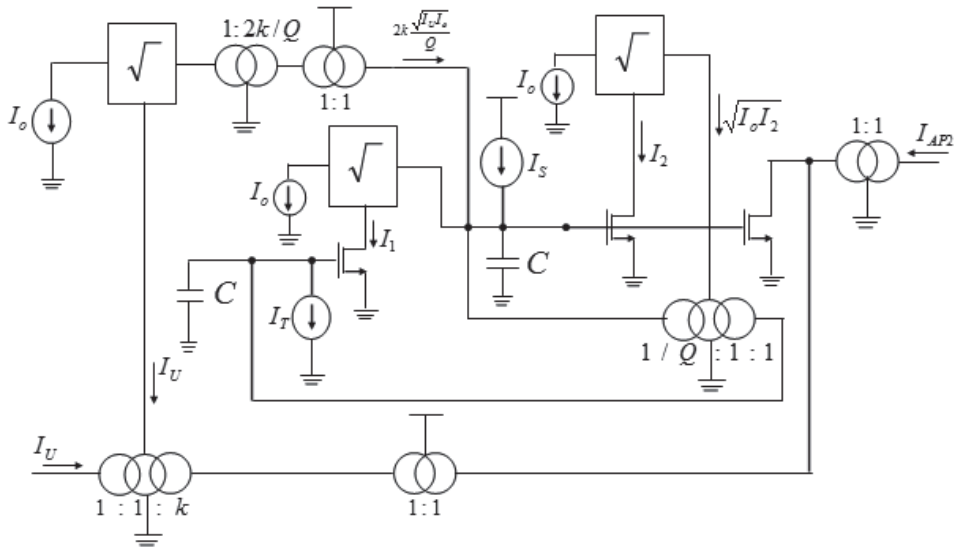

Figure 3. Proposed low-voltage SRD design of second-order AP filter

SIMULATION RESULTS

In order to verify the theoretical predictions contained in the previous section, the proposed low-order AP circuits shown in Figures 2 and 3 are simulated using Taiwan semiconductor manufacturing company 0.25µm CMOS process parameters. For both the filters, the aspect ratio of transistors used in the current mirror is W/L = 20µm/2µm and those used in the GM cell are given in Table 1.

Table 1. Aspect ratios of metal oxide semiconductor (MOS) transistors of GM cell

Transistor	W/L (µm/µm)
M_{p1}-M_{p3}	11.6/2
M_{p4}	5.8/2
M_{p5}	14/2
M_{p6}-M_{p10}	28/2
M_{n1}-M_{n4}	3.6/2
M_{n5}	20/2
M_{n6}-M_{n7}	30/2
M_{n8}-M_{n9}	10/2

The simulated value of pole frequency is found to be 100 kHz for V_{DD} = 1.5 V, V_{SS} = 0V, C_1 = C_2 = 56.27pF and I_0 = 5µA. Figures 4 and 5 depict the simulated magnitude and phase responses of first- and second-order AP filters respectively. Furthermore, the simulated frequency responses of LP and band-pass filters, the intrinsic building blocks of the low-order and high-order AP filters, are shown in Figure 6. The simulated phase responses obtained from low-order AP filters of Figures 2 and 3 are shown in Figure 7. It is worth mentioning here that the simulated ideal curves of Figure 7 were obtained by implementing equations (1) and (11)

using ideal voltage-controlled current sources with the same set of coefficients as those chosen for the SRD design.

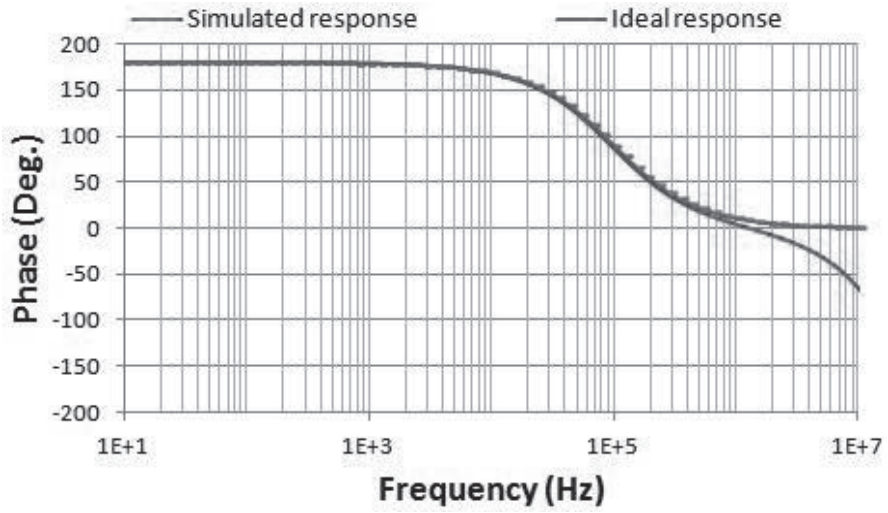

(a)

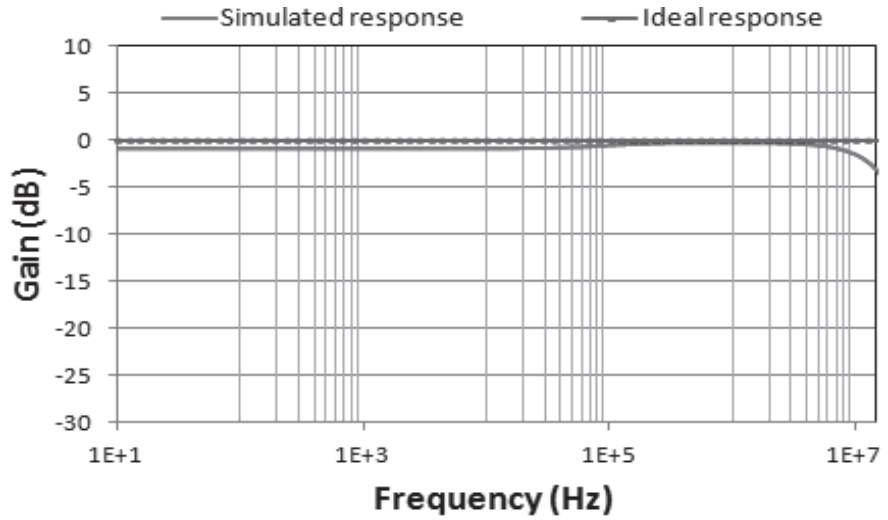

(b)

Figure 4. Simulated responses of first-order AP filter: (a) magnitude response; (b) phase response

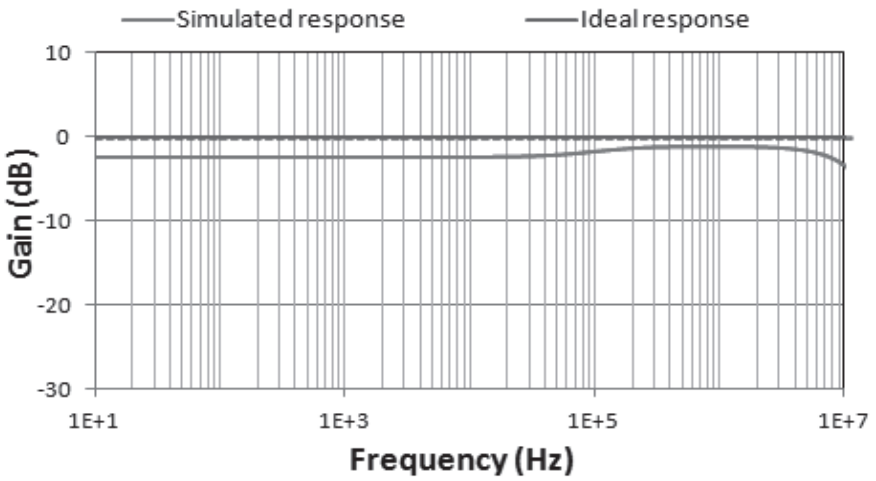

(a)

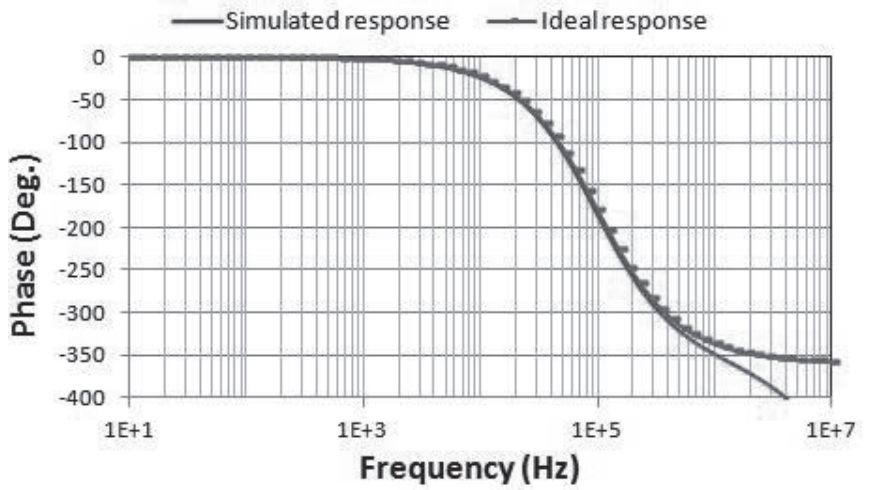

(b)

Figure 5. Simulated responses of second-order AP filter: (a) magnitude response; (b) phase response

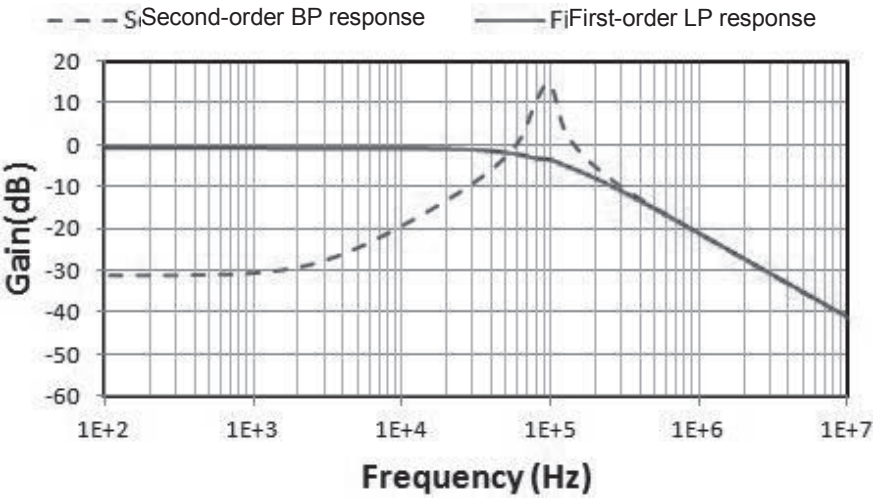

Figure 6. Simulated magnitude responses of first-order LP filter and second-order band-pass filter

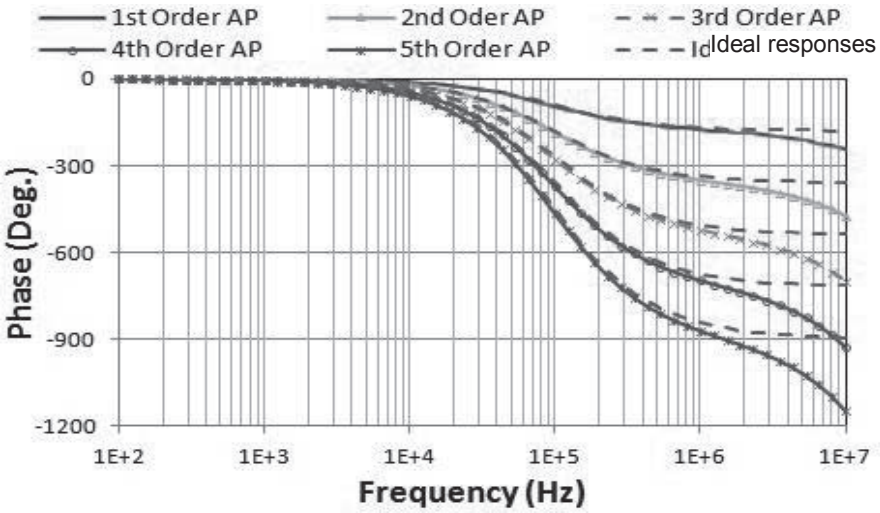

Figure 7. Simulated phase responses of higher-order AP filters

To demonstrate the electronic tunability of the proposed circuits, I_0 was varied and the results obtained for 1.25µA, 5µA and 20µA are depicted in Figure 8. Additionally, the performance of the proposed AP filters was evaluated for the parameters of linearity, noise and mismatching. The obtained results are summarised in Table 2.

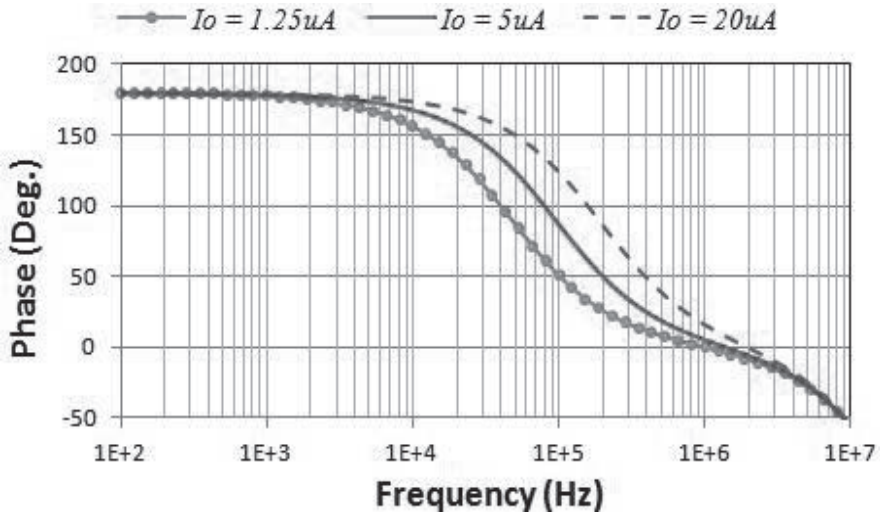

Figure 8. Demonstration of electronic tunability of the proposed AP designs

Table 2. Performance factor results for the proposed AP filters

Performance factor	Value		
	1st-Order AP	**2nd-Order AP**	**5th-Order AP**
Power dissipation	250µW	475µW	1.03mW
Dynamic range	49.2dB	48.7dB	47.1dB
Sensitivity of ω_0	76.4kHz	79.4kHz	83.5kHz

CONCLUSIONS

Novel low-voltage SRD first-order and second-order AP filter structures having electronic tunability feature and amenability for monolithic integration are presented. A systematic synthesis procedure for deriving the filter circuits together with their use in the design of high-order AP filters is also given. The circuits, besides consuming low power, consist merely of a few SRD cells and grounded capacitors.

REFERENCES

1. E. A. Vittoz, "Low-power low-voltage limitations and prospects in analog design", in "Analog Circuit Design: Low-Power Low-Voltage, Integrated Filters and Smart Power" (Ed. R. J. van de Plassche, W. M. C. Sansen and J. Huijsing), Kluwer Academic Publisher, Boston, **1995**, pp.3-14.
2. A. L. Coban, P. E. Allen and X. Shi, "Low-voltage analog IC design in CMOS technology", *IEEE Trans. Circuits Syst. I*, **1995**, *42*, 955-958.
3. E. Sánchez-Sinencio and A. G. Andreou, "Low-Voltage/Low-Power Integrated Circuits and Systems: Low-Voltage Mixed-Signal Circuits", Wiley-IEEE Press, New York, **1999**, p.207-237.
4. S. Yan and E. Sánchez-Sinencio, "Low voltage analog circuit design techniques: A tutorial", *IEICE Trans. Analog Integr. Circ. Syst.*, **2000**, *E00-A*, 1-17.
5. S. S. Rajput and S. S. Jamuar, "Low voltage analog circuit design techniques", *Circ. Syst. Mag. IEEE*, **2002**, *2*, 24-42.
6. N. A. Shah and F. A. Khanday, "Synthesis of SIFO electronically tunable log-domain universal biquad", *Frequenz*, **2008**, *62*, 30-36.
7. N. A. Shah and F. A. Khanday, "A DC stabilized log-domain nth-order multifunction filter based on the decomposition of nth-order HP filter function to FLF topology", *Int. J. Circ. Theory Appl.*, **2009**, *37*, 1075-1091.
8. N. A. Shah and F. A. Khanday, "A MISO electronically tunable log-domain universal biquad with digital programmability", *Frequenz*, **2009**, *63*, 36-41.
9. N. A. Shah and F. A. Khanday, "A multiple-input-multiple-output log-domain universal biquad filter", *Indian J. Pure Appl. Phys.*, **2012**, *50*, 928-934.
10. N. A. Shah and F. A. Khanday, "A generic current mode design for multifunction grounded capacitor filters employing log-domain technique", *Act. Pass. Electron. Compon.*, **2011**, *2011*, Article ID 313580.
11. C. Psychalinos, "Log-domain SIMO and MISO low-voltage universal biquads", *Analog Integr. Circ. Sig. Process.*, **2011**, *67*, 201-211.
12. C. Kasimis, G. Souliotis and C. Psychalinos, "Novel log-domain frequency-adaptive filter", *Int. J. Electron.*, **2012**, *99*, 197-209.
13. G. J. Yu, J. J. Chen, H. Y. Lin, B. D. Liu and C. Y. Huang, "A low-voltage low-power log-domain band-pass filter", Proceedings of IEEE International Symposium on VLSI Technology, Systems, and Applications, **2003**, Hsinchu, Taiwan, pp.219-222.
14. G. J. Yu, B. D. Liu, Y. C. Hsu and C. Y. Huang, "Design of log domain low-pass filters by MOSFET square law", Proceedings of 2nd IEEE Asia Pacific Conference on ASICs, **2000**, Cheju, South Korea, pp.9-12.

15. M. H. Eskiyerli, A. J. Payne and C. Toumazou, "State space synthesis of integrators based on the MOSFET square law", *Electron. Lett.*, **1996**, *32*, 505-506.
16. A. J. Lopez-Martin and A. Carlosena, "A 3.3 V tunable current-mode square-root domain biquad", Proceedings of IEEE International Symposium on Circuits and Systems**, 2000**, Geneva, Switzerland, pp.5-8.
17. F. A. Khanday, C. Psychalinos and N. A. Shah, "Square-root-domain realization of single cell architecture of complex TDCNN," *Circ. Syst. Sig. Process.*, **2013**, *32,* 959-978.
18. E. Stoumpou and C. Psychalinos, "Square-root domain linear transformation filters", *Int. J. Circ. Theory Appl.*, **2011**, *39*, 719-731.
19. C. Laoudias, C. Psychalinos and E. Stoumpou, "1.5 V square-root domain universal biquad filters", *Int. J. Circ. Theory Appl.,* **2013**, *41*, 307-318.
20. E. Stoumpou, F. A. Khanday, C. Psychalinos and N. A. Shah, "A low-voltage square-root domain n-th order multi-function FLF filter topology", *Analog Integr. Circ. Sig. Process.*, **2009,** *61,* 315-322.
21. A. Kircay and U. Cam, "A novel log-domain first-order multifunction filter", *ETRI J.*, **2006**, *28*, 401-404.
22. C. Psychalinos, "Realization of log-domain high-order transfer functions using first-order building blocks and complementary operators", *Int. J. Circ. Theory Appl.*, **2007**, *35*, 17-32.
23. S. Ozoguz, T. M. Abdelrahman and A. S. Elwakil, "Novel approximate square-root domain all-pass filter with application to multiphase oscillators", *Analog Integr. Circ. Sig. Process.*, **2006**, *46*, 297-301.
24. S. Olmez and U. Cam, "A novel square-root domain realization of first order all-pass filter", *Turk. J. Elec. Eng. Comp. Sci.*, **2010**, *18*, 141-146.
25. A. Kircay and M. S. Keserlioglu, "Novel current-mode second-order square-root-domain highpass and allpass filter", Proceedings of IEEE International Conference on Electrical and Electronics Engineering, **2009**, Bursa, Turkey, pp. II-242 – II-246.
26. A. J. Lopez-Martin, A. Carlosena and J. Ramirez-Angulo, "Very low voltage MOS translinear loops based on flipped voltage followers", *Analog Integr. Circ. Sig. Process.*, **2004**, *40*, 71-74.

Maejo International Journal of Science and Technology

ISSN 1905-7873
Available online at www.mijst.mju.ac.th

Full Paper

Tiger hair morphology and its variations for wildlife forensic investigation

Thitika Kitpipit* and Phuvadol Thanakiatkrai

Department of Applied Science, Faculty of Science, Prince of Songkla University, Thailand

* Corresponding author, e-mail: thitika.k@psu.ac.th

Received: 15 February 2013 / Accepted: 6 November 2013 / Published: 11 November 2013

Abstract: Tiger population has dramatically decreased due to illegal consumption and commercialisation of their body parts. Frequently, hair samples are the only evidence found in the crime scene. Thus, they play an important role in species identification for wildlife forensic investigation. In this study, we provide the first in-depth report on a variety of qualitative and quantitative characteristics of tiger guard hairs (24 hairs per individual from four individuals). The proposed method could reduce subjectivity of expert opinions on species identification based on hair morphology. Variations in 23 hair morphological characteristics were quantified at three levels: hair section, body region, and intra-species. The results indicate statistically significant variations in most morphological characteristics in all levels. Intra-species variations of four variables, namely hair length, hair index, scale separation and scale pattern, were low. Therefore, identification of tiger hairs using these multiple features in combination with other characteristics with high inter-species variations (e.g. medulla type) should bring about objective and accurate tiger hair identification. The method used should serve as a guideline and be further applied to other species to establish a wildlife hair morphology database. Statistical models could then be constructed to distinguish species and provide evidential values in terms of likelihood ratios.

Keywords: wildlife forensic science, tiger, *Panthera tigris*, hair morphology, tiger hairs, animal hairs

INTRODUCTION

Tigers (*Panthera tigris*) are critically endangered; only approximately 3.2% of the population size estimated in 1990 remains in the wild [1-5]. This is mainly due to extreme poaching of tigers for their skins and body parts. A number of organisations such as the Convention on International Trade in Endangered Species of Wild Flora and Fauna (CITES) and

the wildlife trade monitoring network (TRAFFIC) have taken an action to enforce tiger trade regulation in order to protect and manage wild tiger populations at a sustainable level [6]. National legislations are enacted in response to these international controls. Forensic science aids law enforcement by determining if seized materials contain tiger body parts.

For species identification, two reliable and court-accepted methods commonly employed by most forensic laboratories are molecular testing and microscopic examination [7, 8]. The advantage of the molecular approach is its high accuracy and sensitivity. However, it is time-consuming, expensive and destructive. Tiger hairs rather than other tissues are commonly found in a crime scene and are sometimes the only evidence found, hence the importance of the non-destructive method. The traditional hair morphological examination is a viable alternative for tiger species identification.

In an actual wildlife crime scene, it is common to find hairs from many species including domestic animals such as cat and dog. Species identification based on hair morphology has been reported in many animal species [9-15]. A wide range of hair morphological features has also been reported in these different species. However, most studies cannot be reliably used in the forensic context, as the critical process of validation is lacking. An important aspect of validation is a large enough sample size and a reporting of scientific findings with statistics such as likelihood ratios. The conventional hair morphology-based method is subjective, relying heavily on expert opinions. Comparisons can only be made when reference samples are readily available. Also, variations in hair morphology, which are biologically meaningful [10], have been overlooked in previous studies.

To our knowledge, trustworthy data on hair morphological features of tiger and quantifiable, statistics-based method for the identification of this species have never been reported. Therefore, in this study, we aim to establish a tiger hair morphological characteristic reference as well as quantify variations due to difference between individuals, body regions and hair sections. Using this information, we hope to identify the characteristics that are suitable for tiger identification. We hope this study should serve as a guideline for how hair morphology in animals should be reported in order to establish a wildlife hair morphology database to assist reporting hair evidence with probability statements.

MATERIALS AND METHODS

Sample Collection and Hair Specimen Preparation

Hair samples were obtained from Songkhla Zoo and Chiang Mai Zoo (Thailand). Hairs were collected from four mature, healthy individuals of *Panthera tigris* with no familial relationship. For each individual, six guard hairs were taken from each of the four body regions: head, dorsum, ventrum and extremities (n = 24 for each individual). These hairs were degreased using an ethanol (95%)-ether mixture (1:1) and then dried prior to further analysis.

From each hair, three types of specimen, i.e. whole mount, scale cast and cross section, were prepared for examination under a light microscope. Whole mount and cross-section specimens were prepared following the methods described by Brunner and Coman [16]. Scale casts were obtained with the clear nail polish method [13].

Morphological Examination

Qualitative characteristics

The qualitative hair characteristics that were recorded for each hair consisted of one whole- mount characteristic and eight hair-section characteristics of the proximal, middle and distal parts. The whole mount characteristic was medulla type. The eight hair-section characteristics were hair colour, cortex colour, scale margin, scale separation, scale pattern, cross-section colour, cross-section shape and cross-section medulla size. The classification of these characteristics was based on Brunner and Coman [16].

Quantitative characteristics

For whole mount specimens, six numerical features were obtained as follows:

1. The length (mm) was directly measured using a metric ruler.
2. The proximal width (μm) was the hair width measured at the middle of the proximal position of hair using a calibrated micrometre in the eyepiece.
3. The maximum width (μm) was the hair width measured at the widest point of hair using a calibrated micrometre in the eyepiece.
4. The medulla width (μm) was measured at three positions of hair (proximal, middle and distal) using a calibrated micrometre in the eyepiece.
5. Hair width index was calculated as follows [15]:

$$\text{Hair width index} = \frac{\text{Hair width at the proximal one third of hair shaft}}{\text{Maximum width along the hair shaft}} \times 100$$

6. Medulla index was calculated as follows [15]:

$$\text{Medulla index} = \frac{\text{Medulla width at the maximum width part along the hair shaft}}{\text{Hair width at the maximum width part along the hair shaft}} \times 100$$

For scale-cast specimens, two numerical features were obtained at three hair sections (proximal, middle and distal) as follows:

1. Scale width (μm) was measured from three cuticle scales randomly selected using a calibrated micrometre in the eyepiece.
2. Scale height (μm) measured from three cuticle scales randomly selected using a calibrated micrometre in the eyepiece.

For cross-section specimens, six numerical features were obtained at three hair sections (proximal, middle and distal) as follows:

1. Cuticle width (μm) was measured using a calibrated micrometre in the eyepiece.
2. Minimum diameter (μm) was measured at the minor axis at the widest point of the hair using a calibrated micrometre in the eyepiece.
3. Maximum diameter (μm) was measured at the major axis at the widest point of the hair using a calibrated micrometre in the eyepiece.
4. Medullary fraction was calculated as follows:

$$\text{Medullary fraction} = \frac{\text{Medulla diameter}}{\text{Hair diameter}} \times 100$$

5. Hair index was calculated as follows [15]:

$$\text{Hair index} = \frac{\text{Minimum diameter of cross section}}{\text{Maximum diameter of cross section}} \times 100$$

6. Cuticle index was calculated as follows [15]:

$$\text{Cuticle index} = \frac{\text{Cuticular thickness of cross section}}{\text{Maximum diameter of cross section}} \times 100$$

Statistical Analysis

The multivariate analysis of variance (MANOVA) was used to determine whether there were statistically significant differences between the different hair sections, body regions and individuals. If MANOVA results were significant, a univariate analysis of variance (ANOVA) was further carried out to determine which morphological characteristics were different. A p-value of less than 0.05 was considered significant.

RESULTS AND DISCUSSION

Tiger Hair Morphological Characteristics

Ninety-six hairs from four tigers were examined using whole mounts, cross-sections and scale casts. The descriptive macroscopic and microscopic morphological characteristics are shown in Table 1 and Table 2. A total of 23 morphological characteristics were investigated on three hair sections: proximal, middle and distal. Of these, 9 characteristics are qualitative data which are reported in the form of percentages (Table 1) and 14 characteristics are quantitative data, of which the means and standard deviations are calculated (Table 2). The overall row indicates an average percentage for each qualitative feature calculated over the three hair sections.

Whole mount

Under the whole mount examination, tiger hairs are presented in four colours: white, black, yellow and brown (Table 1). The proximal and distal hair parts are dominantly white and black, whereas black, white and yellow are almost equally found in the middle part. The existence of such colour patterns is common in felid species such as bobcat and cougar [17] while domestic animal hairs are usually unbanded [13].

The tiger hair length in this study is 14.4 mm on average (range of 5.2-45.0 mm) (Table 2). The range is broader than 17.9-20.3 mm reported by Soni *et al.* [18], which is the only previous study of tiger hair characteristics but with no intra-species variations reported. The disparity in range is probably due to the difference in sample size. A very small sample size (ten hairs) was used in the previous study, resulting in a considerably narrow range of tiger hair length compared to ours. The average hair length of tiger (14.4 mm) is shorter than those of domestic cat (25.4 mm) and domestic dog (31.9 mm) [15]. The ranges of tiger hair proximal and maximum widths are found to be 15.0-97.5 μm and 22.5- 120.0 μm respectively, giving the hair width index of 68.3±13.3. Both maximal width and hair width index are quite similar to those of domestic cat (35.3-102.9 μm and 68.6±13.4) but smaller than those of domestic dog (50.0-165.0 μm and 75.0±13.6) [15].

Tiger hair medulla is narrow, resulting in a small medulla index (35.2±11.3) when compared with that of domestic cat (67.8±7.4), domestic dog (57.5±9.4) [15], mongoose (59.6±0.4 to 79.2±0.5) [11] and wild ungulates [9, 19, 20]. On the other hand, tiger hair medulla index is larger than that of four Indian bear species (4±0.3 to 36±0.9) [12].

Table 1. Qualitative characteristics of tiger hairs. All qualitative variables are shown in percentages.

Feature	Hair colour				Cortex colour				Medulla type			
	Black	Brown	White	Yellow	Black	Brown	White	Yellow	Simple	Uniserial ladder	Absent	Mixed
Proximal	28.1	9.4	56.3	6.3	0.0	36.5	55.2	8.3	64.6	4.2	24.0	7.2
Middle	34.4	2.1	38.5	25.0	5.2	42.7	28.1	24.0				
Distal	47.9	9.4	21.9	20.8	21.9	37.5	15.6	25.0				
Overall	36.8	6.9	38.9	17.4	9.0	38.9	33.0	19.1				

Feature	Scale margin				Scale separation				Scale pattern				
	Crenate	Rippled	Smooth	Mixed	Close	Distant	Near	Mixed	Regular wave	Single chevron	Irregular wave	Streaked	Mixed
Proximal	16.7	1.0	76.0	6.3	0.0	19.8	79.2	1.0	100.0	0.0	0.0	0.0	0.0
Middle	49.0	20.8	27.1	3.1	13.5	0.0	85.4	1.0	39.6	44.4	10.8	4.2	1.0
Distal	27.1	67.7	0.0	5.2	93.8	0.0	6.3	0.0	9.5	78.3	4.9	4.2	3.1
Overall	30.9	29.9	34.4	4.9	35.8	6.6	56.9	0.7	49.7	40.9	5.2	2.8	1.4

Feature	Cross-section colour						Cross-section shape				Cross-section medulla size	
	Black	Brown	Red	White	Yellow	Mixed	Circular	Concavo-convex	Oval	Absent	Medium	Small
Proximal	39.6	0.0	1.0	22.9	20.8	15.6	50.0	29.2	20.8	2.1	81.3	16.7
Middle	40.6	1.0	1.0	15.6	28.1	13.5	41.7	27.1	31.3	2.1	84.4	13.5
Distal	45.8	0.0	2.1	16.7	20.8	14.6	55.2	27.1	17.7	11.5	79.2	9.4
Overall	42.0	0.3	1.4	18.4	23.3	14.6	49.0	27.8	23.3	5.2	81.6	13.2

Table 2. Quantitative characteristics of tiger hairs. Quantitative variables are given as means ± standard deviation and range ([]). Length, proximal width, maximum width, hair width index, and medulla index are whole hair features.

Feat.	Length (mm)	Proximal width (µm)	Maximum width (µm)	Medulla width (µm)	Scale width (µm)	Scale height (µm)	Cuticle width (µm)	Minimum diameter (µm)	Maximum diameter (µm)	Medullary fraction
Prox.				16.2±11.8 [2.5-62.5]	36.4±9.4 [14.2-74.2]	8.6±2.1 [2.5-18.3]	1.4±0.7 [0.6-5.0]	53.8±20.3 [20-162.5]	61.2±23.0 [21-192.5]	34.9±8.9 [4.0-59.5]
Midd.	14.4±7.9 [5.2-45.0]	50±19.1 [15.0-97.5]	73.1±21.1 [22.5-120.0]	26.3±13.9 [2.5-85.0]	46±12.6 [12.5-72.5]	7.3±1.7 [2.5-11.3]	1.8±1.1 [0.5-7.5]	67.4±19.8 [17-105.0]	77.6±23.0 [23-187.5]	42.8±8.7 [21.1-59.1]
Dist.				27±10.3 [5.0-52.5]	34.4±13.6 [10.0-72.7]	5.1±1.7 [1.5-10]	1.9±1.2 [0.5-6.3]	55.5±21.1 [7-157.5]	62.5±23.4 [10-197.5]	40.7±8.0 [11.5-55.6]

Feat.	Hair width index	Medulla index	Hair index	Cuticle index
Prox.			87.9±8.7 [64.0-100]	2.4±1.6 [0.7-13.3]
Midd.	68.3±13.3 [46.2-100]	35.2±11.3 [12.9-73.9]	86.9±9.8 [53.1-100]	2.4±1.6 [0.6-10.3]
Dist.			89.1±11.4 [8.75-100]	3.4±2.0 [0.7-11.9]

The medulla of tiger hairs consists of three types, viz. simple, uniserial ladder and a mixture of both (Figure 1). The medulla type of each hair does not change along the length of the hair but the width becomes narrow towards the distal end. This characteristic is quite unique for tiger and can be used to distinguish it from other species such as ungulates (filled lattice medulla), mongoose (wide medulla with cortical intrusions and vacuoles), and bear (amorphous medulla) [9, 11, 12].

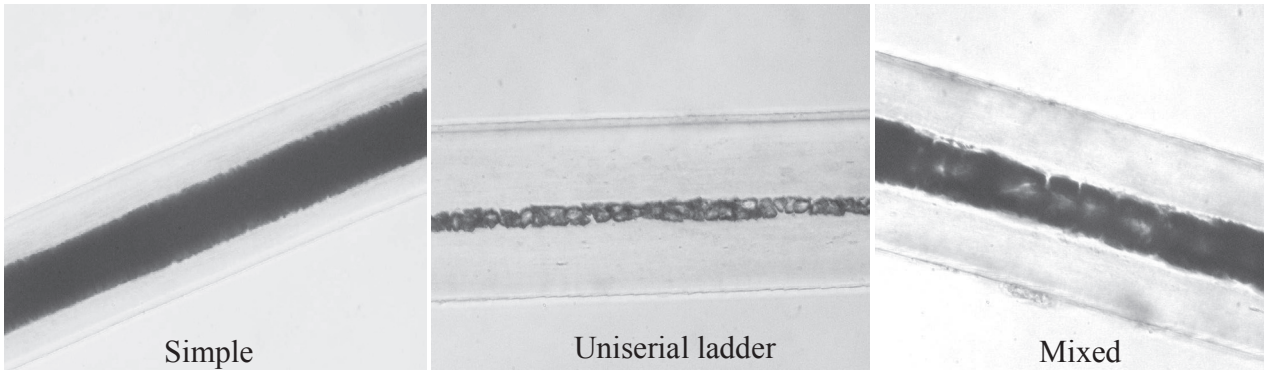

Figure 1. Three types of medulla observed in tiger hairs

Scale cast

Five types of scale pattern, i.e. regular wave, single chevron, irregular wave, streaked and a mixture of these, are observed in tiger hairs (Figure 2). It is worth noting that the scale pattern, scale margin and scale separation are distinctively different among hair parts (Table 1). The scale pattern present in the proximal part is all regular wave with a smooth margin and near separation (Figure 2). The major pattern found in the middle and distal parts is single chevron. The scale margin in the middle part is mostly crenate and shows near separation while rippled scale margin and close scale separation is the majority in the distal part. Scale margins and separations in tiger are similar to those in Indian bear, deer family and mongoose [11-13]. While tiger hairs rarely have distant scale separation, the majority of ungulates have it [9]. Single chevron found in almost half of tiger hairs in this study is quite uncommon among other species and thus can be useful for identifying tigers in wildlife crimes [9].

Tiger hair scale width and height also shows hair section variations (Table 2). The scale width in the middle part shows the highest value (46±12.6 μm) compared to other parts (proximal, 36.4±9.4 μm; distal, 34.4±13.6 μm). Scale height shows a decreasing trend towards the distal end.

Cross section

The cross-section shape of tiger hairs is found in three forms: circular, concavo-convex and oval, with mostly medium-sized medulla (Table 1). While in general the cross-section shapes are similar to Asiatic lion, Indian bear and mongoose, tiger hairs lack the oblong and dumbbell shapes found in ungulates [19]. They also lack the ellipsoidal shape found in roe deer [20], and the cigar shape found in leopard [18].

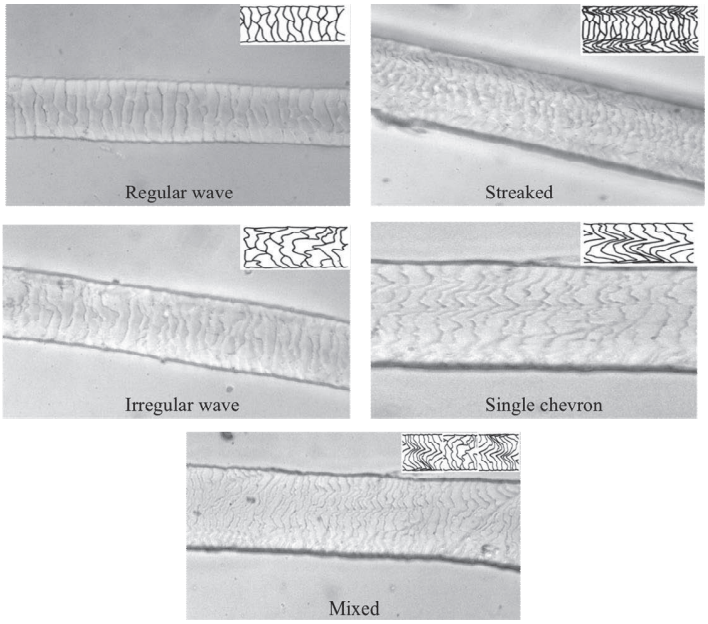

Figure 2. Five types of scale pattern observed in tiger hairs

The cross-section diameter of tiger hairs in our study ranges between 7.0-197.5 μm (Table 2), which overall is similar to that of domestic cat (min: 49.4±12.4 μm, max: 59.3±15.6 μm) but shorter than that of domestic dog (min: 76.4±20.7 μm, max: 95.3±23.7 μm) [15]. As for hair index, all three species are very similar (tiger: 86.9±9.8; domestic cat: 84.5±10.8; domestic dog: 80.1±8.9).

Variations in Tiger Hair Morphology

Three types of hair morphological variation are of interest, viz. variations due to hair section, body region and individual animal. Results of MANOVA are all highly significant ($p < 0.001$), meaning that there are significant differences between the means of the groups being compared.

Variation due to hair section

Of the 17 observed variables measured for all three hair sections, only cross-section colour, cross-section shape, and hair index are not significantly different ($p > 0.05$). All the other 14 variables are significantly different ($p < 0.001$), indicating that these characteristics are different in each hair section (Table 3). It is apparent that if measurements of scale pattern were only made in the proximal part, information regarding the variations in this characteristic would have been lost, possibly leading to misidentification of species. Therefore, when hair evidence are encountered at crime scenes, investigators must report not only the characteristics of the hairs, but also from which hair part the measurements are taken from, in order to achieve an accurate identification.

Variation due to body region

Ten of 23 observed characteristics are not significantly different between the four body regions studied. These are scale separation, cross-section shape, proximal width, maximum width, medulla width, scale width, minimum diameter, hair width index, hair index, and cuticle index. This means that these features are consistent among tiger body areas. The other 13 characteristics

measured show body region variation (Table 3). Obviously, it is expected that some variables such as length would differ significantly between the four anatomical regions, as it is normal for animals to have longer hairs in the ventral area compared with the extremities (e.g. 8.6-45.0 mm for the ventral region and 5.2-16.0 mm for the extremities in our tigers). We advise that, as performed by van den Broeck *et al.* [10], any future study that reports on hair morphological characteristics include hairs from many anatomical regions to quantify these variations as well.

Table 3. P-values of variations of tiger hairs within hair section, body region and individual for each morphological characteristic. NC = not compared. Bolded values indicate statistical significance ($p < 0.05$).

Features	Hair section	Body region	Individual
Hair colour	**<0.001**	**<0.001**	**<0.001**
Cortex colour	**<0.001**	**<0.001**	**<0.001**
Medulla type	NC	**<0.001**	**<0.001**
Scale margin	**<0.001**	**0.044**	**<0.001**
Scale separation	**<0.001**	0.062	0.150
Scale pattern	**<0.001**	**0.006**	0.876
Cross-section colour	0.849	**<0.001**	**<0.001**
Cross-section shape	0.205	0.383	**<0.001**
Cross-section medulla size	**0.022**	**<0.001**	**<0.001**
Length	NC	**<0.001**	0.598
Proximal width	NC	0.831	**<0.001**
Maximum width	NC	0.606	**<0.001**
Medulla width	**<0.001**	0.053	**<0.001**
Scale width	**<0.001**	0.245	**<0.001**
Scale height	**<0.001**	**<0.001**	**<0.001**
Cuticle width	**0.001**	**0.023**	**<0.001**
Minimum diameter	**<0.001**	0.073	**<0.001**
Maximum diameter	**<0.001**	**0.042**	**<0.001**
Medulla fraction	**<0.001**	**0.019**	**0.021**
Hair width index	NC	0.253	**<0.001**
Medulla index	NC	**0.027**	**<0.001**
Hair index	0.317	0.107	0.066
Cuticle index	**<0.001**	0.094	**<0.001**

Variation due to individual

Of the 23 observed characteristics, 19 are significantly different among the four tiger individuals. Only scale separation, scale pattern, hair length, and hair index are not significantly different between the four individuals (Table 3), indicating a low intra-species variation of these hair characteristics in tigers. Three of these four characteristics, namely scale separation, scale pattern, and hair length are also found to have high inter-species variation [10, 13, 15]. In order to distinguish between different species, a characteristic that has low intra-species variation and high inter-species variation should be used. Hence, these three characteristics should be the main variables for differentiating tiger hairs from other species. The results correspond to the FBI study on animal hairs [13], in which scale casts are recommended for separation of deer family. Other

characteristics that can help include scale count index, medulla type and medulla index, which have been reported as the most reliable characteristics in other studies [11, 12, 17]. Scale count index is not reported in this study, however, and although medulla index and medulla type are different to a certain degree from some other wildlife species and domestic animals, the high intra-species variation observed here suggests that they are of limited value in tigers. Colour patterns have also been recommended [11, 17].

Therefore, to obtain a more reliable identification of tiger hairs, a combination of the main characteristics showing low intra-species variations and other characteristics showing high inter-species variations is recommended. The establishment of a database that contains hair morphological characteristics and their variations of commonly traded or endangered species would be ideal. This database should form the basis for probability calculations (as per the DNA gold standard [21]). Species identification can then be performed using statistical procedures, such as discriminant analysis and cluster analysis, to assign weights to different hypotheses. All these will lead to increased confidence in using hair morphology in species identification and will be beneficial for wildlife forensic investigation.

CONCLUSIONS

In this study, 23 tiger hair morphological characteristics were quantified and the key features useful for tiger identification were noted. It is hoped that the output reported in this study will serve as a guideline for tiger hair identification and raise caution about using data from studies that overlook internal variations of hair morphology. We have shown that there are some variations due to hair section, body region and individual animal in most tiger hair characteristics. We expect to perform a similar study in other species to construct a database of hair morphological characteristics. With such a database, it will be possible to use statistical methods to achieve classifications based on a combination of both quantitative and qualitative hair characteristics, which should help to assign probabilities using likelihood ratios in reporting forensic species identification.

ACKNOWLEDGEMENTS

The authors acknowledge the support of the Research Fund (2008) of the Faculty of Science, Prince of Songkla University. We would like to thank Songkhla Zoo and Chiang Mai Zoo (Thailand) for providing tiger hair samples. Much appreciation is also expressed to Assistant Professor Dr. Waraporn Promwikorn.

REFERENCES

1. K. Nowell and P. Jackson, "Wild Cats: Status Survey and Conservation Action Plan", International Union for Conservation of Nature, Gland (Switzerland), **1996**.
2. R. L. Tilson and U. S. Seal, "Tigers of the World: The Biology, Biopolitics, Management and Conservation of an Endangered Species", Noyes Publications, New Jersey, **1987**.
3. J. Seidensticker, B. Gratwicke and M. Shrestha, "Regional reviews: Status of tiger", in "Tigers of the World" (Ed. T. Ronald and J. N. Philip), 2nd Edn., William Andrew Publishing, Boston, **2010**, Ch. 4.
4. V. Morell, "Wildlife biology: Can the wild tiger survive?", *Science*, **2007**, *317*, 1312-1314.

5. V. G. Heptner and A. A. Sludskii, "Mammals of the Soviet Union Volume II, Part 2: Carnivora (Hyaenas and Cats)", Amerind Publishing, New Delhi, **1992**.
6. G. Hemley and J. A. Mills, "The beginning of the end of tigers in trade?", in "Riding the Tiger: Tiger Conservation in Human-dominated Landscapes" (Ed. J. Seidensticker, S. Christie and P. Jackson), Cambridge University Press, Cambridge, **1999**, Ch. 14.
7. L. Wilson-Wilde, "Combating wildlife crime", *Forensic Sci. Med. Pathol.*, **2010**, *6*, 149-150.
8. A. Linacre and S. S. Tobe, "An overview to the investigative approach to species testing in wildlife forensic science", *Investig. Genet.*, **2011**, *2*, 2-9.
9. A. M. D. Marinis and A. Asprea, "Hair identification key of wild and domestic ungulates from southern Europe", *Wildlife Biol.*, **2006**, *12*, 305-320.
10. W. van den Broeck, P. Mortier and P. Simoens, "Scanning electron microscopic study of different hair types in various breeds of rabbits", *Folia Morphol.*, **2001**, *60*, 33-40.
11. V. Sahajpal, S. P. Goyal, R. Raza and R. Jayapal, "Identification of mongoose (genus: *Herpestes*) species from hair through band pattern studies using discriminate functional analysis (DFA) and microscopic examination", *Sci. Justice*, **2009**, *49*, 205-209.
12. V. Sahajpal, S. P. Goyal, R. Jayapal, K. Yoganand and M. K. Thakar, "Hair characteristics of four Indian bear species", *Sci. Justice*, **2008**, *48*, 8-15.
13. D. W. Deedrick and S. L. Koch, "Microscopy of Hair Part II: A Practical Guide and Manual for Animal Hairs", *Forensic Sci. Comm.*, **2004**, *6*, N3.
14. E. O. Espinoza, B. W. Baker, T. D. Moores and D. Voin, "Forensic identification of elephant and giraffe hair artifacts using HATR FTIR spectroscopy and discriminant analysis", *Endang. Species Res.*, **2008**, *9*, 239-246.
15. H. Sato, H. Matsuda, S. Kubota and K. Kawano, "Statistical comparison of dog and cat guard hairs using numerical morphology", *Forensic Sci. Int.*, **2006**, *158*, 94-103.
16. H. Brunner and B. J. Coman, "The Identification of Mammalian Hair", Inkata Press, Sydney, **1974**.
17. R. L. Harrison, "Evaluation of microscopic and macroscopic methods to identify felid hair", *Wildlife Soc. Bull.*, **2002**, *30*, 412-419.
18. V. C. Soni, Y. Ashalatadevi and D. Nishith, "Hair structure is an ideal criterion to identify various species of genus *Panthera*", *J. Tissue Res.*, **2004**, *4*, 161-163.
19. V. Sahajpal, S. P. Goyal, M. K. Thakar and R. Jayapal, "Microscopic hair characteristics of a few bovid species listed under Schedule-I of Wildlife (Protection) Act 1972 of India", *Forensic Sci. Int.*, **2009**, *189*, 34-45.
20. D. Kulak and M. Wajdzik, "Morphological characteristics of hairs in the roe deer (*Capreolous capreolus* Linneus, 1758) from the Polish part of the Carpathian mountains", *Electron. J. Polish Agric. Univ.*, **2006**, *9*(4).
21. E. Ziętkiewicz, M. Witt, P. Daca, J. Zebracka-Gala, M. Goniewicz, B. Jarząb and M. Witt, "Current genetic methodologies in the identification of disaster victims and in forensic analysis", *J. Appl. Genet.*, **2012**, *53*, 41-60.

Maejo Int. J. Sci. Technol. **2013**, *7*(03), 444-455

Maejo International Journal of Science and Technology

ISSN 1905-7873
Available online at www.mijst.mju.ac.th

Full Paper

Determining the size and location of longans in bunches by image processing technique

Chawaroj Jaisin [1], Siwalak Pathaveerat [1, 2,*] and Anupun Terdwongworakul [1, 2]

[1] Department of Agricultural Engineering, Faculty of Engineering at Kamphaengsaen, Kasetsart University, Kamphaengsaen, Nakhon Pathom 73140, Thailand
[2] The Centre of Excellence for Agricultural and Food Machinery, Kasetsart University, Kamphaengsaen, Nakhon Pathom 73140, Thailand

* Corresponding author, e-mail: fengslp@ku.ac.th

Received: 14 November 2012 / Accepted: 11 November 2013 / Published: 20 November 2013

Abstract: An experimental sorting system was developed for bunches of longan fruits by using an image processing technique. Specifically, a machine-vision system was developed for determining the size and location of individual longans in the bunch. The experimental system involved the use of a camera with a charge coupled device to record images of longan fruits in bunches, which were subsequently converted into digital data using a TV card installed within a microcomputer. The analysis was performed with an image processing software which determined the size and location of each individual longan. The HSB (hue, saturation and brightness) colour model was adapted to the images of longan fruits in bunches, including branches and leaves, to separate the objects of interest from the background. The images of longans were further processed to eliminate noise and convert the images to gray scale while a Canny edge detector was operated as an image processing tool to detect edges in the images of longan fruits. Since the shape of longans is roughly circular, a circular Hough transform was also applied to the images in searching for longans. The results show that the overall margin of error of the size determination using the developed image processing technique, as compared to actual sizes of longan fruits, was less than 10%. In addition, the aforementioned image technique could locate 90% of individual longans which were not overlapped and detect 79% of the overlapped longan fruit in the images.

Keywords: image processing, longan, sorting system, circular Hough transform

INTRODUCTION

Longan (*Dimocarpus longan* Lour., *Euphoria longana* Lamk. or *Nephelium longana* Camb.) is considered one of the most popular fruits in Thailand. Fresh longan contains 81% water, 17% carbohydrate and 1% protein [1], and provides an assortment of nutrients such as glucose, sucrose, fructose and vitamins C, B1 and B2 [1, 2]. In Thailand, there are two kinds of longan products: fresh longan and processed longan (dried longan and freeze-dried longan). In 2012, Thailand exported more than 600,000 tons of fresh and processed longan, with a total value exceeding US$650 million [3].

One of the most important postharvest operations is quality evaluation, in which fruits are sorted based on size, colour, degree of maturity, shape, and defect. Such an operation requires several parameters to be quickly identified and managed at the same time. The efficiency and effectiveness of sorting governs the quality standard of the product, which in turn determines its marketability [4]. Accordingly, there is a need for a robust, consistent, rapid and cost-effective sorting method.

One of the major postharvest operations for longan is size sorting and trimming of fruits in bunches. While the sizing of fresh longan is customarily done by either diameter sizing or weight sizing [5], Thai agriculturists have a preference for diameter sizing in grading whole bunches of fresh longan [6]. This operation is currently done by hand as follows [6]. A sorter picks up a single branch containing about 10 fruits and visually inspects them to determine the size. If undersized fruits are detected, the fruit size is checked with a circular template and the undersized fruits trimmed off. Each branch is graded based on the size of the majority of the fruits in the branch. The sorter then combines roughly 10 sorted branches to form a large bunch weighing approximately 1 kg. This sizing and trimming operation is time-consuming, labour-intensive, inconsistent and requires expert sorters. Therefore, it would be desirable to develop an automatic sorting and trimming machine to perform such operation. The first step in developing such a machine is to develop a system that can determine the size and location of longans in a small bunch on a single branch.

Machine-vision is an electro-optical technique that can be used to determine the size and location of multiple objects. In this technique, the reflectance characteristic of a product illuminated by a light source can be determined using a visible-wavelength camera equipped with a charge coupled device (CCD) which assesses the image by either an area-scan or a line-scan. Various image processing techniques have been used to determine the size, location, and shape of objects. In agricultural applications, several researchers have used the machine-vision technique to locate fruits on trees.

Jiménez *et al.* [7] presented a comprehensive review of various machine-vision techniques used by a number of researchers to locate fruits on trees in orchards. Slaughter and Harrel [8] developed a classification model that used only colour information in a digital colour image to discriminate oranges from the natural background of an orange grove. Zhao *et al.* [9] presented methods of locating both red and green apples in cluttered environments on a single- image frame. They presented a procedure and selected textural properties and redness as the image processing tool for locating apples in an image. Vaysse *et al.* [10] presented a method for determining the size and colour of fruits in shipping bins. Computation of the gradient of luminance in a colour image was used to determine a geometrical model. They applied the technique to apples and were successful in estimating the size of the fruits with only 10% false detection.

Whittaker *et al.* [11] used circular Hough transform (CHT) to locate and identify tomatoes in an image that had been acquired under natural field conditions. Using a modified CHT method, they were able to locate tomatoes based on shape and not colour, even when the scenes contained substantial background noise. In another example, Rizon *et al.* [12] applied the separability filter and CHT technique to identify circular-shaped objects in a noisy and cluttered image.

The problem of determining the size and location of longan fruits in bunches is somewhat different from that for other kinds of fruits on trees in natural settings, where there is usually a greater extent of noise, lighting variation and interfering objects in the background. Longan fruits and branches are a highly uniform light brown colour and, fortunately, longan is fairly circular-shaped. Thus, image processing and CHT technique can be utilised for sizing and locating longans in bunches. Briefly, this study aims to develop a practical and much-needed method for determining the sizes and locations of longans in a bunch. Although the method is based on known image processing techniques, the information gained would be very useful for further development of automatic sorting and packaging (bunching) of longan for export. The results should include less time used for sorting, greater accuracy of size and improved competitiveness in the global marketplace.

MATERIALS AND METHODS

Hardware

The system consisted of a CCD camera (VCC-4795PE, Sanyo), which was mounted in front of a controlled light box at a distance of 35-50 cm from the target. The CCD provided a resolution of 540 horizontal TV lines. Three 14W fluorescent energy-saving lamps (Essential model, CDL E27, 220-240V, 1CT, Philips) with reflective covers were mounted on three sides of the box (top, left and right) to provide a uniform light intensity with minimal shadows. The interior surfaces of the controlled light box were covered with white fabric, except the background, which was covered with black fabric. The CCD captured the image when the frame grabber (FlyTV-34FM Tuner PCI, LifeView) commanded and returned image signals to the frame grabber. The image signals were converted into digital signals by the frame grabber. Next, the digital image signals were sent to a microcomputer for analysis (Figure 1). The digital image was constructed using an AMD Sempron 2200+ processor with a clock speed of 1.8 GHz and 768MB RAM with a clock speed of 400 MHz. The operating system was Microsoft Windows XP. The image was fed into the light box controller and the whole longan bunch was evaluated. The grade of each bunch was defined using three indicators: AA grade, A grade and B grade.

Software

The analysis was performed with a developed image-processing software. The computer programme was written for a specific application in locating each longan and determining its size. Figure 2 shows the entire processing procedure. The first step was to obtain the input image of a bunch of longans in RGB (red, green, blue) colours with a resolution of 640 × 480 pixels at 96 dpi (Figure 3). The image was acquired by the CCD camera and the digital data of the image were obtained by the frame grabber. The image consisted of longans, foliage and branches, but only the longans were of interest. The next step was therefore to eliminate the foliage and branches as much as possible. The foliage can be eliminated from the image by using the colour threshold. HSB (hue, saturation and brightness) thresholding was chosen as the tool to eliminate the foliage

in the image because the difference between green foliage and brown longans is relatively strong. The threshold value was calculated using iterative threshold selection [13].

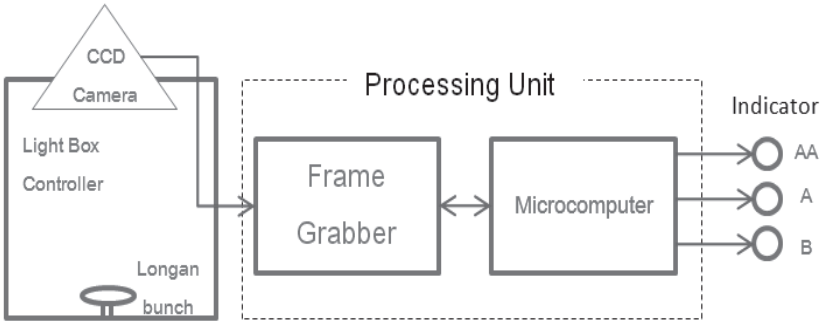

Figure 1. Experimental diagram for longan evaluation system

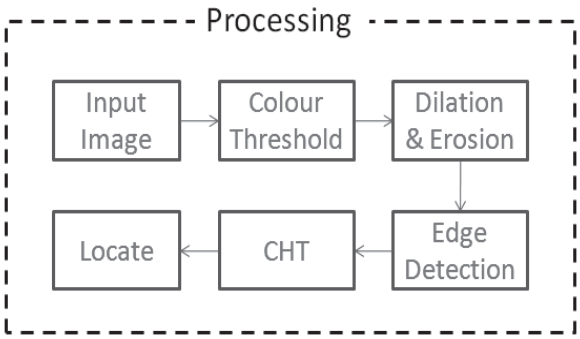

Figure 2. Block diagram of image processing steps

Figure 3. Longans in bunch with leaves and branches

Figure 4(a) shows the image after the green leaves have been removed by colour thresholding. It is more difficult to eliminate the branches by colour thresholding because the colour of the brown branches is not much different from that of the longans. However, due to the prominent difference in thickness between the branches and the longans, the technique of dilation and erosion can be used to solve this problem. In this process, the image was first converted into

a grayscale image (Figure 4(b)). Then a thin erosion process [14] was performed to erode away the thin branches (Figure 5(a)). Since the erosion process also eroded away the perimeters of the longans, it was necessary to perform a dilation process [14] to restore the previous size of the longans (Figure 5(b)) before commencing the next procedure.

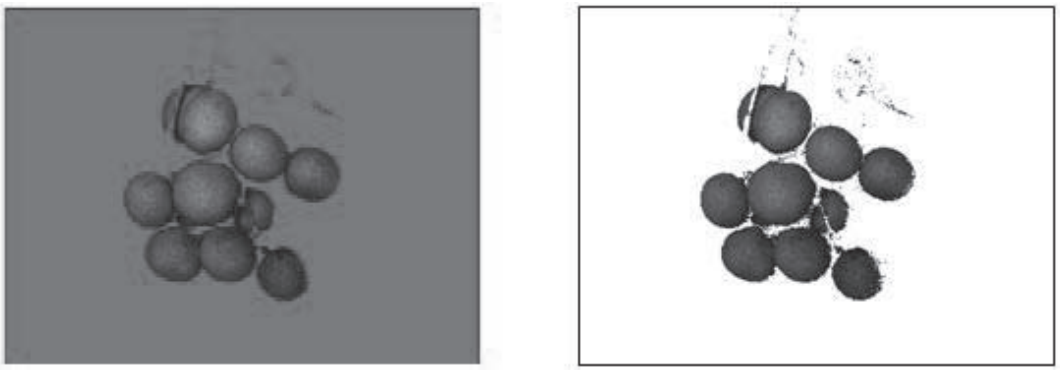

(a) (b)

Figure 4. Image of longans: (a) without green leaves; (b) without leaves in grayscale

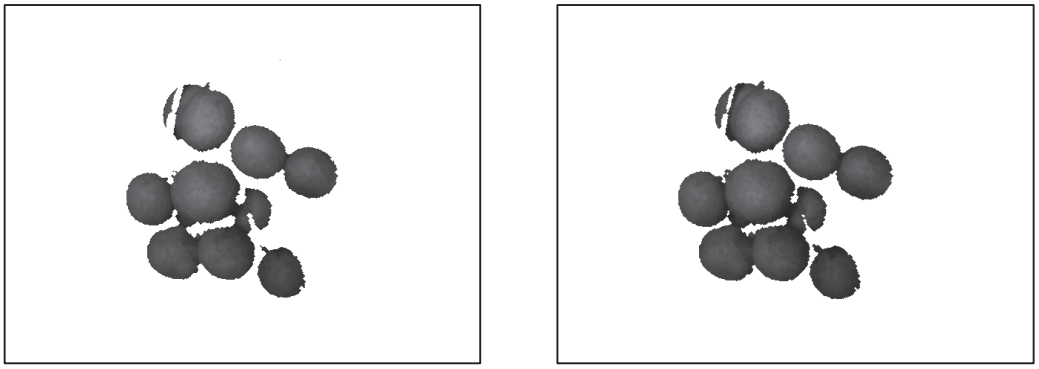

(a) (b)

Figure 5. Image of longans: (a) after thin erosion process; (b) with restored size after dilation process

The next step was edge detection. The purpose of edge detection in general is to significantly reduce the amount of data in an image while preserving the structural properties to be used for further image processing. The Canny edge detection algorithm [15] was selected because it is one of the most commonly used image processing tools that detect edges in a very robust manner. Applying the Canny edge detection algorithm to the grayscale image of longans in Figure 5(b) resulted in an image containing only the edges of the fruit (Figure 6). Then the resolution of the edge image was reduced to 160 × 120 pixels in order to minimise the processing time in the next step. The CHT technique was then used to determine the location and size of each longan from the edges. A brief description of the CHT technique is provided below.

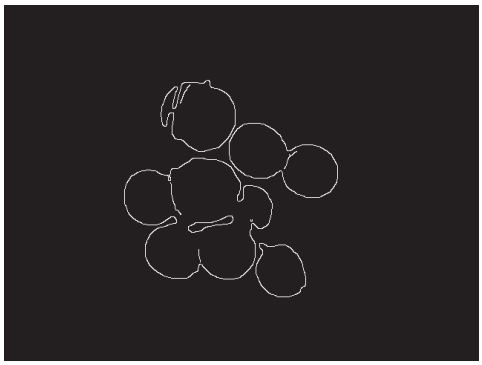

Figure 6. Image of only the edges of longans

In Figure 6, which is the edge image, a circle with a chosen radius was drawn at each edge point with the centre at that edge point. A circle with radius R and centre of pseudo circle (a, b) was described with the parametric equations (1) and (2) [16, 17]:

$$x = a + R\cos\theta \quad (1)$$

$$y = b + R\sin\theta \quad (2)$$

where x and y are coordinates on a two-dimensional matrix and θ is the angle that sweeps through the full 360-degree range. An example of the CHT is demonstrated in Figure 7; each point in the geometric space (left) generates a circle in the parameter space (right). At any coordinates where the perimeter of the drawn circle passes through, the frequency of occurrence is incremented in an accumulator matrix which has the same size as the parameter space. The accumulator contains numbers corresponding to the number of circles passing through the individual coordinates (xn, yn). Thus, the highest numbers correspond to the centres of the circles in the image. For example, if there is a circle with radius R1 and centre (x1, y1) in the image, the CHT algorithm that draws circles with radius R1 will give the highest number of occurrences at (x1, y1) because all the circles drawn with centres on the perimeter of that circle will intersect at (x1, y1). The centres of the circles were obtained by means of thresholding the values at individual points in the accumulator matrix.

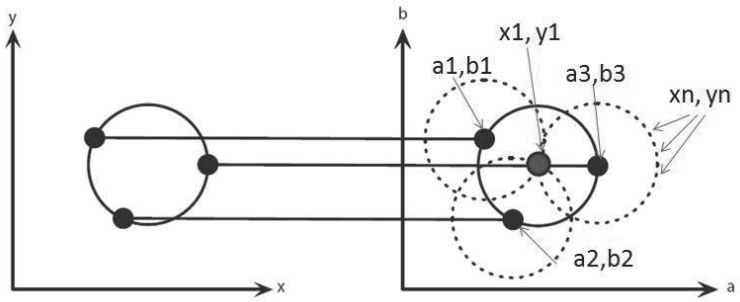

Figure 7. A CHT from the x,y-space (left) to the parameter space (right)

In an image of a fruit bunch (Figure 6), the circles may not intersect exactly at the centre, resulting in groups of high-value points that represent candidates for the centres. The following thresholding procedure was developed to locate the centres. The thresholding of values in the accumulator matrix was performed by first finding the maximum value in the matrix and then removing all the values in the matrix that were below 0.6 of the maximum (Figure 8(a)). Then the

average of the values of the remaining points was calculated and all the remaining points with values below the average value were eliminated. This process resulted in a number of small groups of high-value points. The point with the maximum value in each group was selected as the candidate for the centre of the circle (fruit). The last step was to check each point by drawing the corresponding circle and checking the colour (hue value) of each pixel in the circle to determine if the majority of the pixels matched the colour of the fruit (Figure 8(b)).

In an image where there were circles of different radii such as an image of longans with different sizes, the CHT would be performed repeatedly with a different radius each time. In the case of longans, the range of size is known, i.e. between 15-35 mm. Therefore the CHT was performed from the minimum radius (R_{min}) to the maximum (R_{max}) with one-pixel increments. At the end of the iterations, the centres of all the circles with radii within the range of R_{min} and R_{max} would be found. Knowing the location of each centre and its corresponding radius, the circles could be mapped on the original image (Figure 9).

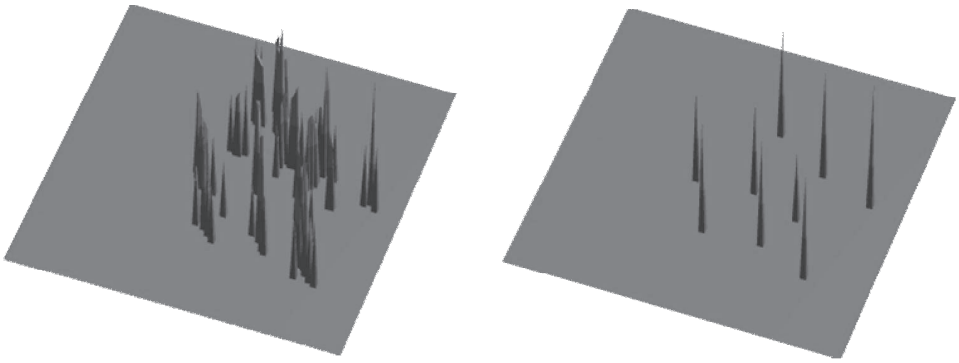

(a) (b)

Figure 8. Surface plots of: (a) all candidates for the centre of each longan in a bunch; (b) true centre of each longan in a bunch

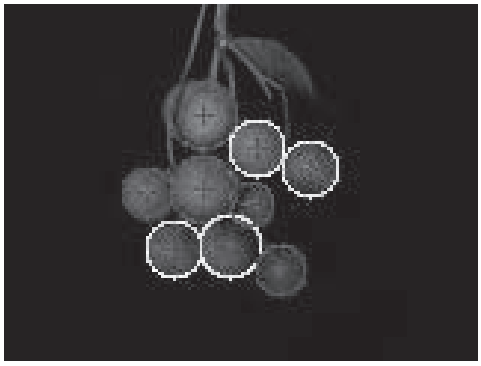

Figure 9. Locations and sizes of longans (circles) found by CHT

ImageJ software [18] was used to perform the first few steps of the image processing up to the end of Canny edge detection. A separate software programme was developed using Borland C++ Builder 5.0 [19] to perform the CHT, the procedure to identify the fruit centres and to draw the circles on the image. The total time to complete the process, starting from inputting the edge line information to the completion of drawing the circles on the image, was approximately 1 sec. This processing speed, even with a personal computer, is acceptable for online sorting of fruit bunches.

Evaluation of the System

The above image processing system was evaluated by processing a total of 140 images of longan bunches. In these images, 997 longans were observed with 658 longans seen as whole fruits (not overlapped) and the remaining partially seen (overlapped). The evaluation was divided into three parts as follows.

Accuracy evaluation of detection of individual fruits in bunch

The system was first evaluated for the ability to detect the individual fruits in a bunch for all images. The performance of the system was tested separately for accuracy in detecting only longans that appeared as whole fruits and those seen as partly overlapped fruits. The overall accuracy was a combination of both performance results.

Evaluation of the accuracy of size determination

A calibration equation was built by regression analysis and used in the determination of the actual size or diameter of individual longans from the measured size in the images. A description of the regression model is as follows. The CCD camera was mounted on an adjustable-length stand. A piece of circular paper was placed on the platform opposite the camera and in the line of sight of the camera lens. The camera was mounted 45 cm away from the paper. The image of the paper was taken, processed and recorded three times. This procedure was repeated for paper sizes of 2.5, 2.8, 3.0, 3.2, 3.5 and 4.0 cm in diameter. The obtained values were constructed as linear equations using Microsoft Excel. The actual size (cm) of the circular paper was submitted as an independent variable and the size measured from the image (pixel) as a dependent variable in the regression analysis. The obtained equation was used to convert the size of the fruit in the image into a determined size, which is the fruit diameter determined by the machine-vision system.

The overall accuracy of size measurement of a group of longans is defined as shown in equation (3):

$$\text{Overall accuracy (\%)} = \frac{100}{n}\sum_{i=1}^{n}\frac{Dd_i}{Dt_i} \qquad (3)$$

where n is the number of longans, and Dd_i and Dt_i are the determined and true diameters of the i^{th} fruit respectively. The evaluation of the size determination was also performed separately for whole fruit and partially seen fruit in the images.

Evaluation of sorting performance based on average fruit size in bunch

Commercially, longans in a bunch command a higher price than individual longans. The National Bureau of Thai Agricultural Commodity and Food Standards [4] classifies longan in a

bunch into five grades by counting the number of fruits per a unit weight, for example fewer than 85 fruits/kg being 1st grade and 85-94 fruits/kg being 2nd grade. The local merchants, however, prefer to measure the diameter because it is easier and faster. The local marketing system classifies longan into three sizes, AA, A and B, for commercial marketing purpose. The AA size is the largest with an average diameter of more than 31 mm. Size A is between 27-31 mm and size B is less than 27 mm [5]. So in practice longan is sorted based on visual inspection of each bunch and the longan size that outnumbers other sizes will represent the bunch grade. Therefore, the third part of the performance test was to evaluate the ability of the system to grade bunches of longan as compared with manual sorting by an experienced sorter.

Each bunch (or image) of longan was first pre-sorted by an experienced sorter into one of three grades (AA, A or B), which refer to the sizes used in current commercial marketing practices. For example, a bunch of longan was judged as grade AA when most of the individual longans were of grade AA. Then they were sorted using the machine-vision system, by which individual fruits (both whole fruits and partially seen fruits) in the bunch were determined for their size and number. The number of correctly sorted bunches was recorded and evaluated for the overall sorting performance by the weight purity index (P_w), as shown in equation (4) [20]:

$$P_w = \sum_i P_{gi} W_i \quad (4)$$

where P_{gi} is the fraction of correct bunches in grade i and W_i is the weight function of grade i. In this case, W_i was given the highest weight for grade AA, as the price of this grade is highest. Grades A and B were assigned less weight in descending order.

RESULTS AND DISCUSSION

Accuracy Evaluation of Individual Fruit Detection in Bunch

The accuracy of individual fruit detection in the images is shown in Table 1. The image processing system could detect 576 out of 658, or 87.5%, of the longans that were not overlapped. The overlapped fruits could be detected in 211 out of 339 cases, or 62.2%. The overall accuracy of detection was 787 out of 997, or 78.9%. This is expected because the overlapped fruits had only partial edge lines. Thus, in the CHT process fewer circles were drawn from each edge line of the overlapped fruit than those drawn from the longer edge line of the whole fruit. As a result, the number of circles passing through the centre (recorded in the accumulator matrix) could, in some cases, be lower than the threshold level and therefore left out in the process of finding the centre from the accumulator matrix.

Table 1. Accuracy of detection of longans in images

Condition	Longans in images	Longans found	Accuracy (%)
Not overlapped	658	576	87.5
Overlapped	339	211	62.2
Overall	997	787	78.9

Evaluation of Accuracy of Size Determination

The readable pixels were estimated by the developed software (Borland C++ Builder 5.0) and converted into a determined size (mm), with the calibration equation obtained by regression analysis at $R^2 = 0.989$ as shown in equation (5):

$$X = \frac{Y + 8.658}{7.523} \quad (5)$$

where X is the predicted diameter (mm) of each longan and Y is the number of readable pixels of each longan from the machine-vision system.

The average percentage of accuracy of size determination, compared with the actual size of each longan, is shown in Table 2. Fruits were sorted into three size-grades according to commercial marketing practices in Thailand: AA (diameter greater than 31 mm), A (diameter between 27-31 mm) and B (diameter less than 27 mm). The percentages of accuracy (above 89%) for all cases indicate that the system can be used to determine the size of longan in relation to their actual size.

Table 2. Accuracy of size determination of longans in images

Condition	Size		
	AA	A	B
Not overlapped	96.3%	96.0%	91.8%
Overlapped	92.0%	93.3%	89.3%
Overall	92.7%	95.6%	90.7%

Note: AA = diameter >31 mm; A = diameter 27-31 mm; B = diameter <27 mm

Evaluation of Sorting Performance Based on Average Size in Bunch

The logans were sorted into three bunch-grades, i.e. AA, A and B. The sorting performance was estimated by the weight purity index. The weight function (W_i) was defined by the market values, yielding (depending on the price of each grade) 0.5, 0.3 and 0.2 for AA, A and B sizes respectively. In this experiment, 140 bunches of longan were fed into the system to be sorted into three bunch-grades. The system could correctly sort 40 bunches out of 59 bunches of AA-grade bunch, while for A and B bunch-grades, the system could correctly sort 50 out of 66 bunches and 12 out 15 bunches respectively. The total number of correctly sorted bunches was 102 out of 140. The ratio of correctly sorted bunches to the number of bunches in each grade was calculated as a fraction of correctly sorted bunches (P_{gi}). P_{gi} and W_i were then used to calculate the weight purity index (P_{wi}) to represent the performance of the sorting system for each grade. The results are shown in Table 3. The total weight purity index of the system is equal to 0.726, i.e. the performance of the sorting system is 72.6%.

Table 3. Performance of sorting system of longan in bunches

Variable	Size			Total
	AA	A	B	
Correctly sorted bunches	40 (59)*	50 (66)*	12 (15)*	102 (140)*
P_{gi}	0.678	0.757	0.8	-
W_i	0.5	0.3	0.2	1.0
P_{wi}	0.339	0.227	0.160	0.726

Note: P_{gi}= fraction of correctly sorted bunches in grade i; W_i= weight function of bunch in grade I;

P_{wi} = weight purity index of grade i

* The number in parentheses represents the total number of bunches in each grade

CONCLUSIONS

An image processing technique has been developed to locate the position and determine the size of longans in a bunch. The circular Hough transform algorithm works well for determining the centre of longan in the image with acceptable accuracy for the number of fruits detected and the size estimation. The processing time is only around 1 sec, which is acceptable for a real-time sorting and trimming operation. This technique should be useful for future development of an on-line size sorting and trimming system for longan in bunches.

ACKNOWLEDGEMENTS

This research grant was supported by the programme of Strategic Scholarships for Frontier Research Network for the Joint Ph.D. Programme for Thai Doctoral Degree from the Office of the Higher Education Commission (Thailand). The authors would also like to express their gratitude for the financial support received from the Postgraduate Education and Research Development Project in Postharvest Technology at Chiang Mai University, the Graduate School at Kasetsart University, and the Postharvest Technology Innovation Centre (PHTIC). All authors would like to dedicate the success of this work to the late Professor Bundit Jarimopas.

REFERENCES

1. Office of Agricultural Extension and Development Region 6, Ministry of Agriculture and Cooperatives, "Longan nutrition", **2010**, http://www.ndoae.doae.go.th/article2010/longan/longan_nutrition.html (Accessed: October 2013).
2. R. E. Paull and N. J. Chen, "Changes in longan and rambutan during postharvest storage", *Hort. Sci.*, **1987**, *22*, 1303-1304.
3. Office of Agricultural Economics, Ministry of Agriculture and Cooperatives, "Agricultural import export", **2013**, http://www.oae.go.th/oae_report/export_import/export_result.php (Accessed: June 2013).
4. National Bureau of Thai Agricultural Commodity and Food Standards (ACFS), Ministry of Agriculture and Cooperatives, "Agricultural Standards Act", **2008**, http://www.acfs.go.th/km/ download/ AGRICULTURAL_STANDARDS_ACT.pdf (Accessed: June 2013).

5. National Bureau of Thai Agricultural Commodity and Food Standards, Ministry of Agriculture and Cooperatives, "Longans", **2003**, http://www.acfs.go.th/standard/download/eng/longans.pdf (Accessed: June 2013).
6. B. Jarimopas, K. Boonyapen and W. Hongsiri, "The study on arrangement of the longan fruit in bunch on relation to the standard sorting and packaging", Proceedings of 5th TSAE National Conference, **2004**, Bangkok, Thailand, pp.308-314.
7. A. R. Jiménez, R. Ceres and J. L. Pons, "A survey of computer vision methods for locating fruit on trees", *Trans. ASAE*, **2000**, *43*, 1911-1920.
8. D. C. Slaughter and R. C. Harrell, "Discriminating fruit for robotic harvest using color in natural outdoor scenes", *Trans. ASAE*, **1989**, *32*, 757-763.
9. J. Zhao, J. Tow and J. Katupitiya, "On-tree fruit recognition using texture properties and color data", Proceedings of IEEE/RSJ International Conference on Intelligent Robots and Systems, **2005**, Alberta, Canada, pp.263-268.
10. P. Vaysse, G. Grenier, O. Lavialle, G. Henry, G. Khay-Ibbat, C. Germain and J. P. Da Costa, "Image processing as a tool for quality assessment of fruits in bulk shipping bins", Proceedings of Information and Technology for Sustainable Fruit and Vegetable Production, **2005**, Montpellier, France, pp.381-388.
11. D. Whittaker, G. E. Miles, O. R. Mitchell and L. D. Gaultney, "Fruit location in a partially occluded image", *Trans. ASABE*, **1987**, *30*, 591-596.
12. M. Rizon, H. Yazid, P. Saad, A. Y. M. Shakaff, A. R. Saad, M. Sugisaka, S. Yaacob, M. R. Mamat and M. Karthigayan, "Object detection using circular Hough transform", *Am. J. Appl. Sci.*, **2005**, *2*, 1606-1609.
13. M. Sonka, V. Hlavac and R. Boyle, "Image Processing: Analysis and Machine Vision", 2nd Edn., PWS Publishing, Pacific Grove (CA), **1998**, pp.127-130.
14. R. C. Gonzalez and R. E. Woods, "Digital Image Processing", 2nd Edn., Prentice Hall, Upper Saddle River (NJ), **2002**, pp.523-528.
15. J. F. Canny, "A computational approach to edge detection", *IEEE Trans. Pattern Anal. Mach. Intell.*, **1986**, *8*, 679-698.
16. N. Jain and N. Jain, "Coin recognition using circular Hough transform", *Int. J. Electron. Commun. Comput. Technol.*, **2012**, *2*, 101-104.
17. S. Liangwongsan, B. Marungsri, R. Oonsivilai and A. Oonsivilai, "Extracted circle Hough transform and circle defect detection algorithm", *World Acad. Sci. Eng. Technol.*, **2011**, *60*, 432-437.
18. M. D. Abramoff, P. J. Magalhães and S. J. Ram, "Image Processing with ImageJ", *Biophotonics Int.*, **2004**, *11*, 36-42.
19. J. Hollingworth, D. Butterfield, B. Swart and J. Allsop, "C++ Builder 5 Developer's Guide", SAMS Publishing, Indianapolis (IN), **2000**, pp.1472-1489.
20. K. Peleg, "Produce Handling, Packaging and Distribution", AVI Publications, Westport (CT), **1985**, p. 567.

Maejo Int. J. Sci. Technol. **2013**, *7*(03), 456-466

Maejo International Journal of Science and Technology

ISSN 1905-7873
Available online at www.mijst.mju.ac.th

Full Paper

On r-duals of some difference sequence spaces

Mikail Et [1], Mahmut Isik [2] and Yavuz Altin [1,*]

[1] Department of Mathematics, Firat University, 23119, Elazığ, Turkey
[2] Department of Statistics, Firat University, 23119, Elazığ, Turkey

* Corresponding author, e-mail: yaltin23@yahoo.com

Received: 8 January 2013 / Accepted: 12 November 2013 / Published: 28 November 2013

Abstract: In this paper we introduce and examine some properties of the sequence spaces $C(\Delta_v^m, \lambda, p)$, $C[\Delta_v^m, \lambda, p]$, $C_\infty(\Delta_v^m, \lambda, p)$, $C_\infty[\Delta_v^m, \lambda, p]$ and $V(\Delta_v^m, \lambda, p)$, and compute the $r\alpha$-, $r\beta$- and $r\gamma$-duals of the sequence spaces $\ell_\infty(v)$, $c(v)$ and $c_0(v)$, and the $r\alpha$- and rN-duals of the sequence spaces $C_\infty(\Delta_v^m)$ and $C_\infty[\Delta_v^m]$.

Keywords: Cesàro sequence spaces, difference sequence, dual space

INTRODUCTION

Let w be the set of all sequences of real or complex numbers and ℓ_∞, c and c_0 be respectively the Banach spaces of bounded, convergent and null sequences $x=(x_k)$ with the usual norm $\|x\|=\sup|x_k|$, where $k \in \mathbb{N}=\{1,2,\ldots\}$, the set of positive integers. Also, by bs, cs, ℓ_1 and ℓ_p, we denote the spaces of all bounded, convergent, absolutely and p-absolutely convergent series respectively.

Let $\lambda=(\lambda_n)$ be a non-decreasing sequence of positive numbers tending to ∞ such that $\lambda_{n+1} \le \lambda_n+1$, $\lambda_1=1$. The generalised de la Vallée-Poussin mean is defined by $t_n(x)=\frac{1}{\lambda_n}\sum_{k\in I_n} x_k$, where $I_n=[n-\lambda_n+1,n]$ for $n=1,2,\ldots$. A sequence $x=(x_k)$ is said to be (V,λ)-summable to a number L if $t_n(x)\to L$ as $n\to\infty$ [1]. If $\lambda_n=n$, then (V,λ)-summability and strongly (V,λ)-summability are reduced to $(C,1)$-summability and $[C,1]$-summability respectively.

The notion of difference sequence spaces was introduced by Kızmaz [2] and it was generalised by Et and Çolak [3]. Recently, the difference spaces bv_p consisting of the sequences $x=(x_k)$ such that $(x_k-x_{k-1})\in\ell_p$ have been studied in the case of $0<p<1$ by Altay and Başar [4], and in the case of $1\le p<\infty$ by Başar and Altay [5], Çolak *et al.* [6] and Başar [7]. Since then

Et and Esi [8] generalised these sequence spaces to the following sequence spaces. Let $v=(v_k)$ be any fixed sequence of non-zero complex numbers and m be a non-negative integer. Then,

$$\Delta_v^m(X)=\left\{x=(x_k)\ :\ (\Delta_v^m x_k)\in X\right\}$$

for $X=\ell_\infty$, c or c_0, where $m\in\mathbb{N}$, $\Delta_v^0 x=(v_k x_k)$ and $\Delta_v^m x=\left(\Delta_v^{m-1}x_k-\Delta_v^{m-1}x_{k+1}\right)$, and so $\Delta_v^m x_k=\sum_{i=0}^{m}(-1)^i\binom{m}{i}v_{k+i}x_{k+i}$.

The sequence spaces $\Delta_v^m(X)$ are Banach spaces normed by

$$\|x\|_\Delta=\sum_{i=1}^{m}|v_i x_i|+\left\|\Delta_v^m x_k\right\|_\infty$$

for $X=\ell_\infty$, c or c_0. Recently the difference sequence spaces have been studied by different research workers [9-29]. The Cesàro sequence spaces Ces_p and Ces_∞ were introduced by Shiue [30], and Jagers [31] determined the Köthe duals of the sequence space $Ces_p\ (1<p<\infty)$. It can be shown that the inclusion $\ell_p\subset Ces_p$ is strict for $1<p<\infty$. Later on the Cesàro sequence spaces X_p and X_∞ of non-absolute type were defined by Ng and Lee [32, 33].

Let X be a sequence space. Then X is called:

i) *Solid* (or *normal*) if $(\alpha_k x_k)\in X$ for all sequences (α_k) of scalars with $|\alpha_k|\le 1$ for all $k\in\mathbb{N}$, whenever $(x_k)\in X$;

ii) *Symmetric* if $(x_k)\in X$ implies $(x_{\pi(k)})\in X$, where π is a permutation of $\mathbb{N}$;

iii) *Sequence algebra* if $x.y\in X$, whenever $x,y\in X$.

The determination of the dual spaces is important in the theory of sequence spaces. The concepts of α-, β- and γ-duality are well known and the topology of the sequence spaces can be defined by duality. The idea of α-, β- and γ- duality was generalised by Et [34] to $r\alpha$-, $r\beta$- and $r\gamma$- duality $(r\ge 1)$. The main purpose of this paper is to introduce the $r\alpha$-, $r\beta$-, $r\gamma$- and rN-duals of some sequence spaces.

MAIN RESULTS

In this section we prove some results involving the sequence spaces $C(\Delta_v^m,\lambda,p)$, $C[\Delta_v^m,\lambda,p]$, $C_\infty(\Delta_v^m,\lambda,p)$, $C_\infty[\Delta_v^m,\lambda,p]$ and $V[\Delta_v^m,\lambda,p]$.

Definition 1. Let $m\ge 1$ and $1\le p<\infty$. We define the following sequence spaces:

$$C\left(\Delta_v^m,\lambda,p\right)=\left\{x=\left(x_k\right):\ \sum_{n=1}^{\infty}\left|\frac{1}{\lambda_n}\sum_{k\in I_n}\Delta_v^m x_k\right|^p<\infty\right\},$$

$$C\left[\Delta_v^m,\lambda,p\right]=\left\{x=\left(x_k\right):\ \sum_{n=1}^{\infty}\left(\frac{1}{\lambda_n}\sum_{k\in I_n}\left|\Delta_v^m x_k\right|\right)^p<\infty\right\},$$

$$C_\infty(\Delta_v^m,\lambda,p)=\left\{x=\left(x_k\right):\ \sup_n\left|\frac{1}{\lambda_n}\sum_{k\in I_n}\Delta_v^m x_k\right|^p<\infty\right\},$$

$$C_\infty\left[\Delta_v^m,\lambda,p\right]=\left\{x=\left(x_k\right):\ \sup_n\frac{1}{\lambda_n}\sum_{k\in I_n}\left|\Delta_v^m x_k\right|^p<\infty\right\},$$

$$V\left[\Delta_v^m,\lambda,p\right]=\left\{x=\left(x_k\right):\ \lim_n\frac{1}{\lambda_n}\sum_{k\in I_n}\left|\Delta_v^m x_k-\ell\right|^p=0\right\}.$$

We get the following sequence spaces from the above sequence spaces, giving particular values to λ, p, v, ℓ and m.

i) For $p=1$, we write $C\left(\Delta_v^m,\lambda\right)$, $C\left[\Delta_v^m,\lambda\right]$, $C_\infty(\Delta_v^m,\lambda)$, $C_\infty\left[\Delta_v^m,\lambda\right]$ and $V\left[\Delta_v^m,\lambda\right]$ instead of $C\left(\Delta_v^m,\lambda,p\right)$, $C\left[\Delta_v^m,\lambda,p\right]$, $C_\infty(\Delta_v^m,\lambda,p)$, $C_\infty\left[\Delta_v^m,\lambda,p\right]$ and $V\left[\Delta_v^m,\lambda,p\right]$ respectively.

ii) For $\lambda_n=n$ for all $n\in\mathsf{N}$ and $p=1$, we write $C\left(\Delta_v^m\right)$, $C\left[\Delta_v^m\right]$, $C_\infty(\Delta_v^m)$, $C_\infty\left[\Delta_v^m\right]$ and $V\left[\Delta_v^m\right]$ instead of $C\left(\Delta_v^m,\lambda,p\right)$, $C\left[\Delta_v^m,\lambda,p\right]$, $C_\infty(\Delta_v^m,\lambda,p)$, $C_\infty\left[\Delta_v^m,\lambda,p\right]$ and $V\left[\Delta_v^m,\lambda,p\right]$ respectively. If $x\in V\left[\Delta_v^m,\lambda,p\right]$, we say that x is Δ_v^m-strongly λ_p-summable to ℓ.

iii) In the case of $v=(1,1,1,...)$, we write $C\left(\Delta^m,\lambda,p\right)$, $C\left[\Delta^m,\lambda,p\right]$, $C_\infty(\Delta^m,\lambda,p)$, $C_\infty\left[\Delta^m,\lambda,p\right]$ and $V\left[\Delta^m,\lambda,p\right]$ instead of $C\left(\Delta_v^m,\lambda,p\right)$, $C\left[\Delta_v^m,\lambda,p\right]$, $C_\infty(\Delta_v^m,\lambda,p)$, $C_\infty\left[\Delta_v^m,\lambda,p\right]$ and $V\left[\Delta_v^m,\lambda,p\right]$ respectively.

iv) In the special case of $p=1$, $\lambda_n=n$ for all $n\in\mathsf{N}$ and $\ell=0$, we write $V_0\left[\Delta_v^m\right]$ instead of $V\left[\Delta_v^m,\lambda,p\right]$.

v) Also in the special case of $p=1$, $v=(1,1,1,...)$ and $m=0$, we write $C(\lambda)$, $C[\lambda]$, $C_\infty(\lambda)$, $C_\infty[\lambda]$ and $V[\lambda]$ instead of $C\left(\Delta_v^m,\lambda,p\right)$, $C\left[\Delta_v^m,\lambda,p\right]$, $C_\infty(\Delta_v^m,\lambda,p)$, $C_\infty\left[\Delta_v^m,\lambda,p\right]$ and $V\left[\Delta_v^m,\lambda,p\right]$ respectively.

Let X denote one of the sequence $C\left(\Delta_v^m,\lambda,p\right)$, $C\left[\Delta_v^m,\lambda,p\right]$, $C_\infty(\Delta_v^m,\lambda,p)$, $C_\infty\left[\Delta_v^m,\lambda,p\right]$ and $V\left[\Delta_v^m,\lambda,p\right]$, and let Y denote one of the sequence $C\left(\Delta^m,\lambda,p\right)$, $C\left[\Delta^m,\lambda,p\right]$, $C_\infty(\Delta^m,\lambda,p)$, $C_\infty\left[\Delta^m,\lambda,p\right]$ and $V\left[\Delta^m,\lambda,p\right]$. We note that the sequence space X is different from the sequence space Y and $X\cap Y\neq\phi$. For this, let $x=\left(k^m\right)$ and $v=\left(k\right)$; then $x\in C_\infty\left[\Delta^m,\lambda,p\right]$, but $x\notin C_\infty\left[\Delta_v^m,\lambda,p\right]$. Conversely, if we choose $x=\left(k^{m+1}\right)$ and $v=\left(k^{-1}\right)$, then $x\in C_\infty\left[\Delta_v^m,\lambda,p\right]$, but $x\notin C_\infty\left[\Delta^m,\lambda,p\right]$.

The above sequence spaces contain some unbounded sequences for $m \geq 1$. For example, the sequence $x = (k^m)$ is an element of $C_\infty[\Delta_v^m, \lambda, p]$ but is not an element of ℓ_∞.

The proof of the following two theorems can be established by using the known standard techniques; therefore we give them without proof.

Theorem 1. Let $m \geq 1$ and $1 \leq p < \infty$; then the sets of sequences $C(\Delta_v^m, \lambda, p)$, $C[\Delta_v^m, \lambda, p]$, $C_\infty(\Delta_v^m, \lambda, p)$, $C_\infty[\Delta_v^m, \lambda, p)]$ and $V[\Delta_v^m, \lambda, p]$ are linear spaces with the coordinate-wise additition and scalar multiplication of sequences.

Theorem 2. Let $m \geq 1$ and $1 \leq p < \infty$; then the following inclusions are strict.

i) $C(\Delta_v^{m-1}, \lambda, p) \subset C(\Delta_v^m, \lambda, p)$,

ii) $C[\Delta_v^{m-1}, \lambda, p] \subset C[\Delta_v^m, \lambda, p]$,

iii) $C[\Delta_v^m, \lambda, p] \subset C(\Delta_v^m, \lambda, p)$,

iv) $C(\Delta_v^m, \lambda, p) \subset C(\Delta_v^m, \lambda, q) \quad (0 < p < q)$,

v) $C_\infty(\Delta_v^{m-1}, \lambda, p) \subset C_\infty(\Delta_v^m, \lambda, p)$,

vi) $C_\infty[\Delta_v^{m-1}, \lambda, p] \subset C_\infty(\Delta_v^m, \lambda, p)$,

vii) $C_\infty[\Delta_v^m, \lambda, p] \subset C_\infty(\Delta_v^m, \lambda, p)$,

viii) $V[\Delta_v^{m-1}, \lambda, p] \subset V[\Delta_v^m, \lambda, p]$,

ix) $V[\Delta_v^m, \lambda, p] \subset C_\infty[\Delta_v^m, \lambda, p]$.

Note that $C(\Delta_v^m, \lambda, p)$ and $c(\Delta_v^m)$ overlap, but neither one contains the other. Actually the sequence $x = (k^m)$ is an element of $c(\Delta_v^m)$ but not an element of $C(\Delta_v^m, \lambda, p)$, and $x = ((-1)^k)$ belongs to $C(\Delta_v^m, \lambda, p)$ but not to $c(\Delta_v^m)$, where $c(\Delta_v^m) = \{x = (x_k) : (\Delta_v^m x_k) \in c\}$.

Theorem 3. The sequence space $C[\Delta_v^m, \lambda, p]$ is a Banach-Coordinate- or *BK*-space normed by

$$\|x\|_1 = \sum_{i=1}^{m} |v_i x_i| + \left(\sum_{n=1}^{\infty} \left(\frac{1}{\lambda_n} \sum_{k \in I_n} |\Delta_v^m x_k| \right)^p \right)^{\frac{1}{p}}, \ (1 \leq p < \infty) . \tag{1}$$

$C_\infty[\Delta_v^m, \lambda, p]$ and $V[\Delta_v^m, \lambda, p]$ are *BK*-spaces normed by

$$\|x\|_2 = \sum_{i=1}^{m} |v_i x_i| + \sup_n \left(\frac{1}{\lambda_n} \sum_{k \in I_n} |\Delta_v^m x_k|^p \right)^{\frac{1}{p}}, \ (1 \leq p < \infty) \tag{2}$$

Proof. We give the sketch of proof for $C_\infty[\Delta_v^m, \lambda, p]$. The others can be proved in the same way. Let (x^s) be a Cauchy sequence in $C_\infty[\Delta_v^m, \lambda, p]$, where $x^s = (x_i^s)_{i=1}^\infty$. Then there exists a positive integer n_0 such that $\|x^s - x^t\|_2 < \varepsilon$ for all $s, t > n_0$.

Hence (x_i^s) (for $i \leq m$) and $(\Delta_v^m(x_k^s))$ for all $k \in \mathbb{N}$ are Cauchy sequence in $\mathbb{C}$. Since $\mathbb{C}$ is complete, these sequences are convergent in $\mathbb{C}$. Suppose that $x_i^s \to x_i$ (for $i \leq m$) and $\Delta_v^m(x_k^s) \to y_k$ for each $k \in \mathbb{N}$ as $s \to \infty$. Then we can find a sequence (x_k) such that $y_k = \Delta_v^m x_k$ for each $k \in \mathbb{N}$. These x_k's can be written as

$$x_k = v_k^{-1}\sum_{i=1}^{k-m}(-1)^m\binom{k-i-1}{m-1}y_i = v_k^{-1}\sum_{i=1}^{k}(-1)^m\binom{k+m-i-1}{m-1}y_{i-m},$$

for sufficiently large k, for instance $k > m$, where $y_{1-m} = y_{2-m} = \ldots = y_0 = 0$.

Thus, $\left(\Delta_v^m\left(x_k^s\right)\right) = \left(\left(\Delta_v^m\left(x_k^1\right)\right), \left(\Delta_v^m\left(x_k^2\right)\right), \ldots\right)$ converges to $\Delta_v^m x_k$ for each $k \in \mathsf{N}$ in C. Hence $\left\|x^s - x\right\|_2 \to 0$ as $s \to \infty$. Since $\left(x^s - x\right)$, $\left(x^s\right) \in C_\infty\left[\Delta_v^m, \lambda, p\right]$ and the space $C_\infty\left[\Delta_v^m, \lambda, p\right]$ are linear, we have $x = x^s - \left(x^s - x\right) \in C_\infty\left[\Delta_v^m, \lambda, p\right]$. Hence $C_\infty\left[\Delta_v^m, \lambda, p\right]$ is complete. Since $C_\infty\left[\Delta_v^m, \lambda, p\right]$ is a Banach space with continuous coordinates, that is, $\left\|x^n - x\right\|_2 \to 0$ implies $\left|x_k^n - x_k\right| \to 0$ for each $k \in \mathsf{N}$ as $n \to \infty$, it is *BK*-space.

In the same way it can be shown that $C\left[\Delta_v^m, \lambda, p\right]$ is a *BK*-space normed by (1) and $V\left[\Delta_v^m, \lambda, p\right]$ is a *BK*-space normed by (2).

Theorem 4. The sequence space $C\left(\Delta_v^m, \lambda, p\right)$ is a *BK*-space normed by

$$\|x\|_3 = \sum_{i=1}^{m}|v_i x_i| + \left(\sum_{n=1}^{\infty}\left|\frac{1}{\lambda_n}\sum_{k\in I_n}\Delta_v^m x_k\right|^p\right)^{\frac{1}{p}}, (1 \le p < \infty)$$

and the space $C_\infty(\Delta_v^m, \lambda)$ is a *BK*-space normed by

$$\|x\|_4 = \sum_{i=1}^{m}|v_i x_i| + \sup_n\left(\left|\frac{1}{\lambda_n}\sum_{k\in I_n}\Delta_v^m x_k\right|\right).$$

Proof. The proof is similar to that of Theorem 3.

Theorem 5. The sequence spaces $C(\lambda)$, $C[\lambda]$, $C_\infty(\lambda)$ and $C_\infty[\lambda]$ are solid and hence monotone, but the sequence spaces $C\left(\Delta_v^m, \lambda, p\right)$, $C\left[\Delta_v^m, \lambda, p\right]$, $C_\infty(\Delta_v^m, \lambda, p)$, $C_\infty\left[\Delta_v^m, \lambda, p\right]$ and $V\left[\Delta_v^m, \lambda, p\right]$ are neither solid nor symmetric, nor sequence algebras for $m \ge 1$.

Proof. Let $x = \left(x_k\right) \in C_\infty[\lambda]$ and $y = \left(y_k\right)$ be sequences such that $|x_k| \le |y_k|$ for each $k \in \mathsf{N}$. Then we get

$$\frac{1}{\lambda_n}\sum_{k\in I_n}|x_k| \le \frac{1}{\lambda_n}\sum_{k\in I_n}|y_k|.$$

Hence $C_\infty[\lambda]$ is solid and hence monotone. Let $p = 1$ and $\lambda_n = n$ for all $n \in \mathsf{N}$. Then $\left(x_k\right) = \left(k^{m-1}\right) \in C_\infty\left[\Delta_v^m, \lambda, p\right]$ but $\left(\alpha_k x_k\right) \notin C_\infty\left[\Delta_v^m, \lambda, p\right]$ when $\alpha_k = (-1)^k$ for all $k \in \mathsf{N}$. Hence $C_\infty\left[\Delta_v^m, \lambda, p\right]$ is not solid. The other cases can be proved on considering similar examples.

DUAL SPACES

The definitions of the $r\alpha$-, $r\beta$-, $r\gamma$- and rN-duals of a sequence space were introduced by Et [34]. Since then the $r\alpha$-duals of some sequence spaces were studied by Bektas *et al.* [35], Chandra and Tripathy [36], and Tripathy and Sarma [37]. In this section we compute the $r\alpha$-, $r\beta$- and $r\gamma$-duals of the sequence spaces $\ell_\infty(v), c(v), c_0(v)$, the rN-duals of the sequence spaces $C_\infty(\Delta_v^m)$, $C_\infty\left[\Delta_v^m\right]$ and $V_0\left[\Delta_v^m\right]$, and the $r\alpha$-duals of the sequence spaces $C_\infty(\Delta_v^m)$ and $C_\infty\left[\Delta_v^m\right]$.

Definition 2 [34]**.** Let X be any sequence space with $1 \le r < \infty$, and define

$$X^{r\alpha} = \left\{ a = (a_k) : \sum_k |a_k x_k|^r < \infty, \text{ for each } x \in X \right\},$$

$$X^{r\beta} = \left\{ a = (a_k) : \sum_k (a_k x_k)^r \text{ is convergent, for each } x \in X \right\},$$

$$X^{r\gamma} = \left\{ a = (a_k) : \sup_n \left| \sum_{k=0}^{n} (a_k x_k)^r \right| < \infty, \text{ for each } x \in X \right\},$$

$$X^{rN} = \left\{ a = (a_k) : \lim_k (a_k x_k)^r = \lim_k a_k x_k = 0, \text{ for each } x \in X \right\} = X^N.$$

Then $X^{r\alpha}, X^{r\beta}, X^{r\gamma}$ and X^{rN} are called $r\alpha$-, $r\beta$-, $r\gamma$- and rN-duals of X respectively. It can be shown that $X^{r\alpha} \subset X^{r\beta} \subset X^{r\gamma}$ and if $X \subset Y$, then $Y^{r\eta} \subset X^{r\eta}$ for $\eta \in \{\alpha, \beta, \gamma, N\}$. If we take $r = 1$ in this definition, then we obtain the α-, β- and γ-duals of X. If $X = (X^{r\alpha})^{r\alpha}$, then X is called $r\alpha$- perfect.

Lemma 1. $x \in C_\infty(\Delta_v^m)$ implies $\sup_n \left(n^{-1} \mid \Delta_v^{m-1} x_n \mid \right) < \infty$.

Proof. Firstly, we have

$$\frac{1}{n} \sum_{k=1}^{n} \Delta_v^m x_k = \frac{1}{n} \left(\Delta_v^{m-1} x_1 - \Delta_v^{m-1} x_{n+1} \right).$$

If $x \in C_\infty(\Delta_v^m)$, then we have

$$\frac{1}{n+1} \left| \Delta_v^{m-1} x_{n+1} \right| \le \frac{1}{n} \left| \Delta_v^{m-1} x_{n+1} \right| \le \left| \frac{1}{n} \sum_{k=1}^{n} \Delta_v^m x_k \right| + \left| \Delta_v^{m-1} x_1 \right|$$

and this implies that $\sup_n \left(n^{-1} \mid \Delta_v^{m-1} x_n \mid \right) < \infty$.

Lemma 2. $\mathrm{Sup}_n \left(n^{-1} \mid \Delta_v^{m-1} x_n \mid \right) < \infty$ implies $\sup_n \left(n^{-m} \mid v_n x_n \mid \right) < \infty$.

Proof. Omitted.

Lemma 3. $x \in C_\infty(\Delta_v^m)$ implies $\sup_n \left(n^{-m} \mid v_n x_n \mid \right) < \infty$.

Proof. Proof follows from Lemma 1 and Lemma 2.

Lemma 4 [35]. Let m be a positive integer. Then

$$[\ell_\infty(\Delta_v^m)]^N = \left[c(\Delta_v^m) \right]^N = \{ a = (a_n) : v_n^{-1} n^m a_n \to 0, \ n \to \infty \}$$

and

$$[c_0(\Delta_v^m)]^N = \{ a = (a_n) : \sup_n \mid \textstyle\sum_{k=0}^{n} \binom{n+m-k-1}{m-1} v_n^{-1} a_n \mid < \infty \},$$

where

$$X(\Delta_v^m) = \{ x = (x_k) : (\Delta_v^m x_k) \in X \} \quad \text{for } X = \ell_\infty, c \text{ and } c_0.$$

Theorem 6. Let $m \ge 1$ and $1 \le r < \infty$. Then

(i) $[C_\infty(\Delta_v^m)]^{r\alpha} = U_1^{(r)}$,

(ii) $\left[U_1^{(r)} \right]^{r\alpha} = U_2^{(r)}$.

where

$$U_1^{(r)} = \left\{ a = (a_k) : \sum_{k=1}^{\infty} k^{rm} \left| v_k^{-1} a_k \right|^r < \infty \right\},$$

$$U_2^{(r)} = \left\{ a = (a_k) : \sup_k k^{-rm} \left| v_k a_k \right|^r < \infty \right\}.$$

Proof. (i) Let $a \in U_1^{(r)}$; then

$$\sum_{k=1}^{\infty} | a_k x_k |^r = \sum_{k=1}^{\infty} k^{rm} | v_k^{-1} a_k |^r \; k^{-rm} | v_k x_k |^r \quad \le \sup_k k^{-rm} | v_k x_k |^r \sum_{k=1}^{\infty} k^{rm} | v_k^{-1} a_k |^r < \infty \qquad (3)$$

for each $x \in C_\infty(\Delta_v^m)$ by Lemma 3. Hence $a \in [C_\infty(\Delta_v^m)]^{r\alpha}$. Since $\ell_\infty(\Delta_v^m) \subset C_\infty(\Delta_v^m)$, we have $[C_\infty(\Delta_v^m)]^{r\alpha} \subset [\ell_\infty(\Delta_v^m)]^{r\alpha} = U_1^{(r)}$; hence $a \in U_1^{(r)}$.

(ii) Let $a \in U_2^{(r)}$ and $x \in U_1^{(r)}$. Then from (3) we have $a \in \left[U_1^{(r)}\right]^{r\alpha}$. Now suppose that $a \in \left[U_1^{(r)}\right]^{r\alpha}$ and $a \notin U_2^{(r)}$. Then we have $\sup_k k^{-rm} | v_k a_k |^r = \infty$. Hence there is a strictly increasing sequence $(k(i))$ of positive integers $k(i)$ such that

$$[k(i)]^{-rm} | v_{k(i)} a_{k(i)} |^r > i^m.$$

We define the sequence $x = (x_k)$ by

$$x_k = \begin{cases} | a_{k(i)} |^{-1}, & k = k(i) \\ 0 \;, & k \ne k(i). \end{cases}$$

Then we have

$$\sum_{k=1}^{\infty} k^{rm} | v_k^{-1} x_k |^r = \sum_{i=1}^{\infty} [k(i)]^{rm} | v_{k(i)} a_{k(i)} |^{-r}$$

$$\le \sum_{i=1}^{\infty} i^{-m} < \infty, \quad m \ge 2.$$

Hence $x \in U_1^{(r)}$ and $\sum_{k=1}^{\infty} | a_k x_k |^r = \sum_{k=1}^{\infty} 1 = \infty$. This contradicts $a \in \left[U_1^{(r)}\right]^{r\alpha}$; hence $a \in U_2^{(r)}$.

Theorem 7. Let $m \ge 1$ and $1 \le r < \infty$. Then

(i) $\left\{C_\infty\left[\Delta_v^m\right]\right\}^{r\alpha} = U_1^{(r)}$,

(ii) $\left[U_1^{(r)}\right]^{r\alpha} = U_2^{(r)}$.

Proof. The proof is similar to that of Theorem 6.

Corollary 1. The sequence spaces $C_\infty(\Delta_v^m)$ and $C_\infty\left[\Delta_v^m\right]$ are not $r\alpha$-perfect for $m \ge 1$.

Let $v = (v_k)$ be any fixed sequence of non-zero complex numbers and let E stand for ℓ_∞, c and c_0. Then we define $E(v) = \{x = (x_k) : (v_k x_k) \in E\}$. In the following theorem we give the $r\alpha$-, $r\beta$- and $r\gamma$-duals of $E(v)$.

Theorem 8. Let $m \ge 1$ and $1 \le r < \infty$. Then $\left[E(v)\right]^{r\eta} = U^{(r)}$ for $\eta \in \{\alpha, \beta, \gamma\}$, where

$$U^{(r)} = \left\{ a = (a_k) : \sum_{k=1}^{\infty} \left| v_k^{-1} a_k \right|^r < \infty \right\}$$

Proof. We give the proof for the case $E = \ell_\infty$ and $\eta = \alpha$. If $a \in U^{(r)}$, then

$$\sum_{k=1}^{\infty} |\, a_k x_k \,|^r \le \sup_k |v_k x_k|^r \;\; \sum_{k=1}^{\infty} |\, \frac{a_k}{v_k} \,|^r < \infty$$

for each $x \in \ell_\infty(v)$; hence $a \in [\ell_\infty(v)]^{r\alpha}$. Now suppose that $a \in [\ell_\infty(v)]^{r\alpha}$ and $a \notin U^{(r)}$. Then there is a strictly increasing sequence (n_i) of positive integers n_i such that

$$\sum_{k=n_i+1}^{n_{i+1}} |\, v_k^{-1} a_k \,|^r > i^r .$$

Let $x \in \ell_\infty(v)$ be defined by

$$x_k = \begin{cases} 0, & 1 \le k \le n_1 \\ v_k^{-1}(\operatorname{sgn} a_k)/i, & n_i < k \le n_{i+1} \end{cases}.$$

Then we may write

$$\begin{aligned} \sum_{k=1}^{\infty} |\, a_k x_k \,|^r &= \sum_{k=n_1+1}^{n_2} |\, a_k x_k \,|^r + \ldots + \sum_{k=n_i+1}^{n_{i+1}} |\, a_k x_k \,|^r + \ldots \\ &= \sum_{k=n_1+1}^{n_2} |\, v_k^{-1} a_k \,|^r + \ldots + \frac{1}{i^r} \sum_{k=n_i+1}^{n_{i+1}} |\, v_k^{-1} a_k \,|^r + \ldots \\ &> 1 + 1 + \ldots = \sum_{i=1}^{\infty} 1 = \infty. \end{aligned}$$

This contradicts $a \in (\ell_\infty(v))^{r\alpha}$; hence $a \in U^{(r)}$. The proofs for the cases $X = c_0$ or c and $\eta \in \{\beta, \gamma\}$ are similar.

Corollary 2. *i*) Let $v_k = 1$ for all $k \in \mathbb{N}$. Then we have

$$[C_\infty(\Delta_v^m)]^{r\alpha} = \left\{C_\infty\left[\Delta_v^m\right]\right\}^{r\alpha} = G_1^{(r)} \text{ and } \left[G_1^{(r)}\right]^{r\alpha} = G_2^{(r)}.$$

where

$$G_1^{(r)} = \{a = (a_k) : \sum_{k=1}^{\infty} k^{rm} |\, a_k \,|^r < \infty\},$$

$$G_2^{(r)} = \{a = (a_k) : \sup_k k^{-rm} |\, a_k \,|^r < \infty\},$$

(*ii*) Let $v_k = 1$ for all $k \in \mathbb{N}$ and $m = 0$. Then we have

$$[C_\infty(\Delta_v^m)]^{r\alpha} = \left\{C_\infty\left[\Delta_v^m\right]\right\}^{r\alpha} = \ell_r = \{a = (a_k) : \sum_{k=1}^{\infty} |\, a_k \,|^r < \infty\},$$

(*iii*) Let $v_k = 1$ for all $k \in \mathbb{N}$. Then we have $U^{(r)} = \ell_r$.

Lemma 5 [35]**.** Let m be a positive integer. Then

i) There exist positive constants, M_1 and M_2, such that $M_1 k^m \le \binom{m+k}{k} \le M_2 k^m, k = 0,1,2\ldots$

ii) $\sum_{k=0}^{n} \binom{n+m-k-1}{m-1} = \binom{n+m}{m} = \binom{n+m}{n}$,

iii) If $x \in c_0(\Delta_v^m)$, then $\binom{m+k}{k}^{-1} v_k x_k \to 0, (k \to \infty)$.

Theorem 9. Let $1 \le r < \infty$, and m be a positive integer. Then

$[C_\infty(\Delta_v^m)]^{rN} = \{C_\infty[\Delta_v^m]\}^{rN} = [C_\infty(\Delta_v^m)]^N = \{C_\infty[\Delta_v^m]\}^N = U_1(v)$ and

$\{V_0[\Delta_v^m]\}^{rN} = \{V_0[\Delta_v^m]\}^N = U_2(v)$

where

$$U_1(v) = \{a = (a_n) : v_n^{-1} n^m a_n \to 0, \ \ n \to \infty\}$$

$$U_2(v) = \{a = (a_n) : \sup_n |\sum_{k=0}^{n} \binom{n+m-k-1}{m-1} v_n^{-1} a_n | < \infty\}.$$

Proof. The proof of the part $[C_\infty(\Delta_v^m)]^N = [C_\infty(\Delta_v^m)]^N = U_1(v)$ is easy. We only show that $\{V_0[\Delta_v^m]\}^N = U_2(v)$. Since $[c_0(\Delta_v^m)]^N = U_2(v)$ and $c_0(\Delta_v^m) \subset V_0[\Delta_v^m]$, we have $[c_0(\Delta_v^m)]^N \subset U_2$. Let $a \in U_2(v)$ and $x \in V_0[\Delta_v^m]$. Then by Lemma 5 *i*), *ii*) and *iii*), we obtain

$$\lim_n a_n x_n = \lim_n (\sum_{k=0}^{n} \binom{n+m-k-1}{m-1}) v_n^{-1} a_n (\sum_{k=0}^{n} \binom{n+m-k-1}{m-1})^{-1} v_n x_n = 0.$$

Hence $a \in \{V_0[\Delta_v^m]\}^N$.

ACKNOWLEDGEMENTS

This research was supported by FUBAP (The Management Union of the Scientific Research Projects of Firat University) under the Project Number: FUBAP 1646. The authors are thankful to the referees whose comments improve the quality of the paper.

REFERENCES

1. L. Leindler, "Über die de la Vallee-Pousinsche Summierbarkeit allgemeiner Orthogonalreihen", *Acta Math. Acad. Sci. Hungar.*, **1965**, *16*, 375-387.
2. H. Kızmaz, "On certain sequence spaces", *Canad. Math. Bull.,* **1981**, *24*, 169-176.
3. M. Et and R. Çolak, "On some generalized difference sequence spaces", *Soochow J. Math.*, **1995**, *21*, 377-386.
4. B. Altay and F. Başar, "The fine spectrum and the matrix domain of the difference operator Δ on the sequence space $\ell_p, (0 < p < 1)$", *Commun. Math. Anal.*, **2007**, *2*, 1-11.
5. F. Başar and B. Altay, "On the space of sequences of p-bounded variation and related matrix mappings", *Ukrainian Math. J.*, **2003**, *55*, 136-147.
6. R. Çolak, M. Et and E. Malkowsky, "Some Topics of Sequence Spaces", Firat University Press, Elazığ, **2004**.
7. F. Başar, "Summability Theory and Its Applications", Bentham Science Publishers, Istanbul, **2012**.
8. M. Et and A. Esi, "On Köthe-Toeplitz duals of generealized difference sequence spaces", *Bull. Malaysian Math. Sci. Soc.*, **2000**, *23*, 25-32.
9. B. Altay and F. Başar, "On the fine spectrum of the difference operator Δ on c_0 and c", *Inform. Sci.*, **2004**, *168*, 217-224.
10. B. Altay, "On the space of p-summable difference sequences of order m, $(1 \le p < \infty)$", *Studia Sci. Math. Hungar.*, **2006**, *43*, 387-402.

11. V. K. Bhardwaj and I. Bala, "Generalised difference sequence space defined by $|\overline{N}, p_k|$ summability and an Orlicz function in seminormed space", *Math. Slovaca*, **2010**, *60*, 257-264.
12. I. Djolović and E. Malkowsky, "Characterizations of compact operators on some Euler spaces of difference sequences of order m", *Acta Math. Sci.*, **2011**, *31B,* 1465-1474.
13. M. Et, "On some generalised Cesàro difference sequence spaces", *Istanbul Univ. Fen. Fak. Mat. Derg.*, **1996/97,** *55/56* , 221-229.
14. M. Et, "Spaces of Cesàro difference sequences of order r defined by a modulus function in a locally convex space", *Taiwanese J. Math.*, **2006**, *10*, 865-879.
15. M. Et and M. Işık, "On $p\alpha$-dual spaces of generalised difference sequence spaces", *Appl. Math. Lett.,* **2012**, *25*, 1486-1489.
16. M. Işık, "On statistical convergence of generalised difference sequences", *Soochow J. Math.*, **2004**, *30*, 197-205.
17. M. Güngör and M. Et, "Δ^r - strongly almost summable sequences defined by Orlicz functions", *Indian J. Pure Appl. Math.*, **2003**, *34*, 1141-1151.
18. E. Malkowsky and S. D. Parashar, "Matrix transformations in spaces of bounded and convergent difference sequences of order m", *Analysis*, **1997**, *17*, 87-97.
19. M. Mursaleen, "Generalised spaces of difference sequences", *J. Math. Anal. Appl*., **1996,** *203*, 738-745.
20. P. D. Srivastava and S. Kumar, "Generalised vector-valued paranormed sequence space using modulus function", *Appl. Math. Comput*., **2010**, *215*, 4110-4118.
21. B. C. Tripathy, Y. Altin and M. Et, "Generalised difference sequence spaces on seminormed space defined by Orlicz functions", *Math. Slovaca*, **2008**, *58*, 315-324.
22. Z. U. Ahmad and M. Mursaleen, "Köthe-Toeplitz duals of some new sequence spaces and their matrix maps", *Publ. Inst. Math. (Belgr.)*, **1987**, *42*, 57-61.
23. E. Malkowsky, "Absolute and ordinary Köthe-Toeplitz duals of some sets of sequences and matrix transformations", *Publ. Inst. Math. (Belgr.)***, 1989**, *46*, 97-103.
24. E. Malkowsky, M. Mursaleen and S. Suantai**,** "The dual spaces of sets of difference sequences of order *m* and matrix transformations", *Acta Math. Sin. Engl. Ser.*, **2007**, *23*, 521-532.
25. M. Mursaleen and A. K. Noman**,** "On some new difference sequence spaces of non-absolute type", *Math. Comput. Model.*, **2010**, *52*, 603-617.
26. B. C. Tripathy and S. Mahanta, "On a class of vector-valued sequences associated with multiplier sequences", *Acta Math. Appl. Sin. Engl. Ser.*, **2004**, *20*, 487-494.
27. B. C. Tripathy and B. Hazarika, "*I*-convergent sequence spaces associated with multiplier sequences", *Math. Inequal. Appl.*, **2008**, *11*, 543-548.
28. B. C. Tripathy and P. Chandra, "On some generalized difference paranormed sequence spaces associated with multiplier sequence defined by modulus function", *Anal. Theory Appl.*, **2011**, *27*, 21-27.
29. B. C. Tripathy and A. Baruah, "Lacunary statistically convergent and lacunary strongly convergent generalized difference sequences of fuzzy real numbers", *Kyungpook Math. J.*, **2010**, *50*, 565-574.
30. J. S. Shiue, "On the Cesàro sequence space", *Tamkang J. Math.*, **1970**, *2*, 19-25.
31. A. A. Jagers, "A note on Cesàro sequence spaces", *Nieuw Arch. Wisk.*, **1974**, *22*, 113-124.

32. P. N. Ng and P. Y. Lee, "On the associate spaces of Cesàro sequence space", *Nanta Math.*, **1976**, *9*, 168-172.
33. P. N. Ng and P. Y. Lee, "Cesàro sequence spaces of non-absolute type", *Comment. Math.*, **1978**, *20*, 429-433.
34. M. Et, "On some topological properties of generalized difference sequence spaces", *Int. J. Math. Math. Sci.*, **2000**, *24*, 785-791.
35. Ç. A. Bektaş, M. Et and R. Çolak, "Generalised difference sequence spaces and their dual spaces", *J. Math. Anal. Appl.*, **2004**, *292*, 423-432.
36. P. Chandra and B. C. Tripathy, "On generalized Köthe-Toeplitz duals of some sequence spaces", *Indian J. Pure Appl. Math.*, **2002**, *33*, 1301-1306.
37. B. C. Tripathy and B. Sarma, "Generalized Köthe-Toeplitz duals of some double sequence spaces", *Fasc. Math.*, **2008**, *40*, 119-125.

Maejo International Journal of Science and Technology

ISSN 1905-7873
Available online at www.mijst.mju.ac.th

Full Paper

Development of dried chewy longan arils

Wiwat Wangcharoen*

Faculty of Engineering and Agro-Industry, Maejo University, Chiang Mai 50290, Thailand

* E-mail: wiwat@mju.ac.th

Received: 5 February 2012 / Accepted: 16 December 2013 / Published: 23 December 2013

Abstract: Dried chewy longan arils were developed by osmotic dehydration with sucrose and glucose syrup solution and hot air drying. The water sorption isotherm of dried longan arils was better fitted by Gugenheim-Anderson de Boer (GAB) model than Brunauer-Emmett-Teller (BET) model and it showed that the water activity and moisture content of dried longan arils were decreased by glucose syrup solution. The most acceptable product was longan aril soaked for 2 days in sucrose solution followed by 2 days in glucose syrup solution before drying. This product showed the antioxidant capacity of at least 0.53±0.08 mg vitamin C equivalent per g dry sample and this antioxidant activity was stable for 12 months. Its shelf life was predicted at 20 months.

Keywords: longan, osmotic dehydration, water sorption isotherm, antioxidant capacity, shelf-life prediction

INTRODUCTION

Longan (*Dimocarpus longan* (Lour.) Steud) is among ten of the most economically important fruits of Thailand. The main region of longan cultivation is in the upper northern part of the country, namely in the provinces of Chiang Mai (31.4%), Lamphun (28.8%) and Chiang Rai (8.8%). 'E Dor', the most popular commercial cultivar, occupies the largest area or 75% followed by 'Haeo', 'Bieo Khieo' and 'Si Chompu', each covering 7% of the total cultivated area [1]. Thailand currently becomes the top exporter of longan, followed by Vietnam [1-2].

Nowadays, longan is available year round in Thailand but the peak period is June-August [3]. The mature longan fruit is small (ca. 1.5-2 cm in diameter), conical, heart-shaped or spherical in shape and light brown in colour. It has thin, leathery and indehiscent pericarp surrounding succulent, edible white aril developed around a relatively large dark brown seed. Longan is non-climacteric and therefore must be harvested when the skin becomes yellow-brown and the flesh reaches optimal maturity at 15.5-16°Brix [4]. In practice, however, the harvest maturity is usually assessed on the basis of colour and flavour [2].

Longan has a very short postharvest life of 3-4 days at ambient temperature [5-6]. The major factors that reduce its storage life and marketability are microbial decay and pericarp browning. Low temperature storage at 1-5°C is used to reduce pathological decay up to approximately 30 days, but the fruit becomes visually unacceptable from pericarp browning and deteriorates rapidly when removed from cold storage. Sulfur dioxide fumigation has been the most effective postharvest treatment for control of pericarp browning in longan, and is used extensively in commercial situations at present [2].

For commercial processing, canning, freezing and drying are widely used for longan [7]. Dried longan is an important product and more than 3,000 hot-air driers are currently in operation in Thailand for its production [8]. Longan drying by a hot-air drier at 45-85°C is an energy-intensive process [9-11]. Both peeled and unpeeled dried longans are available in the local market and for export, but they are only suitable for use as ingredients for cooking or further processing because most of them have tough or hard texture. Combinations between hot-air driers and other processes such as microwave [12], two-stage superheated steam [13] and far-infrared radiation [14], have been studied in order to improve the drying process and the products. Some commercialised crispy longan arils [15, 16] have been produced by higher drying technology such as freeze-drying. They are suitable for direct consuming as snack or serving with drinks, yogurt or salad. A high content of vitamin C is claimed [16].

This work presents another method for preserving longan and developing another a dried longan snack with chewy texture. Longan arils were osmotically dehydrated before they were dried by a hot-air drier. The type of sugar solution used in osmotic dehydration was studied. A water- sorption isotherm of dried longan arils was created and an acceptance test of selected dried chewy longan arils was performed. The water activity, water content and antioxidant capacity of the most acceptable samples were evaluated during 12 months of storage at room temperature, and the shelf life of the product was predicted.

MATERIALS AND METHODS

Preparation of Dried Longan Arils

Longan arils (E Daw cultivar) purchased from a local fruit canning company were dipped in boiling water for 1 min. They were then soaked in 70°Brix sugar solution (longan arils: sugar solution = 1:1 (wt/wt) [17]) at room temperature (28$\pm$5°C) for 24 hr, and were transferred to a new 70°Brix sugar solution every 24 hr. This osmotic dehydration was carried out by separately soaking for: (I) 3 days in sucrose solution; (II) 2 days in sucrose solution followed by 2 days in glucose syrup solution; (III) 1 day in sucrose solution followed by 3 days in glucose syrup solution; and (IV) 4 days in glucose syrup solution. The average weight and total soluble solid of the aril samples were recorded at day 0, 1, 2, 3 and 4. The osmotically dehydrated arils were dipped in boiling water for 1 min. to wash out the stickiness before they were dried in a hot-air drier at 50$\pm$2°C for 24 hr. They were left in airtight plastic boxes for moisture equilibration for 48 hr before measurement of shear force, water activity and moisture content (% dry basis).

The average weight was obtained by an electronic precision balance (BP610: Sartorius AG, Germany). The total soluble solid was recorded by a set of portable refractometers (FG 103/113, FG 104/114 and FG 106/116: Beijing Zhongjin Tech Metallurgical Equipment Corp., China). The shear force was measured by a Warner Bratzler shear (Salter: G-R Elec. Mfg. Co., USA). The water activity was measured by a water activity meter (AquaLab Series 3: Decagon

Device Inc., USA), and the moisture content (% dry basis) was determined by AOAC method [18].

Water Sorption Isotherm

Dried longan arils were placed over various saturated salt solutions (LiCl, CH_3COOK, $MgCl_2$, K_2CO_3, $Mg(NO_3)_2$, NaCl, KCl, $BaCl_2$ and K_2SO_4) in airtight plastic boxes at room temperature (28±5°C) for moisture equilibration (3-10 days) before their water activity and moisture content were determined. The moisture content was then plotted against water activity to create a water sorption isotherm of dried longan arils, which was then fitted by models of Brunauer-Emmett-Teller (BET) and Gugenheim-Anderson de Boer (GAB) [19-21] as follows.

$$BET : Aw/[(1-Aw)*m] = 1/(mo*c) + [(c-1)/(mo*c)]*Aw$$

$$GAB : Aw/m = (k/mo)*((1/c)-1)*Aw^2 + (c-2)/(mo*c)*Aw + 1/(mo*c*k)$$

where Aw = water activity; m = moisture content (% dry basis); mo = monolayer moisture content; c = energy constant; and k = constant

Sensory Evaluation

An acceptance test of selected dried chewy longan arils was performed. One hundred and twenty consumers were requested to evaluate samples of the dried longan arils with respect to appearance, flavour, texture and overall preference by using a 9-point hedonic scale: 1 = extremely dislike, 5 = neither like nor dislike, 9 = extremely like [22].

Shelf-life Study and Antioxidant Capacity

The most accepted samples of the dried longan were packed in 190-ml polypropylene plastic boxes (100 g per box) and kept at room temperature (25.4±6°C) for 12 months. Their water activity, moisture content and antioxidant capacity during storage were determined. The antioxidant capacity was measured by 3 different methods, namely ferric reducing/antioxidative power (FRAP) assay [23], improved ABTS radical-cation decolourisation assay [24] and DPPH free radical scavenging activity [25] with some modification as previously described [26]. Vitamin C was used as a standard for all methods and results were reported as mg vitamin C equivalent/ g dry sample. The change of water activity and moisture content was used to predict the shelf life of the products by the following linear equation [27]:

$$\ln [(m_e - m_0)/(m_e - m_c) = [K / \alpha] t$$

where m_e = Equilibrium moisture content of product (% dry basis)
m_0 = Initial moisture content of product (% dry basis)
m_c = Moisture content of product at the end of acceptance point (% dry basis)
K = Moisture transmission rate (g water/ g solid.time)
α = Slope of liner regression (g water/ g solid)
t = Shelf life of product (time)

Statistical Analysis

All experiment was done in triplicate. Completely randomised design was used for analysis of variance for almost all of the data except those for sensory evaluation, for which randomised complete block design was used. Tukey (a)'s w test was used for the Post Hoc test.

RESULTS AND DISCUSSION

Sample Preparation

The average weight and total soluble solid of longan arils measured at day 0, 1, 2, 3 and 4 are shown in Figure 1. The average weight of longan arils decreased whilst the total soluble solid increased because there was a diffusion of water and some solutes from tissues of longan arils into the sugar solution and a simultaneous counter-diffusion of solutes from the sugar solution into the tissues of longan arils. The rate of diffusion depends on several factors including the size and geometry of material [28]. The glucose syrup in this study was the original glucose syrup (dextrose equivalent=42) which contained glucose, maltose and higher molecular-weight sugars [29]. Its solution could better absorb water (Figure 1a) but more slowly increase total soluble solid in longan arils than did sucrose solution (Figure 1b). This osmotic dehydration could be accelerated to reduce processing time by increasing the temperature of the sugar solution [17, 28].

Shear force, water activity and moisture content of the dried longan arils are shown in Table 1. The shear forces of longan arils soaked in sucrose and glucose syrup solutions were much lower than those of the arils soaked in sucrose or glucose syrup solution alone because the crystallisation of sucrose was retarded in the former case and sugars with higher molecular weights in the glucose syrup helped to give body and chewiness to the longan arils [30]. Higher-molecular-weight sugars also caused toughness of longan arils and this is why the shear force of longan arils soaked in sucrose or glucose syrup solution only was higher. Moreover, glucose syrup solution helped to decrease the water activity and moisture content of longan arils due to its humectant property [31]. Since only dried longan arils (II and III) which were soaked in sucrose and glucose syrup solutions had the chewy texture, they were selected for the sensory evaluation.

Table 1. Shear force, water activity and moisture content of dried longan arils

	Longan arils (I)	Longan arils (II)	Longan arils (III)	Longan arils (IV)
Shear force (kg)	9.48 ± 2.53^{a}	1.52 ± 0.33^{b}	2.30 ± 0.39^{c}	7.72 ± 2.21^{a}
Water activity	0.713 ± 0.012^{a}	0.658 ± 0.016^{b}	0.630 ± 0.022^{bc}	0.602 ± 0.021^{c}
Moisture content (% dry basis)	17.79 ± 2.05^{a}	13.12 ± 1.42^{b}	11.18 ± 1.56^{b}	9.37 ± 1.29^{b}

Note: Longan arils (I) were soaked for 3 days in sucrose solution before drying.
Longan arils (II) were soaked for 2 days in sucrose solution followed by 2 days in glucose syrup solution before drying.
Longan arils (III) were soaked for 1 day in sucrose solution followed by 3 days in glucose syrup solution before drying.
Longan arils (IV) were soaked for 4 days in glucose syrup solution before drying.
Means with different letters in the same row are significantly different ($p<0.05$).

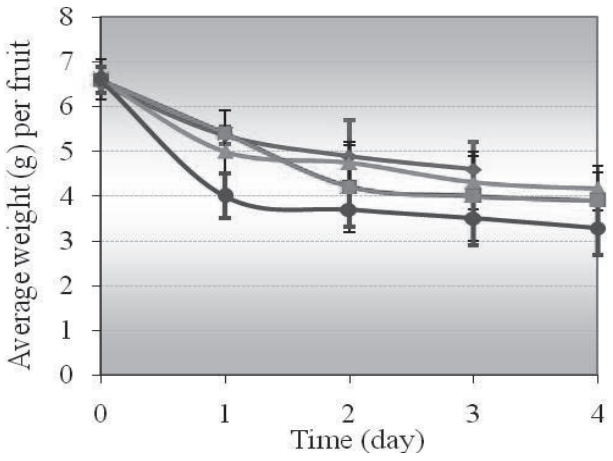

(a)

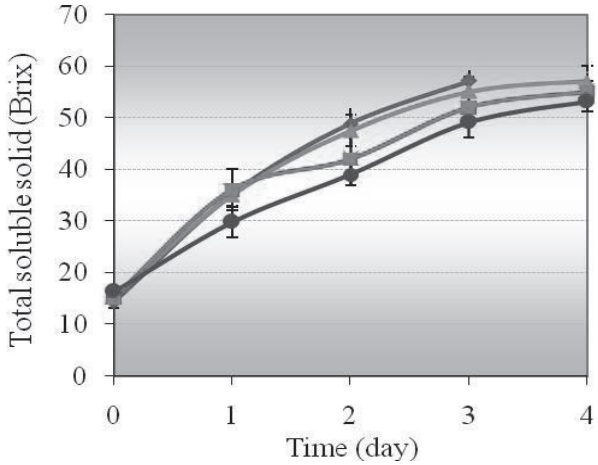

(b)

Figure 1. Average weight (a) and total soluble solid (b) of longan arils soaked for: (I) 3 days in sucrose solution (♦); (II) 2 days in sucrose solution followed by 2 days in glucose syrup solution (▲); (III) 1 day in sucrose solution followed by 3 days in glucose syrup solution (■); and (IV) 4 days in glucose syrup solution (●)

Water Sorption Isotherm

To create a water sorption isotherm of dried longan arils, the equilibrium moisture content and the water activity of longan arils placed over saturated salt solutions were plotted as shown in Figure 2a. It is a Flory-Huggins (type III) isotherm because sugars in dried longan arils have a fairly low adsorption of water until the water activity becomes sufficient for solubilisation when adsorption increases [32-33]. This type-III isotherm was also reported in a previous study with fresh and osmotically dehydrated apples, which showed that at a constant water activity the equilibrium moisture content decreased with increasing sugar content of the products [34]. The equilibrium moisture content of dried and osmotically dehydrated longan arils at each water activity value in this study was also lower than that of dried longan arils without osmotic dehydration reported by Janjai *et al.* [8].

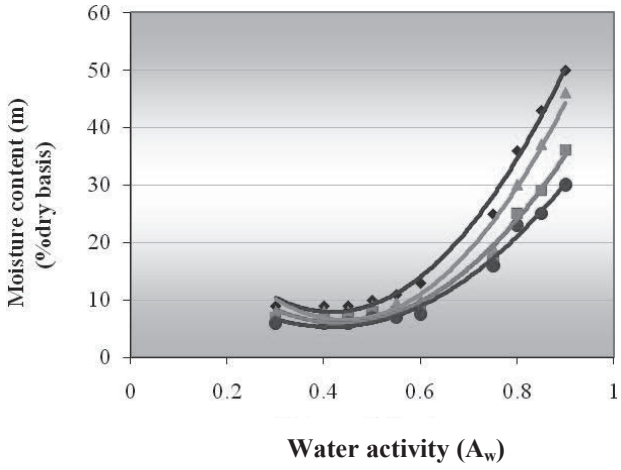

(a)

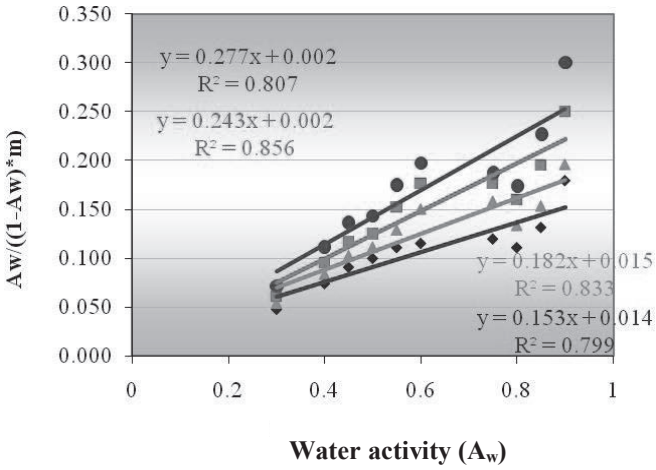

(b)

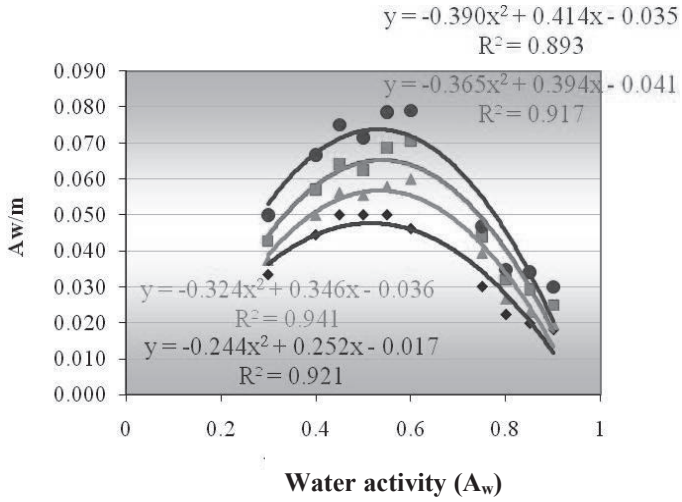

(c)

Figure 2. Water sorption isotherms (a), BET model (b), and GAB model (c) of longan arils soaked for: (I) 3 days in sucrose solution (♦); (II) 2 days in sucrose solution followed by 2 days in glucose syrup solution (▲); (III) 1 day in sucrose solution followed by 3 days in glucose syrup solution (■); and (IV) 4 days in glucose syrup solution (●), before drying

When the water sorption isotherms of dried longan arils were fitted by models of BET and GAB, they were found to be better fitted to the GAB model (R^2 = 0.893 – 0.941) than the BET model (R^2 = 0.799-0.856) (Figures 2b and 2c). These findings agree with previous work [34-35]. The GAB model has become very popular because the activity range covered by this model is much wider (A_w = 0.05-0.80 or 0.90) than that by the BET model (A_w = 0.05-0.30), and it has been recommended by the European Project Group COST 90 on Physical Properties of Food as the fundamental equation of water sorption by food materials [36].

Since water adsorption is one of the main factors that affect the physical state and stability of products [32], its prediction can be useful for estimating the shelf life of the products. In this present work, fungal growth could be observed when the moisture content of dried longan arils was higher than 20% and this value was used as the end of acceptance point of product in the shelf-life study.

Sensory Evaluation

Dried longan arils (II and III) soaked in sucrose and glucose syrup solution which had the chewy texture were selected for sensory evaluation. Longan type II was preferred to type III by 120 consumers as shown in Table 2. This result may be correlated with sweet taste, less sticky texture and appearance of longan type II, as apparent from the comparative values of total soluble solid and shear force (Figure 1 and Table 1). This product was therefore used for the shelf-life study.

Table 2. Sensory evaluation of dried chewy longan arils by 120 consumers with 9 point-hedonic scales

	Longan arils (II)	Longan arils (III)
Appearance	6.23 ± 1.08^{a}	5.83 ± 1.44^{b}
Flavour	6.68 ± 1.28^{a}	5.84 ± 1.45^{b}
Texture	6.59 ± 1.44^{a}	5.45 ± 1.62^{b}
Overall preference	6.71 ± 1.19^{a}	5.86 ± 1.38^{b}

Note: Means with different letters in the same row are significantly different ($p<0.05$).

Shelf-life Study and Antioxidant Capacity

The water activity, moisture content and antioxidant capacity of longan type II were determined during 12 months of storage (Table 3). The fluctuation of water activity and moisture content was found to be due to the change of relative humidity of air [37]. The product adsorbed or desorbed moisture when the relative humidity of air was higher or lower than the water activity of the product. When the values of water activity and moisture content were plotted on the water sorption isotherm, a linear regression, $y = 91.64x - 45.57$, from the minimum moisture content during storage to moisture content at maximum relative humidity of air during storage (A_w = 0.800) was created as shown in Figure 3. The slope of linear regression in Figure 3 was used as the value of 'α' in the equation for predicting shelf life. To predict the shelf life of product, the transmission rate, K, during storage was first calculated from the equation for predicting shelf life and then its value was used for determining the product's shelf life from the same equation as elaborated below.

From equation $\ln [(m_e - m_0)/(m_e - m_c) = [K / \alpha] t$, when m_e = 30% (equilibrium moisture content at highest relative humidity of air during storage, A_w = 0.800), m_0 = 9.36% (minimum moisture content during storage), m_c = 16.61% (maximum moisture content during

storage), α = 91.64 g water/ g solid (slope of linear regression, y = 91.64x - 45.57, in Figure 3), and t = 12 (months of storage), a moisture transmission rate (K) of 3.305 g water/ g solid.month was obtained. This K value, with the end of acceptance point of product observed from water sorption isotherm section (20% moisture content), m_e = 30%, m_0 = 9.36% and α = 91.64, was used to predict the shelf life of product (t), which turns out to be about 20 months.

Table 3. Water activity, moisture content and antioxidant capacity of dried chewy longan arils (type II)

Storage time (month)	Relative humidity* (%)	Water activity	Moisture content (% dry basis)	Antioxidant capacity (mg vitamin C equivalent/ g dry sample)		
				FRAP ^{ns}	ABTS ^{ns}	DPPH ^{ns}
0		0.658±0.016 ^{ab}	13.12±1.42 ^{cd}	0.86±0.12	0.62±0.05	0.97±0.10
1	70	0.666±0.026 ^{ab}	16.61±1.76 ^{b}	0.76±0.10	0.59±0.03	0.92±0.08
2	64	0.657±0.033 ^{ab}	15.92±1.07 ^{bc}	0.72±0.07	0.53±0.08	0.83±0.14
3	47	0.589±0.071 ^{b}	12.62±1.99 ^{cd}	0.77±0.09	0.56±0.12	0.88±0.21
4	47	0.617±0.062 ^{ab}	12.46±1.43 ^{cd}	0.83±0.06	0.58±0.05	0.74±0.08
5	39	0.618±0.044 ^{ab}	10.52±0.90 ^{de}	0.79±0.09	0.62±0.01	0.65±0.21
6	53	0.591±0.034 ^{b}	9.36±1.01 ^{e}	0.81±0.11	0.56±0.04	0.74±0.16
7	63	0.620±0.026 ^{ab}	10.06±0.89 ^{de}	0.84±0.12	0.61±0.06	0.92±0.08
8	70	0.649±0.019 ^{ab}	10.88±1.16 ^{de}	0.72±0.01	0.58±0.02	0.90±0.10
9	80	0.692±0.012 ^{a}	13.36±1.96 ^{a}	0.80±0.14	0.61±0.02	1.06±0.21
10	75	0.689±0.009 ^{a}	13.04±1.32 ^{b}	0.70±0.01	0.61±0.06	0.97±0.02
11	74	0.668±0.010 ^{ab}	12.47±1.31 ^{cd}	0.82±0.01	0.54±0.12	0.76±0.29
12	68	0.654±0.017 ^{ab}	11.09±1.47 ^{de}	0.64±0.12	0.55±0.02	1.04±0.10

Note: Means with different letters in the same column are significantly different ($p<0.05$).
^{ns} Means in the same column are not significantly different ($p>0.05$).
* Data from Titi Tudorancea Bulletin [37]

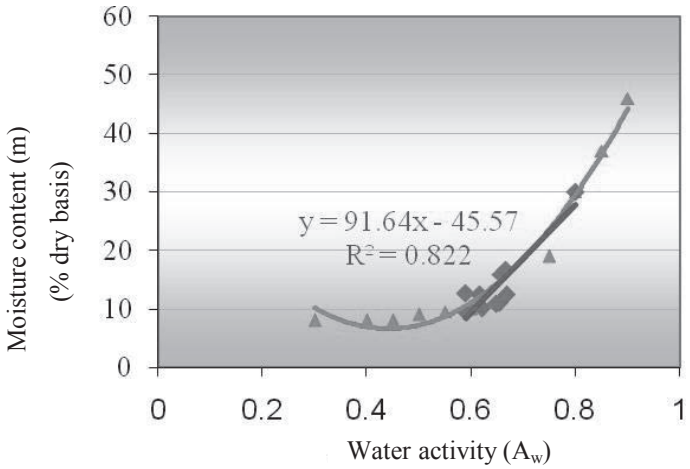

Figure 3. Water sorption isotherm (▲) and linear regression of water activity and moisture content during storage of dried chewy longan arils type II (♦)

As seen in Table 3, the antioxidant capacity did not significantly change ($p>0.05$) during 12 months of storage. This antioxidant capacity has been shown to be the result of compounds present in longan fruits such as phenolic/flavonoid glycosides and ellagitannins [38], vitamin C

[39] and browning pigments formed during heat treatment [26, 40-41]. In addeition, antioxidant compounds in fresh longan may decompose during drying and storage whilst browning pigments are formed. From Table 3, FRAP and DPPH values, which have been found highly correlated with browning pigment formation, are obviously higher than ABTS values, which are highly correlated with phenolic compounds in our previous work [26]. Browning pigment formation, therefore, was likely to be the main factor which made for a more or less constant antioxidant capacity in this study.

From Table 3, the minimum value of antioxidant capacity of dried chewy longan arils is 0.53$\pm$0.08 mg vitamin C equivalent/ g dry sample. Recommended intake or daily value of vitamin C for adults or children from four years of age, based on a caloric intake of 2,000 calories, is 60 mg [42], and a product which contains at least 20% of the daily value of vitamin C can be claimed as 'high in antioxidant vitamin C', although this claim can be used only for antioxidant vitamins in products which include vitamin C, vitamin E and beta-carotene [43]. However, an analysis of antioxidant capacity as mg of vitamin C equivalent can be used to show the antioxidant potential of these dried chewy longan arils.

CONCLUSIONS

Longan preservation by osmotic dehydration and hot air drying, resulting in longan arils with a chewy texture suitable for snacks or similar products, seems to be an alternative method which may be useful for local manufacturers when longan is readily available and low-priced in the peak season.

ACKNOWLEDGEMENTS

This work is a part of a research project supported by a grant from the Office of Agricultural Research and Extension at Maejo University.

REFERENCES

1. S. Somsri and S. Vichitrananda, "Tropical Fruit Production and Marketing in Thailand", Department of Agriculture, Bangkok, **2007**, pp.11-12.
2. Y. M. Jiang, Z. Q. Zhang, D. C. Joyce and S. Ketsa, "Postharvest biology and handling of longan fruit (*Dimocarpus longan* Lour.)", *Postharvest Biol. Technol.*, **2002**, *26*, 241-252.
3. Department of Agricultural Extension, "Fruits in Thailand", Ministry of Agriculture and Cooperatives, Bangkok, **2004**, pp.14-15.
4. O. Wara-Aswapati, D. Sroymano, S. La-Ongsri and S. Gomolmanee, "Development of maturity indices for longan", Proceedings of "Postharvest Handling of Tropical Fruit", **1994**, Australian Centre for International Agricultural Research (ACIAR), Canberra, Australia, pp.341-342.
5. J. Siriphanich, "Post-harvest problems in Thailand: Priorities and constraints", Proceedings of Symposium on "Post-harvest Technology in Asia—a Step forward to Stable Food Supply Production" **1998**, Tsukuba, Japan, pp.17-23.
6. H. T. Lin, S. J. Chen, J. Q. Chen and Q. Z. Hong, "Current situation and advances in post-harvest storage and transportation technologies of longan fruit", *Acta Hort.*, **2001**, *558*, 343-351.
7. R. X. Lu, X. J. Zhan, J. Z. Wu, R. F. Zhuang, W. N. Huang, L. X. Cai and Z. M. Huang, "Studies on storage of longan fruits", *Subtrop. Plant Res. Commun.*, **1992**, *21*, 9-17.

8. S. Janjai, P. Intawee, K. Tohsing, B. Mahayothee, B. K. Bala, M. A. Ashraf and J. Müller, "Neural network modeling of sorption isotherms of longan (*Dimocarpus longan* Lour.)", *Comput. Electron. Agric.*, **2009**, *66*, 209-214.
9. R. Attabhanyo, K. Ngamsomsut, A. Attabhanyo, S. Arrayarungsarit, Y. Chaowanapoonpon and J. Kitchaijaroon, "Longan Process Industry", Faculty of Agriculture, Chiang Mai University, Chiang Mai, **1998** (in Thai).
10. A. Achariyaviriya, S. Soponronnarit and J. Tiasuwan, "Study of longan flesh drying", *Drying Technol. Int. J.*, **2001**, *19*, 2315-2329.
11. A. Achariyaviriya, J. Tiansuwan and S. Soponronnarit, "Energy optimization of whole longan drying: Simulation results", *Int. J. Ambient Energy*, **2002**, *23*, 212-220.
12. J. Varith, P. Dijkanarukkul, A. Achariyaviriya and S. Achariyaviriya, "Combined microwave-hot air drying of peeled longan", *J. Food Eng.*, **2007**, *81*, 459-468.
13. T. Somjai, S. Achariyaviriya, A. Achariyaviriya and K. Namsanguan, "Strategy for longan drying in two-stage superheated steam and hot air", *J. Food Eng.*, **2009**, *95*, 313-321.
14. A. Nathakaranakule, P. Jaiboon and S. Soponronnarit, "Far-infrared radiation assisted drying of longan fruit", *J. Food Eng.*, **2010**, *100*, 662-668.
15. Alibaba, "Crispy longan", http://www.alibaba.com/showroom/crispy-longan.html (Accessed: December 2011).
16. Crispy Veg and Fruit, "Crispy longan", http://www.crispyvegandfruit.com (Accessed: January 2012).
17. W. Wangcharoen, "Effect of temperature on sucrose penetration and browning reactions in longan aril during osmotic dehydration", *Maejo Int. J. Sci. Technol*., **2009**, *3*, 434-445.
18. W. Horwitz (Ed.), "Official Methods of Analysis of AOAC International", 17th Edn., Association of Official Analytical Chemists (AOAC), Gaithersburg (MD), **2000**.
19. R. Boquet, J. Chirife and H. A. Iglesias, "Equations for fitting water sorption isotherms of foods. II. Evaluation of various two-parameter models", *Int. J. Food Sci. Technol*., **1978**, *13*, 319-327.
20. Y. H. Roos, "Water activity and physical state effects on amorphous food stability", *J. Food Process. Preserv.*, **1993**, *16*, 433-447.
21. E. O. Timmermann, J. Chirife and H. A. Iglesias, "Water sorption isotherms of foods and foodstuffs: BET or GAB parameters?", *J. Food Eng*., **2001**, *48*, 19-31.
22. M. C. Meilgaard, G. V. Civille and B. T. Carr, "Sensory Evaluation Techniques", 3rd Edn., CRC Press, Boca Raton, **1999**, pp.242-244.
23. I. F. F. Benzie and J. J. Strain, "Ferric reducing/ antioxidant power assay: Direct measure of total antioxidant activity of biological fluids and modified version of simultaneous measurement of antioxidant power and ascorbic acid concentration", *Meth. Enzymol.,* **1999**, *299*, 15-27.
24. M. J. Arts, G. R. Haenen, H. P. Voss and A. Bast, "Antioxidant capacity of reaction products limits the applicability of the Trolox equivalent antioxidant capacity (TEAC) assay", *Food Chem. Toxicol*., **2004**, *42*, 45-49.
25. W. Brand-William, M. E. Cuvelier and C. Berset, "Use of a free radical method to evaluate antioxidant activity", *LWT. Food Sci. Technol.*, **1995**, *28*, 25-30.
26. W. Wangcharoen and W. Morasuk, "Effect of heat treatment on the antioxidant capacity of garlic", *Maejo Int. J. Sci. Technol*., **2009**, *3*, 60-70.

27. P. Chinachoti, "Food products shelf-life stability", Seminar on "Food Products Shelf-life Stability", 26-28 November 1996, Department of Product Development, Faculty of Agro-Industry, Kasetsart University, Bangkok, Thailand.
28. N. K. Rastogi, K. S. M. S. Raghavarao and K. Niranjan, "Developments in osmotic dehydration", in "Emerging Technologies for Food Processing" (Ed. D. W. Sun), Elsevier Academic Press, London, **2005**, Ch.9.
29. P. Hull, "Glucose Syrups: Technology and Applications", Wiley-Blackwell, Oxford, **2010**, pp. 45-60.
30. D. Stansell, "Caramel, toffee and fudge", in "Sugar Confectionary Manufacture" (Ed. E. B. Jackson), 2nd Edn., Aspen Publication, Gaithersberg (MD), **1999**, Ch.8.
31. E. B. Jackson and D. Howling, "Glucose syrups and starch hydrolysates", in "Sugar Confectionary Manufacture" (Ed. E. B. Jackson), 2nd Edn., Aspen Publication, Gaithersberg (MD), **1999**, Ch.2.
32. Y. H. Roos, "Phase Transitions in Foods", Academic Press, San Diego (CA), **1995**, pp.86-90.
33. B. R. Bhandari and B. P. Adhikari, "Water activity in food processing and preservation", in "Drying Technologies in Food Processing" (Ed. X. D. Chen and A. S. Mujumdar), Blackwell Publishing, Oxford, **2008**, Ch.2.
34. S. Bellagha, A. Sahli, M. Ben Zid and A. Farhat, "Desorption isotherms of fresh and osmotically dehydrated apples (Golden delicious)", *Rev. Energ. Renouvel. SMSTS'08 Alger*, **2008**, 45-52.
35. A. M. Elmonsef Omar and Y. H. Roos, "Water sorption and time-dependent crystallization behaviour of freeze-dried lactose–salt mixtures", *LWT Food Sci. Technol.*, **2007**, *40*, 520-528.
36. E. O. Timmermann, "Multilayer sorption parameters: BET or GAB values?", *Colloid. Surface. A: Physicochem. Eng. Aspects*, **2003**, *220*, 235-260.
37. "Weather in Chiang Mai, Thailand", **2012**, http://www.tititudorancea.com/z/weather_chiang_mai_thailand.htm (Accessed: February 2012).
38. N. Rangkadilok, S. Sittimonchai, L. Worasuttayangkurn, C. Mahidol, M. Ruchirawat and J. Satayavivad, "Evaluation of free radical scavenging and antityrosinase activities of standardized longan fruit extract", *Food Chem. Toxicol.*, **2007**, *45*, 328-336.
39. Nutrition Division, "Nutrient Composition per 100 Grams Edible Portion", Department of Health, Ministry of Public Health, Bangkok, **1987** (in Thai).
40. Y. Yilmaz and R. Toledo, "Antioxidant activity of water-soluble Maillard reaction products", *Food Chem.*, **2005**, *93*, 273-278.
41. S. Benjakul, W. Visessanguan, V. Phongkanpai and M. Tanaka, "Antioxidant activity of caramelisation products and their preventive effect on lipid oxidation in fish mince", *Food Chem.*, **2005**, *90*, 231-239.
42. Center for Food Safety and Applied Nutrition, **"**Guidance for industry: A food labeling guide**"**, **2008**, http://www.cfsan.fda.gov/guidance.html (Accessed: April 2008).
43. U.S. Food and Drug Administration, "Food labeling; Nutrient content claims: Definition for 'high potency' and definition of 'antioxidant' for use in nutrient content claims for dietary supplements and conventional foods", *Fed. Regist.*, **1997**, *62*, 49868-49881.